BCL-X_L PROTECTS PANCREATIC BETA-CELLS FROM HIGH GLUCOSE-INDUCED FAILURE BY DAMPENING MITOCHONDRIAL METABOLISM

by

Alexis Zi Le Shih

B.Sc. & ARCS, Imperial College London, 2012

A THESIS SUBMITTED IN PARTIAL FULFILLMENT OF

THE REQUIREMENTS FOR THE DEGREE OF

MASTER OF SCIENCE

in

The Faculty of Graduate and Postdoctoral Studies

(Cell and Developmental Biology)

THE UNIVERSITY OF BRITISH COLUMBIA

(Vancouver)

April 2015

Abstract

Chronic nutrient oversupply, such as seen in obesity, increases metabolic load and oxidative stress in the insulin-secreting β-cells. This progressively impairs β-cell function and survival, contributing to the development of type 2 diabetes. Bcl-x_L is an antiapoptotic protein of the Bcl-2 family. Recent studies have shown additional non-apoptotic functions of Bcl-x_L in suppressing glucose signaling of non-diabetic β-cells. Conceivably, this metabolic dampening may be beneficial to counter β-cell dysfunction during nutrient excess of type 2 diabetes. To test the hypothesis that Bcl-x_L protects β-cell function during metabolic stress via regulation of mitochondrial physiology, we examined the effects of gene deletion and overexpression of Bcl-x_L in β-cells. In normal conditions, islets of β-cell-specific Bcl-x knockout (BclxβKO) mice tend to be metabolically more active compared to BclxβWT islets. This metabolic effect of Bcl-x_L is further enhanced after prolonged high glucose culture, where BclxβKO islets display a pre-toxic state of metabolic amplification with dysregulated intracellular Ca^{2+} and insulin secretion. Islets overexpressing Bcl-x_L display suppressed intracellular Ca^{2+} responses, in agreement with our knockout studies. Interestingly, cells expressing Bcl-x_L at high levels have increased mitochondrial aggregates. We also demonstrated that Bcl-x_L suppresses superoxide levels and cell death induced by ribose, but not islet-cell death under glucolipotoxic conditions. In conclusion, we propose that endogenous Bcl-x_L protects β-cells from high glucose-induced failure by dampening mitochondrial activity, as well as suppressing oxidative stress-induced cell death.

Preface

This thesis presents original and unpublished work by the author, Alexis Zi Le Shih.

Certificates of Approval

All animal work carried out in this study was approved by the University of British Columbia Animal Care Committee. The following certificates and trainings were completed by Alexis Zi Le Shih prior to the study.

UBC Animal Care Center, Biology and Husbandry of the Laboratory Rodent training (#RBH-235-12).

Canadian Council on Animal Care (CCAC)/ National Institutional Animal User Training (NIAUT) Program (Certificate # 5615-12, issued on September 10th, 2012)

Table of Contents

List of Tables

List of Figures

List of Abbreviations

ATP	Adenosine triphosphate
Bcl	B Cell Lymphoma
BclxβKO	β-cell specific Bcl-x knockout
BclxβWT	β-cell specific Bcl-x wildtype
bp	Basepair
Ca^{2+}	Calcium ion
CCCP	Carbonyl cyanide *m*-chlorophenyl hydrozone
Co-A	Coenzyme A
Cre	Cre recombinase
DHE	Dihydroethidium
ETC	Electron transport chain
Gck	Glucose kinase
GDP	Guanosine diphosphate
Glut2	Glucose transport 2
H_2O_2	Hydrogen peroxide
Ins	Insulin gene
Kb	Kilo base pair
KO	Knock out
KRB	Kreb's Ringer's Buffer
MafA	V-Maf Avian Musculoaponeurotic Fibrosarcoma Oncogene Homolog A
Pdx-1	Pancreas and duodenal homeobox 1
PI	Propidium iodide

RT-qPCR	Real time- quantitative polymerized chain reaction
T1D	Type 1 diabetes
T2D	Type 2 diabetes
TCA	Ticarboxylic acid cycle
TMRE	Tetramethylrodamine, ethyl ester
UCP	Uncoupling protein
WT	Wild type
$\Delta\psi_m$	Mitochondrial membrane potential

Acknowledgements

First and foremost, I want to thank my loving parents, David and Teresa, who have inspired and supported me in so many ways that I am forever indebted to them. Their wisdom, kindness and generosity towards my upbringing have turned the teacher's worst nightmare into a master scientist (almost)! My achievements over the years also stem from Miss. Webb, the best biology teacher and Mrs. Prophet, the ultimate life guru.

The past 2.5 years have been an eye-opening experience. I thank Dr. Luciani for the opportunity to play with the confocal microscope and work on mitochondrial biology. It has been a pleasure to have Drs. Jan Ehses, Francis Lynn and Robert Nabi as my committee members, who manage to keep my project on track. I also have to thank Dr. Paul Orban for his expertise in molecular cloning, which has enabled me to make my first ever adenovirus. My project wouldn't have come together without the help of many others including Mitsu Komba for islet isolation, Dr. Jingsong Wang for microscopy training, Lisa Xu for FACS and Rose Shumiatcher for genotyping my mice.

My life as a grad student would've been a lot harder without Sarah White's advice, from scruffing a mouse to drinking regularly. She helped me to settle in and introduced me to all the incredible people at CFRI and UBC. I also very much enjoy lab life with my partner in crime, Annika Sun. Her laughter and insanity at times (or rather all the time) had brought life to mundane experiments. Our silly songs, disco ball and secret stash of snacks had definitely made 12 hours straight of calcium imaging possible. Last but not least, I would like to thank Thilo Speckmann for making this a worthwhile experience. Thilo is always there to listen to my practice talks and other gibberish even when he's half asleep, bring me my favourite salad rolls when I'm hungry, cheer me up when I'm sad and amuse me whenever possible!

Thanks everyone!

Chapter 1: Introduction

1.1 Diabetes

1.1.1 Overview of diabetes

Diabetes is a rapidly growing disease affecting over 382 million individuals in 2013 (1). According to the World Health Organization, diabetes is predicted to be the 7th most deadly disease by 2030 due to hyperglycemia-associated complications such as cardiovascular diseases, kidney failure and neuropathy (2). Diabetes is a disease of chronic hyperglycemia that is caused by a complex interplay between genetic and environmental factors (3). Based on the etiology of dysregulated hyperglycemic control, diabetes can be classified into type 1, type 2 and other rare forms of the disease.

Type 1 diabetes (T1D) is an autoimmune disease, where the patient's immune system is activated to elicit a proinflammatory attack on its own insulin-producing β-cells, resulting in β-cell death and insulin insufficiency (4). The exact trigger for such an immune attack remains largely unknown. Some of the proposed environmental triggers include viral infection and compositions of the gut microbiome (4). There is also a genetic component associated to T1D. For instance, polymorphisms of the Human Leukocyte Antigen (HLA) region, which regulates the immune system and distinguish the body's proteins from those of foreign pathogens, strongly increases the risk of developing T1D (5). Although T1D can develop at all ages, it is most commonly identified in children. Hence it is often referred to as juvenile diabetes. The discovery and isolation of insulin in 1922 by Drs. Frederick Banting, Charles Best and their colleagues has turned diabetes into a manageable disease (6). However, the use of insulin is not a cure and insulin therapy remains sub-optimal with the associated risks of complications. Islet transplantation and other cell-based therapies have a promising future in diabetes treatment (7). To achieve that, extensive research is invested to elucidate the pathophysiology of diabetes.

Type 2 diabetes (T2D) contributes to approximately 90% of all diabetes diagnosis (8). T2D develops over many years with a period known as prediabetes, where insulin resistance progressively develops in peripheral tissues (9). The β-cells are able to compensate for insulin

resistance and maintain glucose homeostasis by increasing cell mass and insulin secretion. Obesity is a major factor for T2D, where high levels of circulating free fatty acids (FFAs) contribute to the onset of insulin resistance (10). Enlarged adipose tissues in obese patients produce and release higher amount of circulating FFAs, which suppress insulin stimulated glucose uptake through glucose transporter 4 and gluconeogenesis in the skeletal muscles (11). Unfortunately the capacity of β-cells to compensate ceases with time and results in full-blown diabetes in some individuals (12). T2D is a highly complex polygenic disease that is associated with diverse genetic variants. People with first-degree relationships with T2D patients are 2 to 4 fold more likely to develop T2D (13). Genetic studies such as candidate gene approach and genome-wide association studies have identified at least 50 genes, which are involved in insulin resistance and β-cells dysfunction in T2D, and many other genes associated to T2D but with currently unknown functions (14,15).

1.1.2 Regulation of blood glucose homeostasis

Blood glucose homeostasis is primarily regulated by two hormones released from the pancreas, they are insulin and glucagon (16), where insulin stimulates glucose uptake in peripheral tissues and glucagon stimulates glycogenolysis and gluconeogenesis in the liver to release glucose. However, glucose regulation involves many other hormones that are released from other parts of the endocrine system, for example the gut releases the glucose-lowering incretin hormones.

Glucagon and insulin are produced by α- and β- cells respectively in the islet of Langerhans in the pancreas. An islet is an amalgam of five endocrine cell types to date; α, β, δ, PP and ε-cells (Table 1). These endocrine cells work in concert to fine tune normoglycaemia in a healthy range of fasting 4.0 – 6.0 mM and 2- hour post meal 5.0 – 7.0 mM (17). Chronic hyperglycemia can lead to destruction of blood vessels and multiple organs contributing to the complications associated to diabetes (18). This thesis specifically focuses on the effects of prolonged exposure to high glucose and fatty acids on islet β-cell physiology.

Cell type	***Proportion of a human/ rodent islet*** (19)	***Hormones***	***Main function***	***Stimulated by***
α	~ 40/20 %	Glucagon	Stimulates gluconeogenesis in the liver	hypoglycemia
β	~ 50/70 %	Insulin	Stimulates glucose uptake and conversion into glycogen in muscle and triglyceride in adipose tissue.	hyperglycemia
		Amylin	Inhibits postprandial glucagon secretion, gastric emptying and food intake	
δ	~ 10/10 %	Somatostatin	Inhibits glucagon and insulin secretion, fine tune insulin secretion by cholinergic signaling (20,21)	hyperglycemia
PP	< 1/1 %	Pancreatic polypeptide	Stimulates glucagon secretion	hypoglycemia
ε	< 1/ 1%	Ghrelin	Inhibits insulin secretion	hypoglycemia

Table 1. Properties of islet endocrine cell types

1.1.3 Current criteria for T2D diagnosis and T2D treatments

According to the Canadian Diabetes Association (CDA), multiple clinical criteria are set up to facilitate accurate diagnosis of diabetes (3). These are 1) Fasting plasma glucose $\geq$ 7.0 mM, where fasting is defined as a lack of calorie intake for at least 8 hours; 2) Random plasma glucose or 2-hour post oral glucose (75 g) tolerance test $\geq$ 11.1 mM; and 3) glycated hemoglobin (A1C) value > 6.5%, where A1C reflects long term (past 2 – 3 months) glycemic control.

Research on the molecular basis of glucose homeostasis over past decades has led to the development of various glucose-lowering drugs to manage T2D, with the aim to reduce the risk of microvascular complications by achieving A1C value < 7.0% (22). Glucose-lowering drugs can be broadly classified into two categories; drugs that act directly on the insulin producing β-cells and drugs that act on non-β-cells. An example of drugs that stimulate insulin secretion in β-cells is sulfonylurea, which binds to a subunit of the K_{ATP} channel known as the SUR1 receptor. Such binding closes the K_{ATP} channel, depolarizes the β-cell membrane and activates the downstream signaling pathway for insulin secretion (22). However these drugs increase the risk of hypoglycemic episodes as insulin secretion can also be stimulated independent of blood glucose levels (23). Other side effects include weight gain, which is not desirable particularly among obese diabetic patients and teenagers. Another group of modern glucose-lowering drugs that stimulate insulin secretion is based on the discovery of the incretin (intestinal secretion insulin) effect. Incretin hormones include glucagon-like peptide 1 (GLP-1) and gastric inhibitory peptide (GIP), which are released upon glucose uptake in the small intestine (24–26). GLP-1 and GIP therefore stimulate insulin secretion in a glucose dependent manner, which reduces the risk of hypoglycemic episodes. However the incretin hormones have a short half-life of approximately 1 to 2 minutes due to rapid degradation by an enzyme called dipeptityl peptidase-4 (DPP-4) (22). Synthetic mimetic of GLP-1 with DPP-4 resistance property such as exenatide and DPP-4 inhibitors such as sitagliptin are designed to prolong drugs action on insulin secretion (22). Despite reduced risk of the dangerous hypoglycemia, there are increasing concerns of pancreatitis, pancreatic cancer and thyroid cancer with the long-term effects of incretin-based treatments (27).

Apart from medications, exercise and nutrition therapy are also effective treatments for T2D, especially for patients with obesity (BMI > 25 kg/m^2) (28). CDA recommends approximately 2.5 hour per week of aerobic activity in combination with resistance training as a prescription to T2D patients. In terms of diet, CDA proposed that the acceptable range of sugar intake is approximately 50 to 65 g per day and fat consumption between 20 – 35 % of daily energy intake. Positive changes in lifestyle such as exercise and nutrient control have been demonstrated to effectively improve long term glycemic control as indicated by reduce A1C values (17).

1.2 The pancreatic β-cell: Function and dysfunction in T2D

1.2.1 Mechanisms of β-cell function – From insulin biosynthesis to secretion

Pancreatic β-cells are highly responsive to blood glucose concentrations. Multiple machineries are in place to activate efficient insulin biosynthesis and secretion to maintain glucose homeostasis. Insulin biosynthesis starts with the production of preproinsulin, which is regulated by glucose both at the transcriptional and translational levels (29,30). Signal peptide of a newly synthesized preproinsulin is guided for translocation to the endoplasmic recticulum (ER), where the signal peptide is then cleaved to release proinsulin (31). Inside the ER, proinsulin is folded into its native structure, ready to be transported to the golgi apparatus, where it is then cleaved by prohormone convertases and carboxypeptidase into mature insulin and C-peptide for packaging into secretory vesicles. Upon nutrient stimulation, mature insulin is immediately available for exocytosis into the blood-stream.

Transcriptional and translational control of insulin biosynthesis:

Glucose-regulated transcription of the *insulin* gene (*Ins*) is mediated by various transcription factors binding to the conserved sequence motifs at the promoter region, which is approximately 340 bp to 90 bp upstream of the insulin transcription start site (29,32). Key transcription factors of insulin include pancreatic/duodenal homeobox1 (Pdx-1), musculoaponeurotic fibrosarcoma oncogene homolog A (MafA), and neurogenic differentiation 1(NeuroD1).

Pdx-1 belongs to the homeobox family and is one of the most studied regulators of insulin transcription. Glucose stimulates the phosphorylation and sumolylation of Pdx-1, which is then translocated to the nucleus (33,34). Binding of Pdx-1 to the insulin regulatory element also stimulates recruitment of transcriptional co-activators such as p300, which couples RNA polymerase activity to transcription factors (35). The importance of Pdx-1 in glucose homeostasis is reflected in a hereditary form of type 2 diabetes, where mutation of Pdx-1 is associated to the development of maturity onset diabetes of the young type 4 (MODY4) due to impaired insulin secretion (36). Another important transcription factor of insulin is MafA, which has a basic leucine zipper domain (37). Similar to Pdx-1, MafA expression in adult pancreas is predominately restricted in β-cells (38) and its expression and binding activity to the insulin

regulatory elements are regulated by glucose (39). The role of MafA in β-cell function is also highlighted in MafA knockout mice, which develop glucose intolerance and diabetes due to impaired glucose-stimulated insulin secretion (40). Moreover, β-cells of diabetic mouse models and T2D patients are often found to have significantly reduced levels of MafA and Pdx1 (41). More recently, it was demonstrated that overexpression of MafA in diabetic mouse model of T2D is able to restore β-cell function and glycemic control (42). Other transcription factors of the insulin gene include NeuroD or BETA2, which has a basic helix-loop-helix domain that binds to the insulin promoter and facilitates its transcription (43). Its translocation to the nucleus is also regulated by glucose via glycosylation (44). Lastly, mutations of NeuroD1 result in an extremely rare form of type 2 diabetes, MODY 6 (45).

Co-operative interactions between Pdx-1, MafA, NeuroD1 and other transcription factors are important to activate insulin gene transcription, which is likely to be mediated by stabilizing transcription factors via p300 (46,47). Acute physiological glucose levels regulate recruitment and subcellular localization of transcription factors to their respective regulatory elements to initiate insulin gene transcription. Apart from acute physiological stimuli, prolonged exposure to glucose and oxidative stress repress expression and binding activities of transcription factors for insulin leading to β-cell failure (48–50), which gives rise to a condition known as glucotoxicity (Chapter 1.2.2).

It has been proposed that mRNA translation in the ribosome is responsible for meeting the immediate demand in insulin biosynthesis. While transcription is largely involved in maintaining long-term supply of insulin (29). The evidence comes from a study, which shows that high glucose stimulation of islets for 1 hour increases proinsulin protein level by 10 fold compared to non-stimulatory condition, while preproinsulin mRNA level is largely unchanged, suggesting a predominant role of translation in proinsulin synthesis to meet immediate demand (51). Interestingly, glucose also maintains the stability of preproinsulin mRNA to enhance rate of translation (52).

The eukaryotic initiation factor 2 alpha (eIF2α) is a critical component necessary to initiate the very first stage of mRNA translation by bringing transfer RNA (tRNA) to the ribosomes (53). The activity of eIF2α is regulated by its phosphorylation status. For example, acute glucose

stimulation dephosphorylates eIF2α, which assembles tRNA to the ribosomes and initiate translation of insulin and other mRNA in the β-cell (54). However, chronic hyperglycemia (gluocotoxicity) and conditions of glucolipotoxicity activate phosphorylation of eIF2α by PERK, which then inhibits translation and insulin synthesis as an ER stress response (55,56).

Regulation of insulin secretion:

Glucose is the main physiological fuel stimulus for insulin secretion. Other stimuli include free fatty acids (FFAs) and amino acids (57). When glucose is transported into the β-cells by glucose transporter (Glut2 in rodent, Glut1 in human), it is quickly phosphorylated by glucokinase and broken down into pyruvate during glycolysis in the cytosol (58). Decarboxylation of pyruvate produces acetyl-CoA, which then enters the mitochondrial tricarboxylic acid (TCA) cycle and fuel the electron transport chain to produce metabolic coupling signals and ATP, which then signal downstream events for insulin secretion (58). Mechanistic details of mitochondrial regulation of glucose-stimulated insulin secretion will be discussed further in Chapter 1.3.1.

Presence of FFAs such as palmitic acid regulates basal insulin secretion and amplifies glucose-stimulated insulin secretion (59,60). Unlike glucose, FFA enters the β-cells freely by diffusion across the plasma membrane as well as by facilitated uptake via fatty acid transporters (61). At basal or fasting condition, FFAs in β-cells are metabolized into long-chain acyl-CoA (LC-CoA) and diacylglycerol (DAG). LC-CoA is then transported into the mitochondria by carnitine palmitoyl transferase-1 (CPT-1), where it is metabolized to acetyl-CoA via β-oxidation. Acetyl-CoA then enters the TCA cycle and downstream events for ATP production. A rise in ATP to ADP ratio closes the K_{ATP} channel, depolarizes β-cells membrane, and activates the opening of voltage-gated Ca^{2+} channel allowing influx of extracellular Ca^{2+}. This increases the level of intracellular Ca^{2+}, which signals insulin secretion. FFAs therefore maintain basal insulin secretion in a K_{ATP} channel-dependent pathway. However after a meal, a rise in glycolysis promotes the production of pyruvate and its conversion to acetyl-CoA, which can then be carboxylated into malonyl-CoA. Malonyl-CoA inhibits the activity of CPT-1 and therefore suppresses the entry of LC-CoA into the mitochondria. This inhibits β-oxidation of fatty acids, which promotes lipolysis and lipogenesis in the cytosol. These two pathways of lipid metabolism increase signaling molecules such as triglyceride and monoacylglycerol (MAG), which activate

the priming of insulin granules containing vesicles to the plasma membrane for exocytosis and therefore amplify glucose-stimulated insulin secretion in a K_{ATP} channel-independent pathway (62,63).

In summary, glucose and FFAs are important regulators of both insulin production and secretion. Acute glucose stimulation has positive effect on insulin secretion. On the contrary, chronic elevation of glucose and fatty acids promotes β-cell functional impairment, which will be discussed next in Chapter 1.2.2.

1.2.2 Mechanisms of β-cell failure in T2D – Glucotoxicity and glucolipotoxicity

Although fasting glucose can be maintained within a normal range during prediabetes, postprandial glucose level often exceeds the normal range due to incomplete β-cell compensation for insulin resistance (12,64). Such intermittent exposure to high glucose has been shown to contribute to β-cell dysfunction, as demonstrated *in vitro* (65). In addition, T2D is also highly associated with obesity. People with BMI of over 30 have an increased chance of developing T2D by 80 times. Since elevated circulating FFAs or dyslipidemia promotes insulin resistance as well as β-cell failure (9). Extensive studies have shown that hyperglycemia and dyslipidemia activate β-cell death (27,66), which have contributed to the concepts of glucotoxicity, lipotoxicity and glucolipotoxicity (67–69).

Glucotoxicity:

Glucotoxicity is a condition where chronic exposure to hyperglycemia results in an irreversible deleterious effect on β-cell function and survival, such as reduced expression and secretion of insulin and increased cell death. Continuous overstimulation of β-cells with high glucose eventually results in a state of β-cell exhaustion, where insulin stores are depleted (70). Multiple interconnected mechanisms of glucotoxicity-induced β-cell exhaustion have been proposed. These include oxidative stress, ER stress, protein glycation and formation of advanced glycation end (AGE) products, islet inflammation, islet amyloid deposition and changes in gene expression (69).

Oxidative stress is a condition where accumulation of reactive oxygen species (ROS) damage cellular lipids, protein and DNA (69). One of the main sources of cellular ROS is the mitochondria, as superoxide is produced as a by-product of ATP synthesis during oxidative phosphorylation. High glucose has been shown to increase ROS formation and expression of oxidative stress markers in both mouse and human islets (71). In addition, antioxidant supplementation and overexpression of antioxidant genes have been demonstrated to protect oxidative stress-induced impairment in insulin gene expression and secretion (71). Oxidative stress can also activate apoptosis through regulation of the Bcl-2 family proteins, which will be discussed more in Chapters 1.3 and 1.4.

ER stress is a condition where there is an increased demand for protein synthesis. As a stress response, it triggers the unfolded protein response (UPR) to downregulate protein synthesis, folding and overall workload. However, under prolong or severe ER stress UPR may fail to maintain ER homeostasis and therefore activate apoptosis (72). During insulin resistance, islet β-cell exerts a high demand for insulin biosynthesis (73). Initially there is an upregulation of UPR genes, which reduces insulin expression and relieves overall β-cell ER stress (74). However, under glucotoxicity, UPR is not sufficient to maintain ER homeostasis and therefore may activate β-cell apoptosis. Increasing evidence has also suggested a close relationships between ER stress and oxidative stress (75).

Protein glycations and AGE products are formed by spontaneous reaction between reducing sugars such as glucose and ribose with amine residues on protein, lipid or DNA (69). AGE products bind to their receptor and can activate signaling pathways resulting in cell death. In mouse islets, hyperglycemia promotes protein glycation and AGE product (76). Inhibitors of AGE can prevent hyperglycemia-induced impairment in insulin gene expression and glucose-stimulated insulin secretion (77,78). Another likely mechanism of AGE induced β-cell failure is oxidative stress. Studies have shown that AGE products promotes ROS production in β-cells and functional impairments, which are prevented by antioxidants (79,80).

Islet inflammation is characterized by increase plasma inflammatory markers such as IL-1β and IL6, which can be found in very early stage of T2D such as prediabetes. Islets from T2D have been shown to be infiltrated with macrophages and have increased IL-1β levels, which also

upregulates Fas-mediated cell death via extrinsic apoptosis (81,82). *In vitro* experiments have shown that high glucose culture of non-diabetic human islets results in increase IL-1 production, which upregulates Fas expression and associated β-cell dysfunction and cell death (83).

Islet amyloid polypeptide (IAPP) is another hormone, which is secreted together with insulin by the β-cells. Aggregation of IAPP into IAPP amyloids is often observed in islets of T2D patients. A buildup of IAPP amyloids is associated with the activation of ER stress and islet inflammation, which promote β-cell death (69,84,85).

Changes in gene expression of β-cells are observed in glucotoxicity. As mentioned, insulin secretion is regulated by glucose at the transcriptional level. Acute glucose stimulation activates transcription factors for insulin transcription. However, chronic hyperglycemia or glucotoxicity significantly impair insulin gene expression and the expression of other β-cell-enriched genes such as glucose transporter 2 (Glut2), glucose kinase (Gck), voltage-dependent Ca^{2+} channels, apoptotic regulators are also targets of glucotoxicity (69,86).

Lipotoxicity and glucolipotoxicity:

Lipotoxicity is a condition where high levels of lipids or hyperlipidemia deteriorate β-cell function and survival (68). High levels of circulating FFAs are characteristic of obese patients due to increased adipose tissues mass and reduced FFA clearance (87). In addition to insulin resistance, high levels of FFAs also contribute to β-cell death through ER stress (88), increased formation of ceramide (89) and ROS (90). In particular, saturated FFAs such as palmitate are more potent in promoting cell death compared to poly-unsaturated FFAs such as linoleate, while mono-unsaturated FFA such as oleate are non-cytotoxic (91).

Glucolipotoxicity is a synergistic, toxic condition of combined hyperglycemia and elevated FFAs. Studies have shown that toxic effects of lipotoxicity are dependent on hyperglycemia (92). This synergistic effect of glucolipotoxicity is partly due to inhibition of fatty acid oxidation in the mitochondria by the TCA cycle (91). Glucolipotoxicity impairs glucose-stimulated insulin secretion (93), insulin gene expression (94–96) and islet viability (97,98). The mechanisms by which glucolipotoxicity contributes to T2D are likely to involve the changes in gene expression

and β-cell death due to accumulation of cholesterol, ceramide and ROS, impaired mitochondrial activities, activation of ER stress and islet inflammation (91,99,100).

In summary, prolonged exposure to high levels of glucose and free fatty acids impair β-cell function and survival through diverse, complex and interrelated mechanisms that range from gene expression to metabolic stress and inflammation. Although there is a large amount of evidence and pathways of β-cells failure and cell death under gluco(lipo)toxicitiy, their functional contribution to the pathogenesis of T2D remain to be further clarified in order to demonstrate a cause and consequence relationship.

1.3 Roles of mitochondria in β-cell function and failure

1.3.1 Mitochondrial metabolic coupling to insulin secretion

Mitochondria of the β-cells translate nutrient input to insulin secretion by providing ATP and additional metabolic coupling factors (MCFs), which contribute to the triggering and amplifying pathways of glucose-stimulated insulin secretion, respectively (58).

Prior to mitochondrial metabolism, glucose is converted into pyruvate by glycolysis in the cytosol. Pyruvate then enters the mitochondria to be converted into acetyl-CoA by pyruvate dehydrogenase. The TCA cycle is fueled by condensation of the acetyl-CoA and oxaloacetate to generate large amounts of reducing equivalents such as NADH and $FADH_2$ and small amounts of ATP (58). Electrons in NADH and $FADH_2$ are then shuttled through the electron transport chain along the mitochondrial inner membrane. The electron transport chain is comprised of five respiratory complexes, which serve to establish an electrochemical gradient to drive ATP synthesis (101,102). Firstly, electrons are transferred from NADH to coenzyme Q (CoQ) via complex I (NADH dehydrogenase), which also transfers protons across to the mitochondrial membrane space. Electrons from $FADH_2$ are transferred to complex II (succinate dehydrogenase), which relays electrons also to coenzyme Q, which in turn reduces cytochrome c via complex III (CoQ-cytochrome c reductase), which also pumps protons across the inner mitochondrial membrane into the intermembrane space. Next electrons are transferred to Complex IV (cytochrome oxidase), which reduces oxygen into water and also contribute to proton transfer to the intermembrane space. The accumulated protons in the mitochondrial intermembrane space result in a highly hyperpolarized mitochondrion, which promotes the re-entry of protons into the matrix though Complex V (ATP synthase) for ATP synthesis. The rise in ATP to ADP ratio then initiates downstream signaling events for insulin secretion primarily via the triggering pathway (58). While ATP and other metabolites produced from the TCA cycle are involved in the amplifying pathway of glucose-stimulated insulin secretion (103).

The triggering pathway of insulin secretion is also referred to as the K_{ATP} channel-dependent pathway. This is because closure of ATP-sensitive K^+ (K_{ATP}) channels in the plasma membrane upon increase ATP to ADP ratio leads to β-cell membrane depolarization and the opening of

voltage-gated Ca^{2+} channels. The increase in intracellular Ca^{2+} then mobilizes the machineries for the docking and fusion of secretory vesicles to the plasma membrane and exocytosis of insulin into the bloodstream (58).

The amplifying pathway also plays a significant role in insulin secretion. In this pathway, the K_{ATP} channel-dependent increase in intracellular Ca^{2+} is bypassed and therefore it is often referred as the K_{ATP} channel-independent pathway. Evidence of this comes from the observation that glucose can also stimulate insulin secretion in fully depolarized β-cells, which are saturated with intracellular Ca^{2+} (104). Metabolism of glucose, FFAs and amino acids generates MCFs, which function as amplifying signals in different stages of glucose stimulated insulin secretion, from Ca^{2+} influx to the final step in mediating exocytosis of insulin granules. Examples of MCFs and their role in mitochondria and glucose-stimulated insulin secretion are described in Table 2. Some of the main MCFs are malonyl-CoA, glutamate, NADH and also ROS. Despite the common misconception that mitochondrial ROS is always destructive, increasing evidence has shown that low levels of ROS are important signaling molecules for cellular physiological activities (105,106). Indeed mitochondria-derived ROS, particularly H_2O_2, are considered as MCFs for glucose-stimulated insulin secretion (107,108). However, compared to the mechanisms of the triggering pathway in glucose-stimulated insulin secretion, the molecular pathways of MCFs in the amplifying pathway remain less understood.

Studies have proposed that the triggering pathway is predominately responsible for the rapid, first phase of insulin secretion, while the amplifying pathway is responsible for the second phase of insulin secretion (104,109–111). However, other studies have proposed that the triggering pathway regulates the oscillatory patterns of Ca^{2+} and pulsatile insulin secretion, while the amplifying pathway contributes to the magnitude of insulin pulses in response to glucose. What is clear is that the mitochondria are central to nutrient metabolism and the control of normal β-cell function in order to maintain normal glucose homeostasis, and mitochondrial failure otherwise will contribute to the development of T2D (112).

Examples of MCFs	*Source in β-cells*	*Role in β-cell insulin secretion*
Malonyl-CoA	Carboxylation of Acetyl-CoA, derived from pyruvate in glycolysis. Inhibits fatty acid β-oxidation to promote fatty acyl-CoA accumulation in the cytosol.	Links glucose & lipid metabolism
Glutamate	Reductive amination of α-ketoglutarate from TCA cycle of glucose metabolism.	Links glucose, amino acids & FFA metabolism Promotes pyruvate cycling via carboxylation and decarboxylation and production of intermediates such as malonyl-CoA
GTP	Phosphorylation of GDP by ATP, TCA, amino acid metabolism	Links glucose, amino acids Promotes insulin exocytosis
NADPH	TCA	Exocytosis, Ca^{2+}
NADH/NAD+	Glucose TCA and ETC	Pyruvate shuttling, reducing equivalents
ATP	Glucose metabolism in ETC	Closure of K_{ATP} channel, stimulates Ca^{2+} influx
cAMP	Conversion of ATP by adenylate cyclase	Activates PKA and Epac2 and downstream insulin exocytotic proteins
ROS, H_2O_2	Glucose metabolism in complex I and III of ETC	Redox control, exocytosis

Table 2. Metabolic coupling factors in the amplifying pathway of glucose-stimulated insulin secretion. Adapted from Prentki 2013 (113). Abbreviations: adenosine triphosphate (ATP), cycle adenosine monophosphate (cAMP), electron transport chain (ETC), guanosine diphosphate (GDP), guanosine triphosphate (GTP), hydrogen peroixde (H_2O_2), nictonamide adenine dinucleotide phosphate (NADH), tricarboxylate acid cycle (TCA),

1.3.2 Mitochondrial dysfunction in β-cells

As mentioned, oxidative stress is one of the mechanisms of glucotoxicity in β-cell failure. A prime target of oxidative damage in β-cells is the mitochondrion due to its close proximity to superoxide production. Given the important role of mitochondrial metabolic coupling for insulin secretion, it is clear that perturbations in mitochondrial metabolism will impair β-cell function. Moreover, other cellular stresses during nutrient overload have been shown to alter the dynamics of mitochondrial morphology, which are all highly interconnected to maintain proper cell function, and this is likely to contribute to diabetes pathogenesis (112).

Mitochondrial ROS and oxidative stress in β-cells:

During oxidative phosphorylation in the electron transport chain, a small proportion of electrons are 'leaked' to partially reduce oxygen into superoxide at complex I and III (112). Mitochondrial production of superoxide can be enhanced by pharmacological inhibition of complex I and III using rotenone and antimycin, respectively (114). Rotenone promotes mitochondrial superoxide by blocking the binding site of coenzyme Q (CoQ) on complex I, which mediates electron transfer from NADH via flavin mononucleotide (FMN) to Co-Q. As a result, rotenone promotes an accumulation of fully reduced FMN and therefore the reduction of oxygen instead of Co-Q. Similarly, antimycin inhibits electron transfer from the reduced CoQ to cytochrome c in complex III and therefore enhances electron transfer to oxygen. The rate of superoxide production is largely determined by the concentrations of reducing equivalents and proportion of their fully reduced state, which in turn is governed by electron flux from nutrient metabolism and electron uptake for ATP synthesis (114). When the rate of ROS production exceeds the rate of ROS clearance, excessive ROS accumulation then results in oxidative stress (115).

The β-cells defense system against oxidative stress involves both antioxidant enzymes and antioxidant molecules (116). Antioxidant enzymes include mitochondrial superoxide dismutase (MnSOD), catalase and glutathione peroxidase (Gpx), while antioxidant molecules include glutathione and vitamins (117). MnSOD catalyzes the conversion of superoxide into hydrogen peroxide, which is a less reactive and membrane permeable ROS species. Hydrogen peroxides can then be converted into oxygen and water by catalase or Gpx. Studies have shown that β-cell-

specific overexpression of Gpx1 in obese diabetic db/db mice is able to improve blood glucose homeostasis through improving insulin secretion and β-cell mass (118). Despite the highly metabolic feature of β-cells, there are relatively low levels of antioxidants compared to other tissue type (119,120). One plausible explanation for such paradoxical adaptation is that ROS themselves are important signals for glucose-stimulated insulin secretion (107,108,117).

Apart from antioxidants, β-cells can modulate mitochondrial ROS formation locally by the mitochondrial uncoupling protein 2 (Ucp2), which shows protective effect against oxidative stress at the expense of reduced glucose-stimulated insulin secretion (121). Ucp2 dissipates proton motive force for ATP production by increasing proton leak and therefore reduces the ROS production associated with coupled mitochondrial respiration (122). Studies have shown that prolonged culture with glucose and FFAs upregulates the expression of Ucp2 in β-cells and that superoxide activates Ucp2 activity to reduce ATP production and overall glucose-stimulated insulin secretion (123,124). In agreement with this, islets from β-cell specific Ucp2 KO mice have increased glucose-stimulated mitochondrial activity and insulin secretion, which are associated with an increase in ROS production (125).

In the case of diabetes, chronic hyperglycemia and hyperlipidemia increase the flux of reducing equivalents including NADH and $FADH_2$ into the mitochondrial electron transport chain and also downregulate antioxidant systems, which collectively promote oxidative-stress induced β-cells dysfunction and cell death (126–128). The mechanisms in which oxidative stress impairs insulin secretion are likely to be mediated through activation of ucp2 activity (129); downregulation of insulin gene expression and its transcription factors including Pdx-1 and MafA (18,41,130), activation of ER stress (73) and intrinsic apoptosis (131).

Mitochondrial morphology and fusion-fission dynamics in β-cells:

Mitochondria are highly dynamic organelles, that take on various shapes and connectivity depending on their cellular environment (132). There is also increasing evidence for the relationship between mitochondrial morphology and metabolic activities in β-cell function and survival (71,133). Mitochondrial morphology is regulated by a series of membrane fusion and fission events. Mitochondrial fission is induced by a dynamin related protein 1 (Drp-1), which is

a cytosolic GTPase, and by a transmembrane protein called Fis-1. Mitochondrial fusion is mediated by another group of mitochondrial GTPases, which include optic atrophy protein 1 (OPA1) on the inner membrane, mitofusin 1 (Mfn1) and mitofusin 2 (Mfn 2) on the outer membrane (134).

The relationship between mitochondrial morphology and functions in β-cells are highlighted in healthy and diabetic animals. Mitochondria of healthy β-cells exist in long tubular and highly connected networks, whereas β-cell mitochondria from diabetic models and T2D patients are fragmented and swollen (129,135,136). Acute stimulation of INS1 cells with glucose promotes a transient shortening or fragmentation of the mitochondria, which correlates with a temporal increase in glucose-stimulated ATP production (137). Moreover, deletions of mitochondrial fusion or fission proteins have been shown to affect insulin secretion in β-cells. For instance, mitochondria from islets of β-cell specific OPA1 KO mice are short and highly fragmented, which are associated with impaired glucose-stimulated insulin secretion (138). The dynamics of mitochondrial morphology are also important to protect cell survival in response to cellular stress and apoptotic stimuli. A study has shown that inhibition of the fission protein Drp1 is able prevent the mitochondrial fragmentation and activation of apoptosis in islet β-cells under conditions of glucolipotoxicity (133).

An imbalance in mitochondrial fusion-fission dynamics may promote oxidative stress in β-cells under conditions of nutrient overload. However, the sequence of events and direct contribution to T2D remain to be deciphered. Interestingly, studies on other cell types have shown that Bcl-2 family members including Bcl-x_L also interact with mitochondrial fusion-fission proteins and contribute the regulation of mitochondrial morphology as part of, or in addition, to their apoptotic functions.

1.4 Bcl-x_L: Programmed cell death and beyond

1.4.1 Overview of apoptosis in T2D

Apoptotic cell death is one of the main contributors to the loss of β-cell mass in both type 1 and type 2 diabetes (139). Apoptosis is characterized by plasma membrane blebbing, chromatin condensation, nuclear fragmentation and engulfment of apoptotic bodies by phagocytes (140). Based on the molecular mechanisms of initiation and execution, apoptosis can be distinguished into the intrinsic and extrinsic pathways (141).

Intrinsic apoptosis is also referred to as the mitochondrial or the Bcl-2-regulated pathway because it involves changes at the mitochondria, which are under tight control by proteins of the Bcl-2 family (141). Intrinsic apoptosis is initiated by intracellular signals such as exposure to elevated glucose or FFAs, which can damage various organelles such as the nuclei, ER and mitochondria (139). Activation of pro-apoptotic members of the Bcl-2 family and the formation of pores in the mitochondrial outer membrane are crucial for the execution of intrinsic apoptosis. Increasing mitochondrial membrane permeability allows cytochrome c, which normally resides within the mitochondrial intermembrane space, to be released into the cytosol and bound to cytosolic protein apoptosis factor-1 (Apaf-1). Assembly of cytochrome c bound Apaf-1 units form a large structure called the apoptosome, which activates the initiator caspase-9 and this activates the effector caspase-3, followed by a series of caspase cascade events that eventually results in the fragmentation of DNA.

Extrinsic apoptosis, which is also called the death-receptor-mediated apoptosis pathway, is initiated by external death signals such as Fas ligand, tumor necrosis factor alpha (TNF-α) and TNF-related apoptosis inducing ligand (TRAIL) (142). Upon binding of these ligands to their respective receptors, adaptors proteins such as the FAS-associated death domain protein are recruited to form the death-inducing signal complex (DISC), which then activates initiator caspase-8 and -10. This is then followed by the activation of effector caspase-3 and -7. In some cell types, including the β-cells, there is cross-talk between the extrinsic and intrinsic apoptotic pathways. In these cells, activation of caspase-8 cleaves the proapoptotic Bcl-2 family member

called Bid, which initiates mitochondrial outer membrane permeabilization and the downstream intrinsic apoptosis (143).

Glucotoxicity and glucolipotoxicity are likely to contribute significantly to the induction of β-cell apoptosis in T2D (69,92). For instance, apoptosis is observed in mouse islets after 6 days culture in 33 mM glucose compared to 5.5 mM control, which is prevented by overexpression of antiapoptotic proteins of the Bcl-2 family (144). Similarly, high glucose culture of human islets results in apoptosis, which contributed to by upregulation of proapoptotic Bcl-2 family proteins and downregulation of antiapoptotic proteins including Bcl-x_L (66). Palmitate has also been shown to promote islet intrinsic apoptosis by altering expression levels of Bcl-2 family members (145). However, increasing evidence has demonstrated the contribution of extrinsic apoptosis to islet cell death under glucotoxicity. Chronic hyperglycemia increases production of the pro-inflammatory cytokine IL1β, which is processed and activated by the inflammasome, increases Fas production and downstream activation of extrinsic apoptosis (82,146). It is likely that β-cell death in T2D is contributed by a complex cross talk between intrinsic and extrinsic apoptosis, and possibly other modes of programmed cell death.

1.4.2 The Bcl-2 family proteins in apoptosis

The Bcl-2 family proteins regulate intrinsic apoptosis through control of the mitochondrial outer membrane integrity. The proteins in this family share one or more of the four common Bcl-2 homology domains (BH 1-4) and are categorized into inducers, executioners, and inhibitors of apoptosis (141). The apoptosis inducers are the Bcl-2 homology 3 (BH-3) only proteins Bid, Bim and Puma. The executioners include Bax and Bak, which following their activation by the inducers will oligomerize and directly promote the mitochondrial outer-membrane permeability for cytochrome c release. Lastly, anti-apoptotic members of the family contain all four BH domains and include Bcl-2, Bcl-x_L (Bcl2l1), Bcl-w (Bcl2l2) and Mcl-1.

The antiapoptotic Bcl-2 proteins can prevent cell death by multiple mechanisms. Biophysical studies (147) have proposed that they inhibit cell death either through direct binding with the

initiator BH-3 only proteins such as Bim (mode 1), by sequestration of the executioner proteins Bax and Bak (mode 2) or by inhibition of both executioner and initiator proteins (unified model). However, variants of Bcl-x_L that could not bind to Bax and Bak still preserve approximately 75% antiapoptotic activity (148), suggesting that they have additional mechanisms of preventing cell death. For instance Bcl-x_L has been shown to prevent cytochrome c release directly by regulating mitochondrial channel proteins that forms the permeability transition pore, such as the voltage-dependent anionic channel (VDAC) (149,150).

In pancreatic β-cells, Bcl-x_L has been shown to be protective against various stress stimuli such as thapsigargin induced ER stress, γ irradiation, Fas ligand and co-culture with IL-1β and IFNγ (151,152). However there is no direct evidence for the involvement of Bcl-x_L in maintaining β-cell survival under glucotoxicity and glucolipotoxicity. High glucose culture (16.7 mM) of human islet for 5 days significantly reduced Bcl-x_L mRNA (45%) and protein (60%) levels while Bcl-2 expression remains stable (66). However, Bcl-2 mRNA expression in islets of Zucker Diabetic fatty rat and human islets is significantly reduced by fatty acids (153,154). Therefore Bcl-x_L and Bcl-2 are likely to have both overlapping and distinct functions in β-cells survival.

1.4.3 Roles of Bcl-x_L in mitochondrial bioenergetics and cell physiology

In addition to apoptosis, increasing evidence has identified novel non-apoptotic functions of Bcl-x_L in cellular physiology and mitochondrial metabolism in β-cells and other cell types (155).

To date only two published studies have demonstrated the roles of Bcl-x_L in pancreatic β-cells. Islets from transgenic mice that overexpress Bcl-x_L specifically in their β-cells are protected from ER-stress induced cell death (151). However, islets from transgenic mice with more than 10-fold increase in Bcl-x_L are compromised in terms of glucose utilization, intracellular Ca^{2+} signaling and insulin secretion in response to glucose. In agreement with this, a recent study by Luciani *et al.* has found that dispersed islet-cells from β-cell-specific Bcl-x knockout (Bcl-x βKO) mice have increase Ca^{2+}responses to glucose and Bcl-x βKO islets show increase glucose-induced NAD(P)H responses, indicating increased mitochondrial metabolism relative to the β-

cells and islets from WT littermate mice (156). This demonstrated that endogenous Bcl-x_L has roles in β-cell physiology via actions on mitochondrial metabolism, and suggest that the loss of β-cell function in Bcl-x_L over-expressing animals was not a transgene-specific effect.

Despite limited studies on the non-apoptotic roles of Bcl-x_L in β-cells, significant data from other cell types, particularly neurons, have provided more mechanistic insights. As discussed in the following, Bcl-x_L has been implicated in the regulation of mitochondrial bioenergetics, intracellular Ca^{2+} homeostasis, ROS and mitochondrial morphology.

1.4.3.1 Bcl-x_L and mitochondrial bioenergetics

Mitochondrial metabolic activity depends on both the inner and outer mitochondrial membranes. Disruptions in either component, such as a loss of mitochondrial inner membrane potential ($\Delta\psi_m$) or uncontrolled opening of the outer membrane permeability result in apoptosis (150,157). The voltage dependent anionic channel (VDAC) is a mitochondrial protein located in the outer membrane. VDAC controls metabolite transport, such as ATP, phosphate and Ca^{2+} ions, and the mitochondrial outer membrane permeability, and contributes to both energy production and cell death (158). VDAC exists in open or closed conformations, which depend on membrane conductance. An open VDAC increases permeability to anions and release of ATP from the mitochondria into the cytosol, while a closed VDAC promotes uptake of cations, such as Ca^{2+}, into the mitochondria. Mitochondrial Ca^{2+} is important for ATP production but chronic high levels of Ca^{2+} promote opening of the mitochondrial transition pore and release of cytochrome c, resulting in apoptosis. Bcl-x_L is shown to physically interact with VDAC (159–161). A study has shown that following induction of apoptotic stimuli, the mitochondrial outer membrane is transiently impermeable to metabolites, which contributes to subsequent loss of mitochondrial membrane integrity, release of cytochrome c and activation of apoptosis. Bcl-x_L has been shown to prevent apoptosis by opening VDAC and maintaining mitochondrial metabolic transfer (159). On the contrary, another group has demonstrated the anti-apoptotic activity of Bcl-x_L is mediated by closing VDAC (160,162), to prevent release of cytochrome c.

Apart from the mitochondrial outer membrane, Bcl-x_L also has interacts with the inner membrane and regulates $\Delta\psi_m$, which is a comprehensive parameter of the energetic state of a cell

(132,163). In neurons, Bcl-x_L is also found to localize to the mitochondrial inner membrane (164), where it enhances ATP synthesis through direct interaction with the β subunit of mitochondrial ATP synthase, which helps maintain $\Delta\psi_m$ and ion flux across the mitochondrial inner membrane (165,166). In the pancreatic β-cells, the importance and mechanisms of Bcl-x_L-mediated regulation of mitochondrial bioenergetics remain to be determined.

1.4.3.2 Bcl-x_L and the control of calcium homeostasis and signaling

While calcium ion (Ca^{2+}) is an integral signaling molecule for cell functions, excessive intracellular Ca^{2+}promotes apoptosis (167). The diverse function of this signaling molecule is likely to be dose dependent. Intracellular concentration of Ca^{2+} is regulated by extracellular and intracellular Ca^{2+} stores, including various organelles such as the mitochondria and ER. These Ca^{2+} active organelles are also home to the Bcl-2 family proteins, and studies have demonstrated actions of Bcl-2 proteins in Ca^{2+} homeostasis (168,169).

As mentioned earlier, Bcl-x_L interacts with the mitochondrial protein VDAC, which promotes mitochondrial Ca^{2+} uptake in its closed conformation. More recently, Bcl-x_L was shown to promote mitochondrial Ca^{2+} uptake via VDAC under basal conditions (170). In addition, single cell biochemical studies have identified binding interactions between Bcl-x_L and the ER inositol triphosphate receptor InsP3R, which facilitates Ca^{2+} transfer from the ER to mitochondria (171). Increase in mitochondrial Ca^{2+} thereby further perturbs mitochondrial membrane permeability. It has been suggested that the antiapoptotic activity of Bcl-x_L is mediated partly by increasing InsP3R sensitivity and promoting its open confirmation to prevent Ca^{2+} overloading in the ER (172).

These studies provide evidence for roles of Bcl-x_L in both physiological and apoptotic conditions through regulation of intracellular Ca^{2+} homeostasis and signaling, but it is not clear if similar mechanisms are important in β-cells.

1.4.3.3 Bcl-x_L and regulation of reactive oxygen species production

The mitochondrion is home to both Bcl-2 family proteins and superoxide production. Bcl-2 family proteins have been indicated to regulate cellular ROS levels (173). Multiple mechanisms have been proposed by which anti-apoptotic Bcl-2 proteins suppress mitochondrial ROS levels, they include increasing mitochondrial level of glutathione (174); maintaining mitochondrial membrane potential (157,166); reducing activity of the mitochondrial electron transport chain (175); and through interaction with ROS modulators such as ROMO1 (176,177). Apart from regulatory roles of Bcl-2 proteins on ROS, the expression of Bcl-2 family proteins is in turn regulated by ROS levels (178,179). In the β-cells, exposure to pro-inflammatory cytokines increases the ratio of proapoptotic to antiapoptotic proteins (Bax:Bcl-2), favoring apoptosis. Overexpression of mitochondria- localized catalase is able to reverse this ratio and prevent apoptosis (180).

Since Bcl-x_L has been implicated in the control of mitochondrial activity and insulin secretion in pancreatic β-cells, it is possible that Bcl-x_L also regulates cellular redox balance under basal and metabolically stressful conditions.

1.4.3.4 Bcl-x_L and mitochondrial morphology

As mentioned in Chapter 1.3.3, mitochondria maintain their functions and adapt to stress through actions of fusion and fission proteins, which dynamically regulate their morphology and connectivity (134). Bcl-2 family members are also involved in control of mitochondrial morphology through direct interaction with these fusion-fission proteins, or indirectly through regulation of overall mitochondrial bioenergetics (181). In HeLa cell lines, Bcl-x_L was found to interact with the fusion protein mitofusin 2 and promotes formation of highly fused mitochondria in a dose-dependent manner (182). Overexpression of Bcl-x_L in other cell lines alters mitochondrial morphology towards a more expanded matrix and reduces cristae spaces via its C-terminal transmembrane domain (183). In addition to fusion, Bcl-x_L also interacts with the fission protein Drp-1 to promote formation of synapses in healthy neurons (184,185). The apparent conflicting interactions of Bcl-x_L with both mitochondrial fusion and fission proteins fusion-fissions are highlighted in another study on neurons, which shows Bcl-x_L increases

activities of both fusion and fission, while overall change in mitochondrial morphology is largely mediated via stimulatory effects of Bcl-x_L on mitochondrial biomass (186). Conceivably, the effects of mitochondrial morphology mediated on β-cells function and survival may involve interactions between the fusion-fission proteins and Bcl-2 family members such as Bcl-x_L (187).

To summarize, although Bcl-x_L is known primarily as an anti-apoptotic protein, emerging studies in islets, neurons and other cell types have demonstrated additional physiological roles in cells that are not necessarily under apoptotic stimuli. However, the molecular mechanisms by which Bcl-x_L carries out such dual activities remain unclear, and the degree to which these non-canonical functions of endogenous Bcl-x_L are involved in the function and failure of β-cells is largely unknown.

1.5 The conditional β-cell specific Bcl-x_L knockout mice

1.5.1 Cre-lox technology: Temporal and tissue specificity of gene deletion

The Cre-lox system was developed in the early 1990s for specific gene modification in order to study a specific gene of interest. Cre recombinase (**c**yclization **re**combination) is derived from the bacteriophage P1 and catalyzes the recombination of specific nucleotide sequences called loxP (locus of crossing over P1) sites (188). Each loxP site is a 34 base pair sequence consisting of two 13 base pair inverted repeats for Cre recognition and an 8 base pair spacer region to define its orientation. LoxP sites that are positioned in the same orientation on the same allele or 'floxed' allele will result in gene excision upon homologous recombination (189). Since optimal temperature of Cre activity is 37^{o}C, the Cre-lox system is a favourable system in mammalian transgenic models, such as mice (189). Breeding of a Cre expressing mouse with a 'floxed' mouse may therefore produce offspring that inherit both Cre and floxed transgene, i.e. knock out mice. In 1992, the first transgenic mice with tissue specific Cre-induced recombination using the Cre-lox system were generated (190).

Germline ablation of specific genes is very useful to study genetically inherited diseases. However very often such global deletions are embryonically lethal or result in impaired post-natal development (189). Therefore inducible and tissue specific forms of Cre were designed, such that recombinase is only functional in the presence of an inducing agent and only be expressed in the cell type specified by a relevant promoter. A commonly used inducible Cre is a fusion protein, where a mutated form of estrogen receptor (ER) ligand-binding domain is fused with Cre (Cre:ER) (189). In the absence of tamoxifen, the fusion protein Cre:ER is sequestered by heat shock protein-90 (HSP90) in the cytosol. Upon administration of tamoxifen, Cre:ER dissociates from HSP90 and is translocated to the nucleus to excise of the floxed gene. Tissue specific expression of Cre:ER can be achieved by placing a relevant promoter upstream of the Cre:ER transgene (189).

The advance of inducible Cre-lox system has revolutionized studies of specific genes of interest with great specificity and flexibility. However attention should be paid to the possibilities of spontaneously Cre-mediated gene deletion, especially with aging mice (191).

1.5.2 Inducible β-cell specific Bcl-x knock out mice

The study presented in this thesis focuses on the role of Bcl-x_L in adult pancreatic β-cell physiology. Bcl-x_L is a one of several isoforms encoded by the *Bcl-x* (also known as *Bcl2l1*) gene, other isoforms include Bcl-xs, Bcl-xβ, Bcl-xγ (152). Depending on the position of the 5' splice site in exon 2, splicing at distal 5' splice site produces pro-apoptotic Bcl-x_S with 3 exons while splicing at proximal 5' splice site produces anti-apoptotic Bcl-x_L with 4 exons (192). Bcl-x_S is highly expressed in cells with rapid turnover while Bcl-x_L is the predominant isoform in stable adult cell types such as neurons and islets (192).

Since Bcl-x_L is essential for the development of all tissue and germline deletion of *Bcl-x* is embryonically lethal in mice at E14.5 (193), an inducible β-cell specific knockout model is necessary to study the role of Bcl-x_L in adult islets. In order to restrict Cre:ER expression in islet β-cells, the promoter of the transcription factor Pdx-1 is used. Pdx-1 is important in pancreas development and β-cells maturation (194). It is first expressed in the foregut, which develops into the ventral and dorsal pancreas. As pancreatic endocrine cells differentiate into specific lineage, high level of Pdx-1 expression is restricted to insulin positive β-cells, while other endocrine cell types maintain low levels of Pdx-1 (195–197).

The BclxβWT and BclxβKO mice used in this study were previously established by Luciani and colleagues (156). Briefly Pdx-1:Cre-ER transgenic mice (provided by Doug Melton, Harvard) were bred with Bclx floxed mice (provided by You-Wen He, Duke), where exon 1 and 2 of *Bcl-x* gene are flanked by the loxP sites thereby deleting all Bcl-x isoforms (198). Offspring that have inherited both cre and floxed Bcl-x transgenes will be Bcl-x_L deficient in their β-cells upon tamoxifen injection.

Pdx-1 controlled Cre expression has previously been observed in the brain in addition to the pancreas of Pdx-1:Cre transgenic mice (199), which has raised concerns about the specificity of Pdx-1 in directing cell-type specific recombination. However, Luciani *et al* (156) confirmed that Bcl-x_L is significantly reduced at both mRNA and protein level in isolated islets, with no changes in islet Bcl-2 levels and no evidence for reduced Bcl-x_L mRNA in the hypothalamus of tamoxifen injected BclxβKO mice.

1.6 Thesis proposal

1.6.1 Rationale

Bcl-x_L is known to protect β-cells against apoptosis induced by various types of cellular stresses. Increasing evidence has indicated functions of Bcl-x_L in regulating several aspects of mitochondrial physiology but such non-apoptotic roles of Bcl-x_L remain largely unexplored in the pancreatic β-cells. Mitochondria are essential for normal glucose-stimulated insulin secretion, and mitochondrial damage and failure are significant aspects of β-cell dysfunction and death in type 2 diabetes. A thorough understanding of Bcl-x_L actions in β-cells during healthy and stressful conditions may therefore be important for our understanding of the pathophysiology of type 2 diabetes, and may help direct the design of new treatments for this complex disease.

1.6.2 Hypothesis

The overall hypothesis is that endogenous Bcl-x_L, by regulation of mitochondrial physiology promotes pancreatic β-cell function and survival under nutrient-induced stress.

1.6.3 Aims

- Characterize non-apoptotic roles of Bcl-x_L in β-cell function with focus on mitochondrial metabolism and oxidative stress *in vitro*
- Characterize the antiapoptotic role of Bcl-x_L in β-cell survival under metabolic stress *in vitro*
- Generate and characterize an adenovirus expressing Bcl-x_L for overexpression studies *in vitro*

Chapter 2: Methods and Materials

2.1 Reagents

Collagenase type XI (#C7657), cornoil (#C8267), palmitate (#P5585), tamoxifen (#T5648), tetramethylrhodamine (TMRE, #87917), fatty-acid free bovine serum albumin (#A8806), D-glucose (#G7528), D-ribose (#R7500), rotenone (#R8875), hydrogen peroxide (H_2O_2, H1009), N-acetyl-L-cysteine (NAC, #A9165) were from Sigma-Aldrich (St. Louis, MO, USA). Fura-2/AM (#F1221), mitotracker deep red (#M224726), dihydroethidium (DHE, #D-1168), hoechst 3342 (#H3570), propidium iodide (PI, #P3566) were from Thermo Fisher Scientific/ Life Technologies (Carlsbad, CA, USA). Carbonyl cyanide *m*-chlorophenyl-hydrazone (CCCP, #215911) was from EMD Millipore/ Calbiochem (Billerica, MA, USA). Dimethyl sulfoxide (DMSO, #BP231) was from Fisher Scientific (Waltham, MA, USA.) eFluor780 (#65-0865-14) was from eBioscience (San Diego, CA, USA).

2.2 Mouse model & genotyping

The inducible β-cell specific Bcl-x KO and WT control littermates were previously generated by Luciani *et al* (156). Briefly, Pdx1-CreER^{TM} (provided by Dr. Douglas Melton, Harvard University) (200) and Bcl-x$^{flox/flox}$ mice (provided by Dr. You-Wen He, Duke University) (198) were bred together to generate Bcl-x$^{flox/flox}$:Pdx1-CreER^{TM} (BclxβKO) and Bcl-x$^{flox/flox}$ (BclxβWT) mice.

For genotyping, each ear notch sample was digested in 150 µl of cell lysis buffer (Qiagen #1045696) containing 1.5 µl proteinase K (Fermentas E0048) at 55^{o}C for 3 to 4 hours. Protein contaminates were removed by addition of 50 µl of protein precipitation solution and centrifugation for 3 minutes at 14,000 xg. DNA from the supernatant was precipitated by 1 sample volume of isopropanol and centrifuged for 8 minutes at 14,000 xg. DNA Pellet was washed with 70% ethanol, air dried prior to rehydration in 20 µl of DNAse RNAse free water. Isolated DNA was stored at -20 until performing PCR for identification of CreER transgene.

The CreER transgene was identified in the presence of an amplification product of 410 bp using the primers listed below. In addition, a set of primers was used as an internal positive control (Tcrd, 200 bp) to ensure successful amplification of mouse DNA. Briefly, PCR (40 cycles: 95^{o}C, 30 sec; 54^{o}C, 1 min; 68^{o}C, 1min. 1 cycle: 68^{o}C, 5min. Hold: 4^{o}C) was prepared in a 15 µl reaction containing 1 µl of DNA, 1X Crimson taq polymerase and buffer (NEB #M3024S), 0.33 mM dNTP (Thermo Scientific #R0192) for each sample. PCR products were analyzed by gel electrophoresis in a 2% agarose gel incorporated with 1X SYBR safe DNA gel stain (Life Technologies #S33102). Gel was run at 140 V for 40 minutes, exposed by UV and imaged using the BioSpectrum 310 imaging system (UVP).

The following primers were used (Fw/ Rv sequences in 5' to 3' direction) for genotyping:

CreER (410 bp),

AACCTGGAAGTGAAACAGGGGC/TTCCATGGAGCGAACGACGAGACC;

Internal positive control, Tcrd (200 bp),

CAAATGTTGCTTGTCTGGTG/ GTCAGTCGAGTGCACAGTTT

2.3 Tamoxifen injection

Tamoxifen was used to induce activation of Cre recombinase in the Pdx-CreER (BclxβKO) positive mice. Littermate control (BclxβWT) mice were also injected with tamoxifen. One week prior to islet isolation from BclxβWT and BclxβKO mice, intraperitoneal injections of tamoxifen (Sigma-Aldrich #T5648) were administered at a dose of 75 µg per body weight (g) at room temperature for 4 days. Body weight was monitored daily during the injection period. Tamoxifen was prepared on the first day of each injection cycle. Briefly, tamoxifen was dissolved in cornoil (Sigma-Aldrich #C8267) to a final concentration of 10 mg/ml. The solution was then vacuum filtered through a 0.22 µm polyethersulfone membrane (Merck Millipore #SCGP00525) and stored at 4^{o}C for up to 4 days.

2.4 Islet isolation

Islets were isolated from mice between 2.8 -3.4 months of age by collagenase (Sigma-Aldrich #C7657) and mechanical digestion as previous described (201). Briefly, collagenase was dissolved in ice-cold 1X HBSS (Life Technology #14185-052) into a concentration of 1000 U/ ml. Surgical dissection of the euthanized animal exposes the common bile duct, which is injected with 5 ml of collagenase to inflate the pancreas. During the procedure, the duodenal opening was clamped with a haemostat to prevent outflow of collagenase into the intestine. The pancreas was excised and incubated in 2 ml of collagenase solution at 37^{o}C for 11 minutes. The pancreas was then homogenized manually with a 3-minute shake. The digested tissues were then washed twice with 1X HBSS + 1 mM $CaCl_2$ and filtered through a 70 μm strainer (Fisher Scientific #352350). The filtrate was then collected into a 100 mm petri dish and cultured (VWR #25384-088) in 11.1 mM glucose RPMI 1640 supplemented with 10 % FBS and 2% P/S (complete RPMI) (Life technology #11875). Islets were picked manually and cultured overnight at 37^{o}C in 5% CO_2 incubator prior to treatments.

2.5 Islet culture and treatments

Whole islets or dispersed islet cells (as described in Chapter 2.6) were cultured in RPMI supplemented with 10% FBS, 2% penicillin-streptomycin (Life technology #11875), at 37^{o}C in 5% CO_2. For hyperglycemic treatments, the desired glucose concentrations (11 mM control, 25 mM high glucose) were prepared by diluting the appropriate amount of 1 M glucose in glucose-free complete RPMI 1640 (Life Technology #11879). For glucolipotoxic treatments, a 20 mM palmitate (PA, Sigma-Alrich #P5585) stock in 30 mM NaOH was prepared at 70^{o}C. A final 1.5 mM PA in 25 mM glucose complete RPMI containing 20% fatty-acid free bovine serum albumin (BSA, Sigma-Aldrich #A7030) was prepared to a final molar ratio of 6:1 (PA:BSA) (202). Treatments with 5 mM NAC (Sigma-Aldrich #A9165) were prepared from a 0.5M stock in dH_20. NAC-containing complete RPMI was adjusted to pH 7.4 with NaOH and filtered sterilized prior to treatments.

2.6 Islet single cell dispersion

Prior to dispersion, intact islets were washed twice with 37^{o}C Minimum Essential Media (MEM, Corning #15015209) in a 1.5 ml low retention microcentrifuge tube (Fisher Scientific #02-681-331). Islets were trypsinised with 0.05% trypin-EDTA (Life Technology #25300-054) in a 1:5 dilution and mechanically dispersed using a P200 pipette into single cells for 1 minute. Dispersed islet cells were then washed in MEM, further dispersed mechanically for 10 seconds and resuspended in complete RPMI. For cell death kinetic imaging experiments, islet cells were seeded in 96 well microplates (Perkin Elmer #6005182) and cultured in 200 μl media. For single time point confocal imaging, single cells were seeded on 25 mm glass coverslips (VWR #102097-880). Single cells were first dispensed on the coverslip as 70 μl droplets at the center of a coverslip, which were allowed to adhere to the surface for 3 hours in the incubator prior to addition of complete RPMI to a final culture volume of 2 ml.

2.7 Mitochondrial membrane potential measurements

Changes in mitochondria membrane potential ($\Delta\psi_m$) were assessed using the mitochondrial specific fluorescence probe, TMRE, which is a positively charged fluorescence probe that labels the negatively charged mitochondria and accumulates in hyperloarized mitochondria undergoing respiration. Since CCCP uncouples mitochondrial respiration and depolarizes $\Delta\psi_m$, it was used as control for TMRE staining and the directionality of $\Delta\psi_m$.

Prolonged culture on $\Delta\psi_m$ of intact islets – Prior to flow cytometry, intact islets were dispersed into single cells as described above and cultured in 3 mM glucose complete RPMI for 1 hour prior to staining with 100 nM TMRE (Sigma-Aldrich #87917) at 37^{o}C for 30 minutes. Islet cells were treated with 5 μM CCCP as a control for TMRE staining and the ability to detect changes in $\Delta\psi_m$. Cells were then washed and resuspended in PBS supplemented with 2% FBS and kept

on ice until measurements by flow cytometry (BD Fortessa) in the PE channel (excitation 561 nm, emission 582/15 nm).

Acute glucose –stimulated changes in $\Delta\psi_m$ of dispersed islet cells – Prior to imaging, cells on coverslips were pre-cultured in 3 mM glucose complete RPMI. Cell were then stimulated with 15 mM glucose or 5 μM CCCP and stained with 50 nM TMRE (Sigma-Aldrich #87917) simultaneously for 20 minute at 37^{o}C. Stained cells were washed once with HEPES-buffered KRB and TMRE fluorescence was excited at 561 nm and collected at emission 566 - 600 nm using a confocal microscopy (Leica SP8).

2.8 Superoxide and cell death measurements

A common method of detecting superoxide is the use of dihydroethidium (DHE). Upon oxidation by superoxide, DHE is metabolized into 2-OH-ethidium, which has a peak excitation at 500 nm and emission 580 nm (203).

Cell viability is assessed using the eFluor780® (eBioscience, #65-0865-14), which has a peak excitation at 633 nm and emission 780 nm. The fluorescence spectrum of eFluor780 therefore does not overlap with DHE. Similar to another common viability dye propidium iodide, eFluor780 labels dead cells based on plasma membrane permeability, which is a common hallmark of various cell death pathways.

Prior to measurements by flow cytometry, intact islets were dispersed into single cells and cultured in 11.1 mM glucose complete RPMI for 1 hour. Cells were first stained with 20 μM of the superoxide indicator dihydroethidium (Molecular Probes, #D-1168) for 20 minutes at 37^{o}C. Cells were then washed and stained with the viability dye eFluor780® in 1:1000 dilution with PBS for 10 minute at room temperature. Cells were then resuspended in PBS supplemented with 2% FBS and kept on ice until superoxide and cell death measurements by flow cytometry (BD Canto) using the PE (ex. 488 nm, em. 575/26 nm) and APC-Alexa780 (ex. 635 nm, em. 780/60 nm) channels, respectively.

2.9 Intracellular Ca^{2+} measurement

Changes in intracellular calcium level $[Ca^{2+}]_i$ was measured by a fluorescent Ca^{2+}indicator Fura-2, which has different fluorescence properties depending on $[Ca^{2+}]_i$. At low $[Ca^{2+}]_i$ or Ca^{2+} free condition Fura-2 is excited at 380 nm, while at high $[Ca^{2+}]_i$ or calcium bound condition Fura-2 is excited at 340 nm. With the same emission wavelength (approximately 510 nm), the ratio in fluorescence intensity between 340 and 380 nm therefore reflects the changes in ratio of Ca^{2+}bound versus unbound.

Intact islets or dispersed islet cells on coverslip were stained with 5 uM Fura-2AM (Molecular Probes #F1221) for 30 minutes at 37^{o}C in 3 mM glucose Ringer's solution (KCl 166 mM; $CaCl_2$ 100mM; $MgCl_2$ 100 mM; HEPES 166 mM; NaCl 166 mM; pH 7.4). Prior to imaging, coverslips were transferred to a 2 ml imaging chamber and cells were washed with 3 mM glucose HEPES-buffered Ringer's solution for 30 minutes. Throughout the experiment, islets were continuously perifused at a flow rate of 2.5 ml/ min. Fura-2 was excited at 340 nm and 380 nm, imaged using widefield microscope (Leica SP8). The ratio of fluorescence intensity at F340/F380 is expressed for $[Ca^{2+}]_{i..}$

2.10 RNA isolation, reverse transcription & real-time qPCR

For each sample, 20 to 40 islets were preserved in 20 ul of RNAlater RNA stabilization reagent (Qiagen #76104) in a microcentrifuge tube at -20^{o}C prior to RNA isolation. Within 4 weeks, collected islets were homogenized using the QIAshredder (Qiagen #79656) followed by mRNA isolation using the RNEasy Mini Kit (Qiagen #74106) according to the manufacturer's manual. Amount and concentration of isolated mRNAs were quantified by nanodrop. Freshly isolated mRNAs (100 ng/ sample) were reverse transcribed into cDNA using the qScript cDNA synthesis kit (Quanta Bioscience #95047-500) and cDNA samples were kept at -20^{o}C until use for gene expression assays. cDNA samples were analyzed in triplicate on a 384 well microplate (Life technologies #4309849) and amplified using PerfeCTa SYBR green Fastmix (Quanta Biosciences #95072) with specific primers (IDT) in a ViiA7 real-time PCR system (Applied

Biosystem). Relative amount of the target gene expressed was calculated using the equation 2^-ΔCt, where ΔCt = Ct (target mRNA) – Ct (internal control). The internal control used was the ribosomal protein gene RPLP0 as the housekeeping gene.

Below is a list of mouse specific primers used (Fw/Rv sequences in 5' to 3' direction):

RPLP0, AGATTCGGGATATGCTGTTGGC/ TCGGGTCCTAGACCAGTGTTC;

Pdx1, GAACCCGAGGAAAACAAGAGG/ GTTCAACATCACTGCCAGCTC;

MafA, TTCAGCAAGGAGGAGGTCAT/ TTCTCGCTCTCCAGAATGTG;

Ins2, GAAGTGGAGGACCCACAAGTG/ GATCTACAATGCCACGCTTCTG;

Glut2, GTCCAGAAAGCCCCAGATACC/ GTGACATCCTCAGTTCCTCTTAG;

Gck, AGCTGCACCCGAGCTTCA/ GATTTCGCAGTTGGGTGTCA;

Ucp2, CAGCCAGCGCCCAGTACC/ CAATGCGGACGGAGGCAAAGC;

Bcl-x (Bcl2l1), exon1/ exon2 (IDT #Mm.PT.58.30208920)

Beta-actin, (IDT #Mn.PT.39a.2214843.q)

2.11 Cell death assay by PI incorporation

Dispersed islet cells were seeded onto a 96 well microplate (Perkin Elmer #6004460) for 24 hours prior to treatment as described. Propidium iodide (0.5 μg/ml per well) and Hoechst (0.1 μg/ml per well) were added during preparation of treatment media. During cell death, increased permeability of plasma membrane allows entry of PI and binding with DNA, which results in fluorescence. At the indicated time point (24, 48 and 72 hour), 3 x 3 non-overlapping images per well were taken using the automated environmental controlled high-throughput microscope (Molecular Device, IXM; kindly made available by Dr. Christopher Maxwell, CFRI). Cell death was analyzed using the imaging analysis software Cell Profiler. A series of actions were assembled in the Cell Profiler pipeline to identify cells based on their fluorescence intensity thresholds, size and shape. Cells identified in the Hoechst and PI channel were categorized as

parent and child respectively. Percentage cell death was then calculated based on the numbers of Hoechst and PI double positive cells relative to total Hoechst positive cells.

2.12 In vitro static insulin secretion and content measurements

For each treatment, insulin secretion was measured from 12 size-matched islets, which were collected in a 1.5 ml low retention microcentrifuge tube at the end of treatment. Islets were pre-cultured in 3 mM glucose Kreb's Ringer's buffer (KRB, NaCl 129 mM; KCl 4.8 mM or 30 mM; $MgSO_4$ 1.2 mM; KH_2PO_4 1.2 mM; $CaCl_2$ 2.5 mM; $NaHCO_3$ 5 mM; HEPES 10 mM; BSA 0.5%) for 1 hour prior to the assay to reach basal metabolic state of the islets. Next islets were incubated sequentially in KRB containing: 3 mM glucose for 1 hour (basal), 20 mM glucose for 1 hour (glucose stimulation), 3 mM glucose for 1 hour (recovery) and 30 mM KCl in 3 mM glucose for 30 minutes (membrane depolarization). At the end of each time point, islets were spun down, the supernatant was collected into a new tube for measurement of secreted insulin. At each step islets were counted to record the number of islets. Islet insulin content was assayed using 5 additional islets, which were from the same batch as, and size-matched to, those used for insulin secretion, at the end of the 6 days treatment. Islets were washed twice in PBS and kept in 250 µl of 0.1M HCl/ 70% EtOH solution at -20^{o}C overnight before sonication with 80 Amps for 4 minutes, pulse on/off for 30 seconds (S-4000 with cuphorn; Misonix).

Samples of both insulin secretion and insulin content were kept at -20^{o}C until measurements using the Ultrasensitive Insulin ELISA kit (Alpco #80-INSMSU-E10) according to manufacturer's manual. Luminescence was measured at 450 nm using a SpectraMaxL luminometer (Molecular Devices, kindly made available by Dr. Francis Lynn, CFRI)

2.13 Transfection of MIN6 cells

Pancreatic β-cell line MIN6 were cultured in high-glucose Dulbecco's modified Eagle's medium (DMEM, Life Technology #11995) supplemented with 10% FBS and 2% penicillin/streptomycin

at 37^{o}C in 5% CO_2. 24 hour prior to transfection, MIN6 cells were seeded on a 6 well tissue cultured plate at a confluency of approximately 70%. On the day of transfection, MIN6 cells were transfected with 1 μg of plasmid DNA (eYFP:Bcl-x_L) using Lipofectamine 2000 (Life Technology # 11668019) in 1 ml of Opti-MEM with reduced serum medium (Life Technology #31985) for 4 hours. After that, cells were cultured in complete DMEM for at least 48 hours prior to assays.

2.14 Electron microscopy

Transfected MIN6 cells with plasmid eYFP:Bcl-x_L were fixed using 2.5 % glutaraldehyde (Sigma #G5882) in 0.1M sodium caocodylate (Sigma #70114) at room temperature for 4 hours. Cells were then scraped from the well, collected into a 1.5 ml microcentrifuge tube, spun down to collect the pellet. The pellets of transfected MIN6 cells and untransfected controls were sent to the Electron Microscopy Facility at McMaster University for embedding onto EM grids. Grids were examined with transmission electron microscopy with the supervisions by Drs. Jenny Bruin and Wayne Vogl at the Life Science Institute (UBC).

2.15 Construction of the eYFP:Bcl-x_L adenovirus (Ad.eYFP:Bcl-x_L)

The donor plasmid expressing eYFP:Bcl-x_L (provided by Dr. James Johnson, UBC) (Bcl-x_L NM_009743.4) was cloned into an E1-substituted adenovirus using the AdenoQuick^{TM} cloning system (O.D.260, #QK-02) according to the supplied manual. Briefly the donor plasmid and the recipient plasmid containing pE.1.1 shuttle vector (provided by Dr. Paul Orban, CFRI) were digested with NheI (Thermo Fisher Scientific #FD0974) and Xba1 (Thermo Fisher Scientific #FD0684). Digested products from the donor plasmid were separated by gel electrophoresis, where the 1.7 kb insert containing eYFP:Bcl-x_L was excised, gel purified (Qiagen #28704) and ligated with the digested recipient shuttle vector using T4 DNA ligase (Life Technology #15224) overnight at 4^{o}C. The ligation product was transformed into DH5-alpha E. coli by electroporation and their recombinant clones were selected on kanamycin containing agar plate.

Recombinant plasmid (pE1.1-YFP:Bcl-xL) was verified by restriction analysis with PvuII, XmnI and Kpn1 individually. Correct clone was further expanded in E. coli and purified DNA using the PureYield^{TM} plasmid miniprep system (Promega #A1222). The resulting plasmid was digested with BstAP1 and the fragment containing eYFP:Bcl-x_L and kan resistance gene was excised, gel purified and ligated with Sfil pre-digested Adenoquick pAd363 (ΔE4). The ligation product was then packaged into the phage λ competent E.coli. Clones resistant to kanamycin and ampicillin were inoculated and their cosmid DNA were verified by restriction analysis with BglII, linearized with Swa1 and transfected into Ad-293 (Stratagene #240085) cells using lipofectamine 2000 (Life technology #11668019) for virus recovery. Crude viral extracts were harvested when cells begin to display cytopathic effect such as rounding of cells and detachment from plate, which began approximately two to three days post transfection. Viruses were released from cells by at least 3 rounds of freeze-thaws followed by centrifugation to remove cell debris. The supernatant was used for the next round of viral amplification in Ad293 cells, which was repeated 6 times such that five 10 cm plate of cells were produced in the last stage.

To extract virus, the combinaed lysates collected at each stage were treated with 10 U/ ml of Benzonase (Sigma #E1014-SKU) to remove DNA from contaminants such as recombinant proteins. The digestion reaction was stopped by addition of dilution buffer (Bicine 20 mM; NaCl 0.6 M; pH 8.4) of the same volume as the lysate. Diluted lysate was purified through Sartobind Q15 anionic exchange filter (Sartorius Stedim #93IEXQ42GB-12--A), washed (Bicine 10 mM; NaCl 0.4 M; pH 8.4) and eluted in (Bicine 10 mM; NaCl 0.61 M; pH 8.2). In order to maintain virus under long-term storage at -80^{o}C, glycerol solution was added to the eluted virus.

2.16 Adenoviral titre determination

Ad293 cells were seeded in a 96 well microplate at a density of ~$10^{\wedge 4}$ cells per well. Serial dilutions of Ad.eYFP:Bcl-x_L were prepared starting from 10^{-3} to 10^{-11}. Cells of the same row except the last two columns were infected by the adenovirus dilution and cultured at 37^{o}C in 5% CO_2. Cells in the last two columns (11 and 12) were cultured in virus-free media as a negative control. Two to four days post infection the number of wells displaying YFP fluorescence per

each row was counted under a microscope. Viral titer was calculated using the equation PFU/ ml = $10^{(x + 0.8)}$, where x is the sum of the fraction of YFP positive wells in each row. PFU/ml of Ad.eYFP:Bcl-x_L is 4.4x $10^{\wedge 10}$.

2.17 Adenovirus transduction in dispersed islet cells

Prior to seeding dispersed islet cells from WT C57B6 mice, coverslips were coated with 500 µl of 804g-extracellular matrix (804g-ECM) in the incubator overnight. The next day, 804g-ECM was removed and coverslips were washed with water. Dispersed islet cells were seeded in the center of each coverslip as a droplet of 70 µl. Single cells were allowed to adhere to coverslips for 4 hours prior to addition of 2 ml of complete RPMI media. The next day cells were transduced with adenovirus. Briefly, cells were infected with Ad.eYFP:Bcl-xL at MOI 5 or Ad.eGFP at MOI 20 in 1ml of serum free media for 3 hours. Adenovirus containing media were then replaced with complete RPMI media for further culture.

2.18 Statistical analysis

All data were represented as mean $\pm$ standard error of the mean (SEM). Data were analyzed by unpaired t-test or 2-way ANOVA in GraphPad Prism software (La Jolla, CA, USA). Statistical significance is determined based on $p < 0.05$, where * indicates a p value ≤ 0.05, ** $p \leq 0.01$, *** $p \leq 0.001$ and **** $p \leq 0.0001$.

Chapter 3: Results

3.1 Knockout studies of Bcl-x_L

3.1.1 Tamoxifen-dependent Cre activation reduces Bcl-x_L transcripts in BclxβKO islets

Previously, our lab has seen indications of tamoxifen-independent activation of Pdx1-CreER^{TM} (191). It was observed that without tamoxifen injection, Bax mRNA was reduced in islets from 6 months old Pdx1-CreER^{TM}:Bax$^{flox/flox}$ mice relative to islets from their Bax$^{flox/flox}$ littermates. This was not seen in islets from 3 months old mice. In this study, mice were therefore injected between 2.8 – 3.4 months of age, at which it is unlikely for them to have significant spontaneous Cre activation (Figure 1A).

In this study, genotype of the mice and the efficiency of Bcl-x_L deletion were confirmed using RT-qPCR. Over 80% reduction in islet Bcl-x_L mRNA is achieved in Bclx fl/fl Cre+ (BclxβKO) mice compared to Bclx fl/fl (BclxβWT) control animals following tamoxifen injection (75 μg/ g body weight) for 4 consecutive days (Figure 1).

Figure 1.

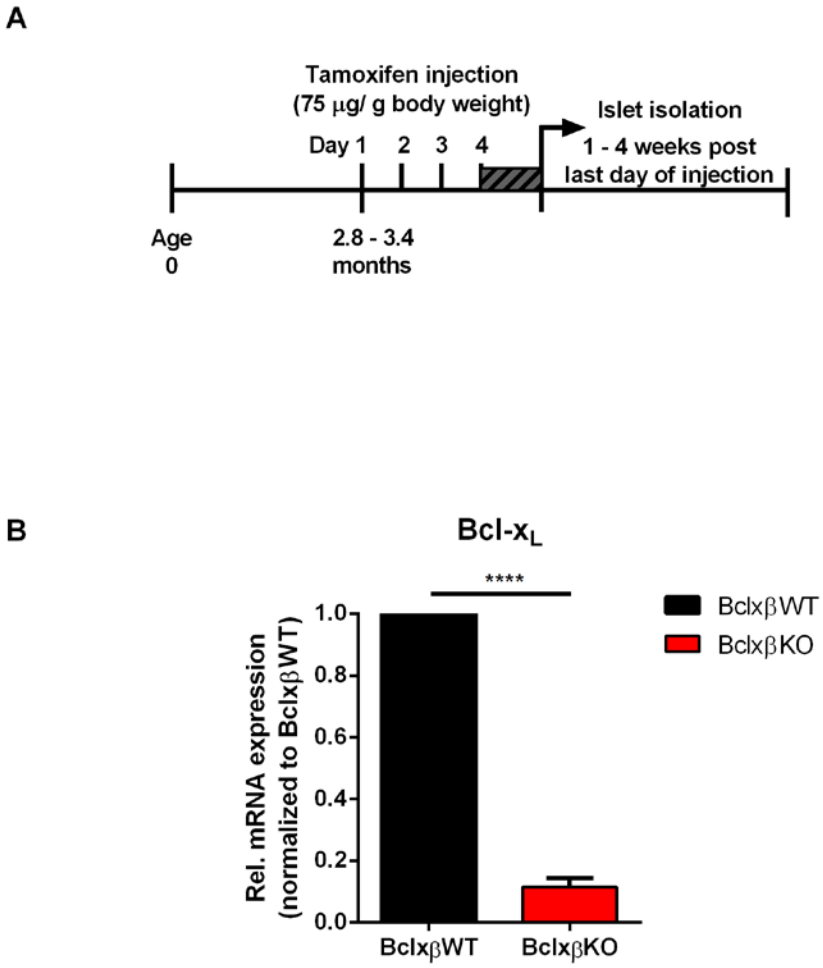

Figure 1. Administration of tamoxifen deletes Bcl-x_L in islets. (A) Experimental Scheme: Bclx fl/fl (BclxβWT) and Bclx fl/fl Cre+ (BclxβWT) mice between the age of 2.8 – 3.4 months were intraperitoneal injected with tamoxifen (75 μg/ g body weight) for 4 consecutive days. Islets were isolated between 1 to 4 weeks post last day of tamoxifen administration. (B) mRNA levels of Bcl-x_L from tamoxifen injected BclxβWT and BclxβKO islets were analyzed by RT-qPCR and expression was normalized to the internal control beta-actin and BclxβWT littermate control islets (n=11). (All data are presented as mean ± SEM)

3.1.2 Loss of Bcl-x_L amplifies islet mitochondrial membrane potential and glucose-stimulated Ca^{2+} responses

Increasing evidence for functions of Bcl-x_L in metabolism (155,156) has promoted us to determine its physiological role in healthy intact islets. Glucose-stimulated insulin secretion is highly dependent on mitochondrial activities and an increase in intracellular Ca^{2+} concentration ($[Ca^{2+}]_i$) (204).We compared glucose-induced mitochondrial membrane potential ($\Delta\psi_m$) and real-time changes of $[Ca^{2+}]_i$ in BclxβWT and BclxβKO islets cultured in regular media with 11 mM glucose for 2 days post islet isolation. Both islet $\Delta\psi_m$ and $[Ca^{2+}]_i$ were imaged at basal non-stimulatory conditions of low glucose (3 mM, 10 min) and in response to a transient-glucose stimulation (15 mM, 20 min). In addition to that, islet $[Ca^{2+}]_i$ continued to be imaged during glucose washout and recovery to baseline (3 mM, 20 min), and finally during membrane depolarization by KCl (30 mM, 5 min). The five different stages of the $[Ca^{2+}]_i$ imaging profile are annotated in (Figure 2A).

Both BclxβWT and BclxβKO islets have similar basal $[Ca^{2+}]_i$ when cultured in regular media (Figure 2B, C). Upon 15 mM glucose stimulation, BclxβWT islets $[Ca^{2+}]_i$ respond in an oscillatory manner, while BclxβKO islets respond with a plateau or a continuous spiking pattern (Figure 2A, B). Due to unsynchronized $[Ca^{2+}]_i$ responses between islets, representative $[Ca^{2+}]_i$ traces from a single intact islet of each genotype are shown on Figure 2A to highlight their differences. In addition, unlike BclxβWT, on no occasion did we observe oscillatory $[Ca^{2+}]_i$ response to glucose in BclxβKO islets (Figure 2C).

To quantitatively compare $[Ca^{2+}]_i$ responses during different stages of glucose stimulation, the average, peak and area under the curve (AUC) of $[Ca^{2+}]_i$ values presented by $[F_{340}/_{380}]$ were analyzed (Figure 2D). Basal $[Ca^{2+}]_i$ is represented by average $[F_{340}/_{380}]$ during the first 10 minute of Ca^{2+} imaging. The first and second phases of $[Ca^{2+}]_i$ are presented as peak $[Ca^{2+}]_i$ during the first 10 minutes and as the average steady state $[Ca^{2+}]_i$ during the last 10 minutes of glucose stimulation, respectively. The ability of islet $[Ca^{2+}]_i$ to recover to baseline during glucose washout, i.e. the recovery period, and the islet response to KCl are quantified by AUC. After 2 days of regular culture, there are no differences in baseline, peak and steady state $[Ca^{2+}]_i$

response to glucose, or in the AUC of the $[Ca^{2+}]_i$ recovery period between BclxβWT and BclxβKO islets. Average steady state $[Ca^{2+}]_i$ response to glucose in BclxβKO islets appears to be slightly higher than BclxβWT islets due to the non-oscillatory, plateau response.

Associated with the differences in $[Ca^{2+}]_i$ response to glucose, $\Delta\psi_m$ of dispersed islet cells tend to be higher in BclxβKO compared to in BclxβWT under both non-stimulatory condition and after 15 mM glucose stimulation (Figure 3), suggesting that islet cells deficient in Bcl-x_L may be metabolically more active.

Figure 2.

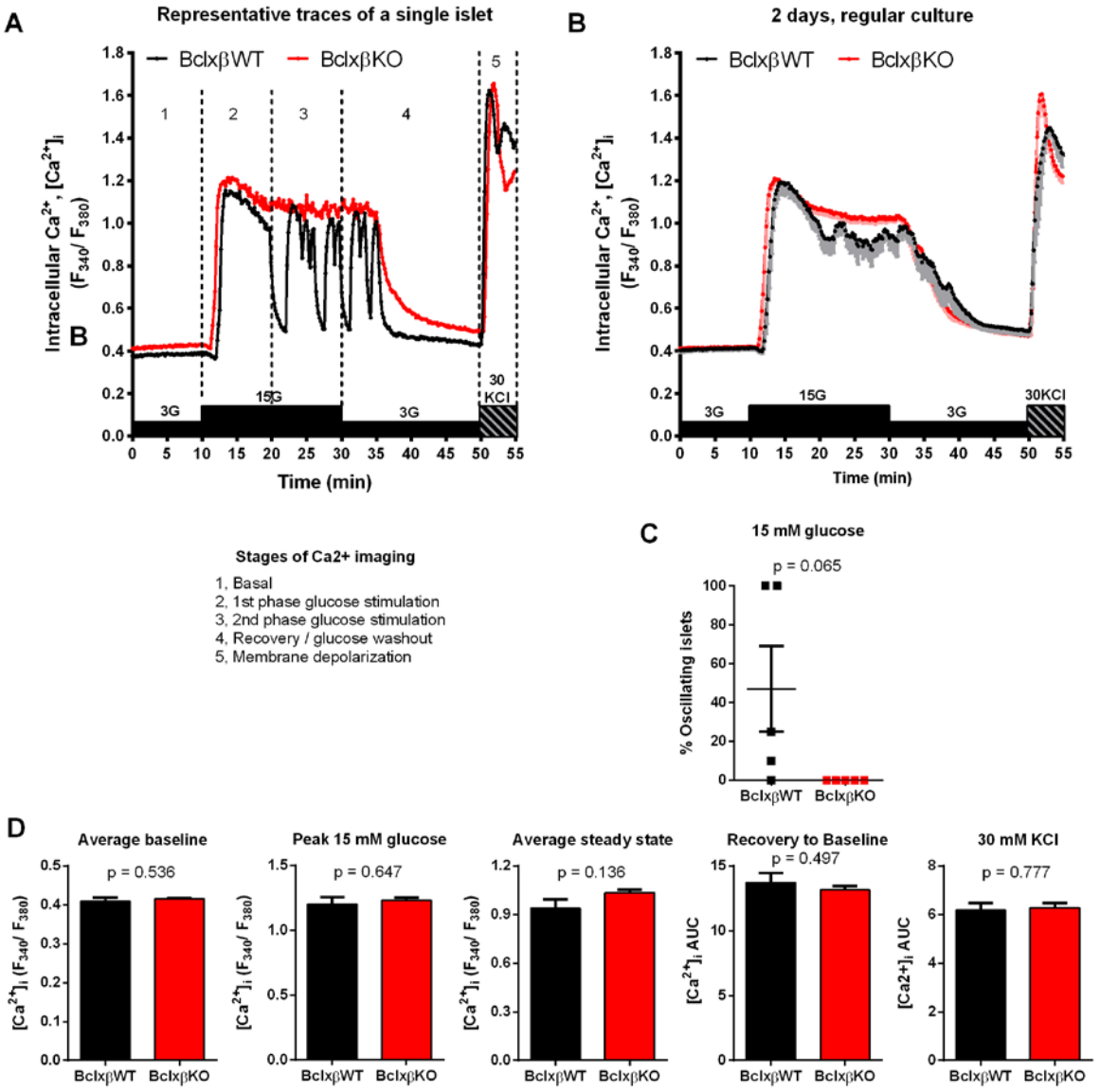

Figure 2. Islets Ca^{2+} responses in BclxβWT and BclxβKO islets. Intact islets from BclxβWT and BclxβKO mice were cultured in regular 11 mM glucose media for 2 days prior to Ca^{2+} imaging. (A) Representative $[Ca^{2+}]_i$ traces of a single islet from each genotype. The course of Ca^{2+} imaging is categorized into stage 1 to 5, beginning at 3 mM glucose (3G, basal condition), followed by 20 minute of 15 mM glucose (15G) stimulation, washout with 3 mM glucose (3G) and β-cell depolarization with 30 mM KCl (30KCl). (B) Averages of islet $[Ca^{2+}]_i$ of each genotype. Shaded bars below data points represent SEM. (C) Quantification of percentage oscillatory islets throughout glucose stimulation in each experiment (n=5 islet preparations). (D) Quantification and comparison of average F_{380}/F_{340} values during baseline, peak and average steady state of F_{380}/F_{340} values in response to glucose, and the AUC of the recovery period to baseline and the response to KCl. (11G n=5). (All data are presented as mean ± SEM)

Figure 3.

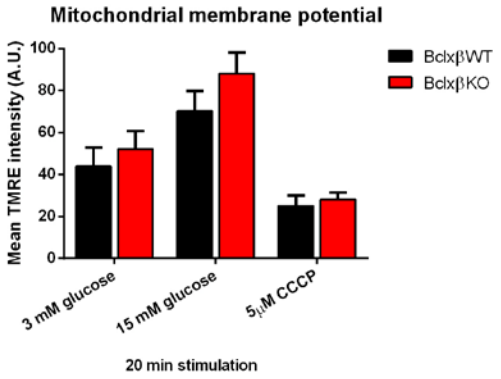

Figure 3. Quantification of mitochondrial membrane potential ($\Delta\psi_m$) in BclxβWT and BclxβKO islets. Dispersed islet single cells of BclxβWT and BclxβKO, were cultured in regular 11 mM glucose media for 2 days prior to confocal imaging. Cells were stained with 25 nM TMRE and fluorescence intensities were measured at 3 mM glucose (basal, non-stimulatory condition) and following stimulation with 15 mM glucose for 20 minute. Mitochondrial depolarization by 5 μM of CCCP was used as a control of TMRE loading and its ability to sense changes in $\Delta\psi_m$ (WT n = 5, KO n = 6). (All data are presented as mean ± SEM)

3.1.3 Loss of Bcl-x_L has little effect on islet function after 2 days of high glucose culture

Luciani *et al* (156) previously reported that deletion of Bcl-x_L increases $[Ca^{2+}]_i$ responses in dispersed islet single cells and intact islet NAD(P)H autofluorescence in response to glucose (156), suggesting a mitochondrial metabolic role of Bcl-x_L. We therefore asked whether such effects of Bcl-x_L on β-cell metabolism and Ca^{2+} responses are amplified under nutrient stress. To test this, BclxβWT and BclxβKO islets were cultured for increasing period of time (2 and 6 days) in control 11 mM glucose (11G) or high glucose at 25 mM (25G).

Results from Ca^{2+} imaging demonstrated that average basal $[Ca^{2+}]_i$ in both BclxβWT and BclxβKO islets are significantly elevated by high glucose culture at 25mM starting at 2 days (Figure 4 A1, A2, B). This is consistent with the reported ability of exposure to high glucose to promote β-cell activation at basal non-stimulatory condition (205).

Interestingly, BclxβWT islets cultured under 25G for 2 days no longer display the oscillatory $[Ca^{2+}]_i$ responses to 15 mM glucose stimulation, which are present in 11G culture (Figure 4 A3). In contrast, BclxβKO islets cultured in either 11G or 25G show the same non-oscillatory $[Ca^{2+}]_i$ plateau response to 15 mM glucose stimulation (Figure 4 A2). The $[Ca^{2+}]_i$ response to glucose in BclxβWT islet thus resembles that of BclxβKO islets after high glucose culture for 2 days. Such changes from oscillatory to plateau $[Ca^{2+}]_i$ response in BclxβWT islets upon high glucose culture likely reflects β-cell metabolic activation. Whereas the consistent plateau glucose-stimulated $[Ca^{2+}]_i$ response in BclxβKO under both normal and high glucose culture likely reflects a lower threshold for β-cell metabolic activation. However, there are no observable differences in peak and average steady state $[Ca^{2+}]_i$ responses to glucose after 2 days of 25G culture compared to 11G (Figure 4 A1, A2), and no differences were observed between BclxβWT and BclxβKO islets (Figure 4 A3, A4)

During the recovery period, BclxβKO islets cultured in 25G have a small but significant increase in the AUC compared to those cultured in 11G, which is not seen in BclxβWT islets (Figure 4B). This suggests reduced ability of BclxβKO islets to recover Ca^{2+} homeostasis after being stimulated by high glucose. Lastly, $[Ca^{2+}]_i$ responses to membrane depolarization induced by KCl are similar between BclxβWT and BclxβKO islets.

Figure 4.

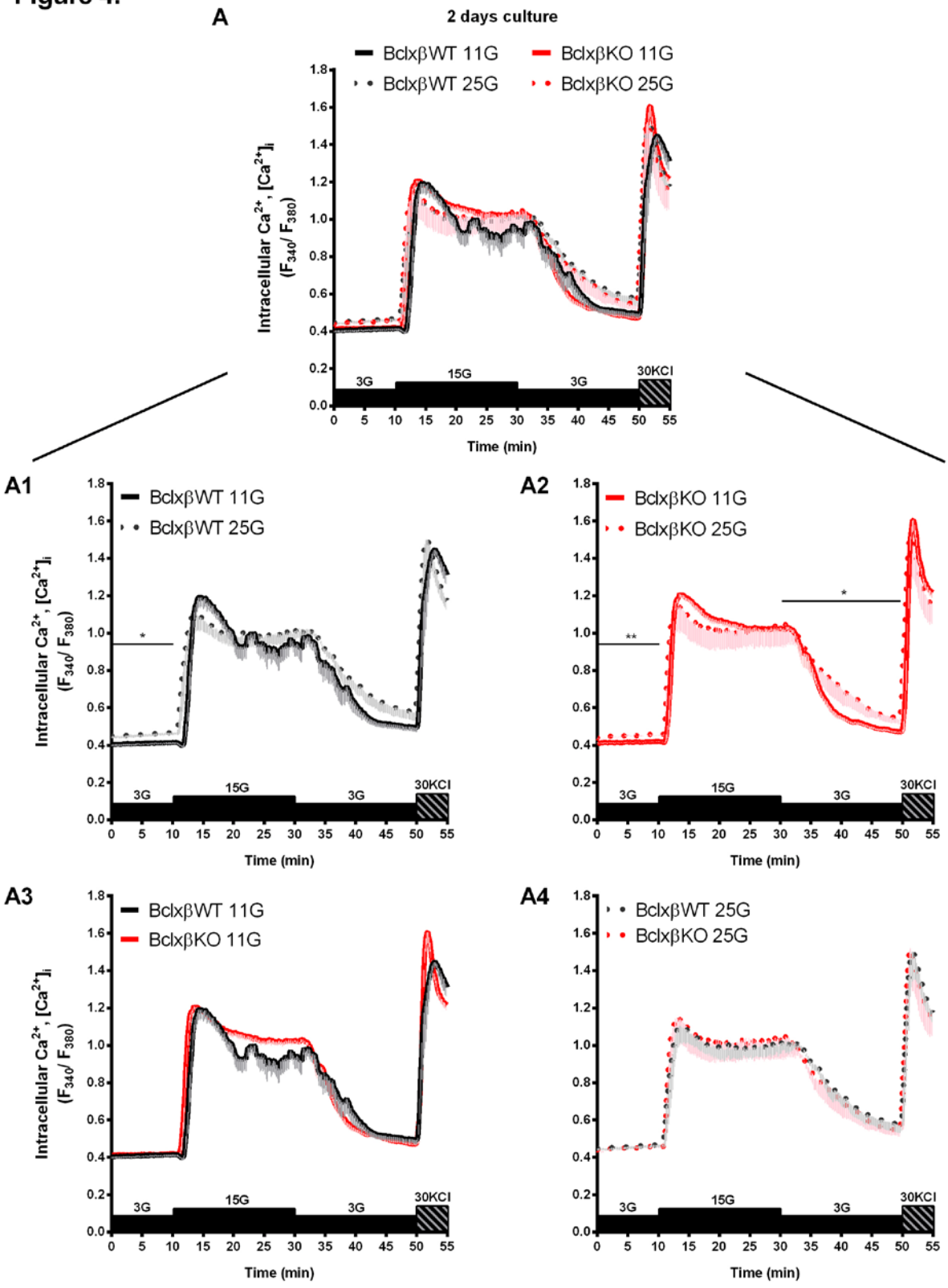
A
2 days culture
BclxβWT 11G
BclxβWT 25G
BclxβKO 11G
BclxβKO 25G
Intracellular Ca2+, [Ca2+]i
(F340/ F380)
3G
15G
3G
30KCl
Time (min)
A1
A2
A3
A4
*
**

Figure 4. ctn

B

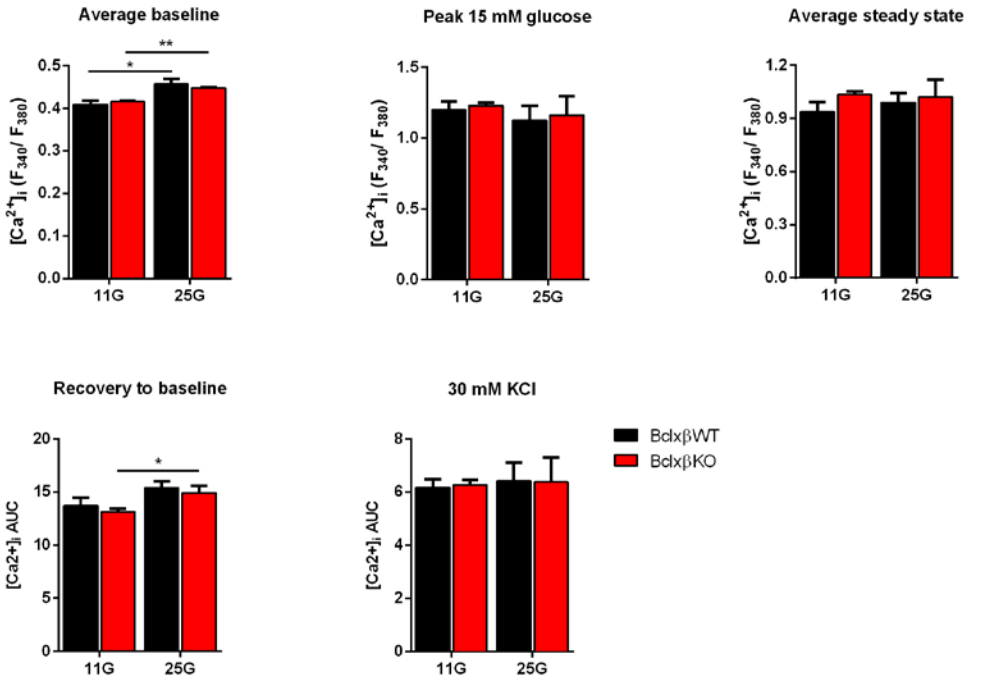

Figure 4. Effects of 2 day culture in 11 or 25 mM glucose on BclxβWT and BclxβKO islet Ca^{2+} response. Intact islets were cultured in media containing regular 11 mM glucose (11G) or 25 mM glucose (25G) for 2 days. (A) Average intracellular Ca^{2+} $[Ca^{2+}]_i$ responses of Fura-2-loaded intact islets isolated from BclxβWT and BclxβKO mice. Shaded bars below data points represent SEM (11G n=5, 25G n=3) (A1) Ca^{2+} traces of BclxβWT only islets cultured in 11G and 25G. (A2) Ca^{2+} traces of BclxβKO only islets cultured in 11G and 25G. (A3) Ca^{2+} traces of BclxβWT and BclxβKO islets cultured in 11G. (A4) Ca^{2+} traces of BclxβWT and BclxβKO islets cultured in 25G. (B) Quantification and comparison of average F_{380}/F_{340} values during baseline, peak and average steady state of F_{380}/F_{340} values in response to glucose, and the AUC of the recovery period to baseline and the response to KCl. (11G n=5, 25G n=3). (All data are presented as mean ± SEM)

3.1.4 Loss of Bcl-x_L worsens islet dysfunction following 6 days of high glucose culture

Published *in vitro* studies of chronic hyperglycemia in islets can span from 2 to 9 days or longer (206,207). Since our results with 2 days of high glucose culture on both BclxβWT and BclxβKO islets do not seem to reflect a state of toxicity, we next examined the effects of longer culture (6 days) under control conditions (11G) and high glucose at 25 mM (25G).

After 6-day culture in control condition, BclxβWT and BclxβKO islets have comparable average basal $[Ca^{2+}]_i$ (Figure 5 A3, B). However basal $[Ca^{2+}]_i$ is significantly elevated by the longer exposure to 25G culture and this effect tends to be amplified in the BclxβKO islets (Figure 5 A1, A2, B). This is associated with a trend towards higher basal $\Delta\psi_m$ in BclxβKO islets after 11G and 25G culture for 6 days, compared to BclxβWT (Figure 6A). This amplification in basal $[Ca^{2+}]_i$ is also mirrored in a small trend towards increased basal insulin secretion after 25G (Figure 6B).

Peak and steady state $[Ca^{2+}]_i$ responses to 15 mM glucose stimulation in both BclxβWT and BclxβKO islets are not significantly different after 6-day culture in 11G and 25G (Figure 5A, B). However, due to the elevated basal $[Ca^{2+}]_i$ after 25G culture, there is a significant reduction in the fold change of peak relative to average basal $[Ca^{2+}]_i$ in both genotypes (Figure 5B).

Following 6 days of 25G culture, the AUC of islet $[Ca^{2+}]_i$ recovery after glucose stimulation is significantly increased in BclxβWT, which is further exacerbated in BclxβKO islets (Figure 5A, B). This dysregulation is also reflected in insulin secretion. The 25G-cultured- BclxβKO islets secrete significantly higher amounts of insulin than similarly cultured BclxβWT islets (Figure 6B). Insulin content of islets from both genotypes are similar after 6 days of 11G and 25G culture (Figure 6C).

Lastly $[Ca^{2+}]_i$ responses to membrane depolarization by 30 mM KCl are comparable in BclxβWT and BclxβKO islets in 11G culture but the $[Ca^{2+}]_i$ response to KCl is significantly increased by 25G culture in BclxβKO islets only (Figure 6B), which is also reflected in the KCl-induced insulin secretion (Figure 5B, Figure 6B). These effects may be a consequence of the impaired

metabolic recovery following the glucose stimulus, and significantly elevated $[Ca^{2+}]_i$ and insulin secretion in BclxβKO islets at the time of KCl stimulation.

Figure 5.

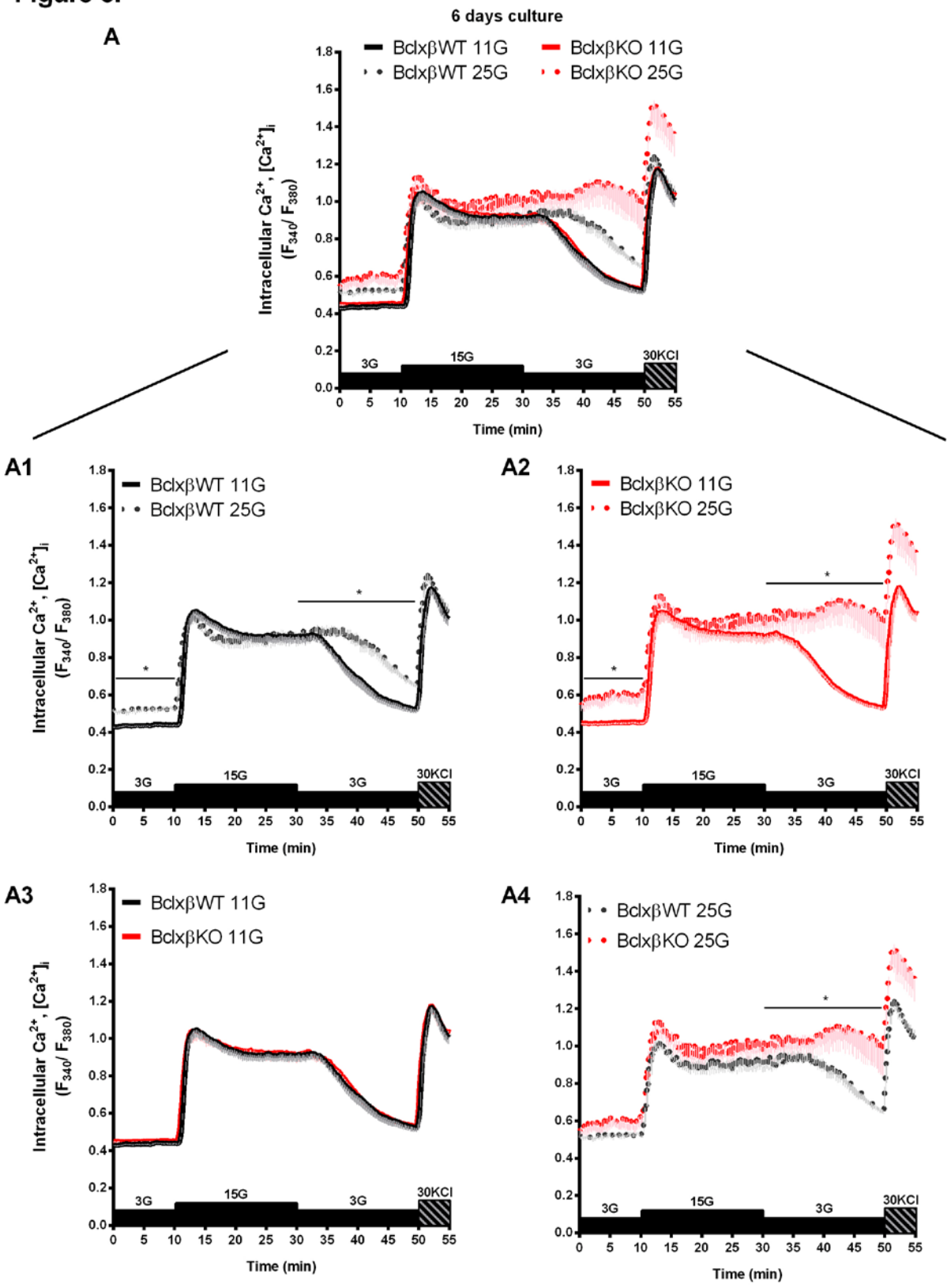
A
6 days culture
BclxβWT 11G
BclxβWT 25G
BclxβKO 11G
BclxβKO 25G
Intracellular Ca2+, [Ca2+]i
(F340/ F380)
3G
15G
3G
30KCl
Time (min)
A1
A2
A3
A4

Figure 5. ctn

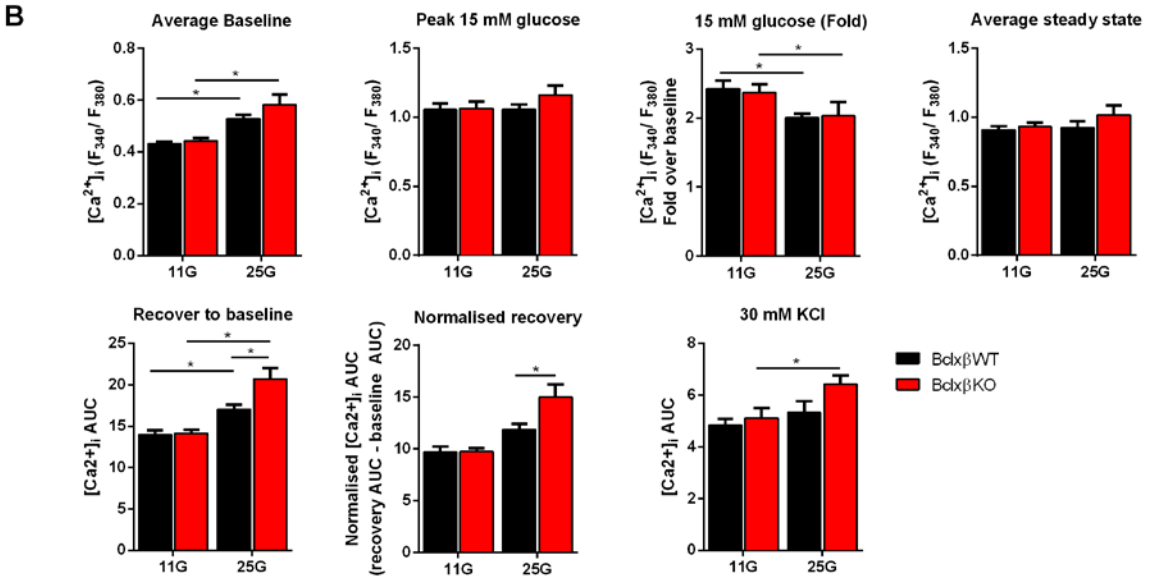

Figure 5. Endogenous Bcl-x_L helps maintains normal Ca^{2+} signaling during prolonged exposure to high glucose. Intact islets from BclxβWT and BclxβKO mice were cultured in either regular 11 mM glucose (11G) or 25 mM glucose (25G) media for 6 days. (A) Average intracellular Ca^{2+} $[Ca^{2+}]i$ responses of Fura-2-loaded intact islets. Shaded bars below data points represent SEM (11G n=5, 25G n=3). The statistical significance indicated in panel A refers to the quantifications of average baseline value and AUC during recovery period, as presented in panel B. (A1) Ca^{2+} traces of BclxβWT only islets cultured in 11G and 25G. (A2) Ca^{2+} traces of BclxβKO only islets cultured in 11G and 25G. (A3) Ca^{2+} traces of BclxβWT and BclxβKO islets cultured in 11G. (A4) Ca^{2+} traces of BclxβWT and BclxβKO islets cultured in 25G. (11G n=5, 25G n=3) (B) Quantification and comparison of average F_{380}/F_{340} values during baseline, peak and average steady state of F_{380}/F_{340} values in response to glucose, and the AUC of the recovery period to baseline and the response to KCl. (11G n=5, 25G n=3).

Figure 6

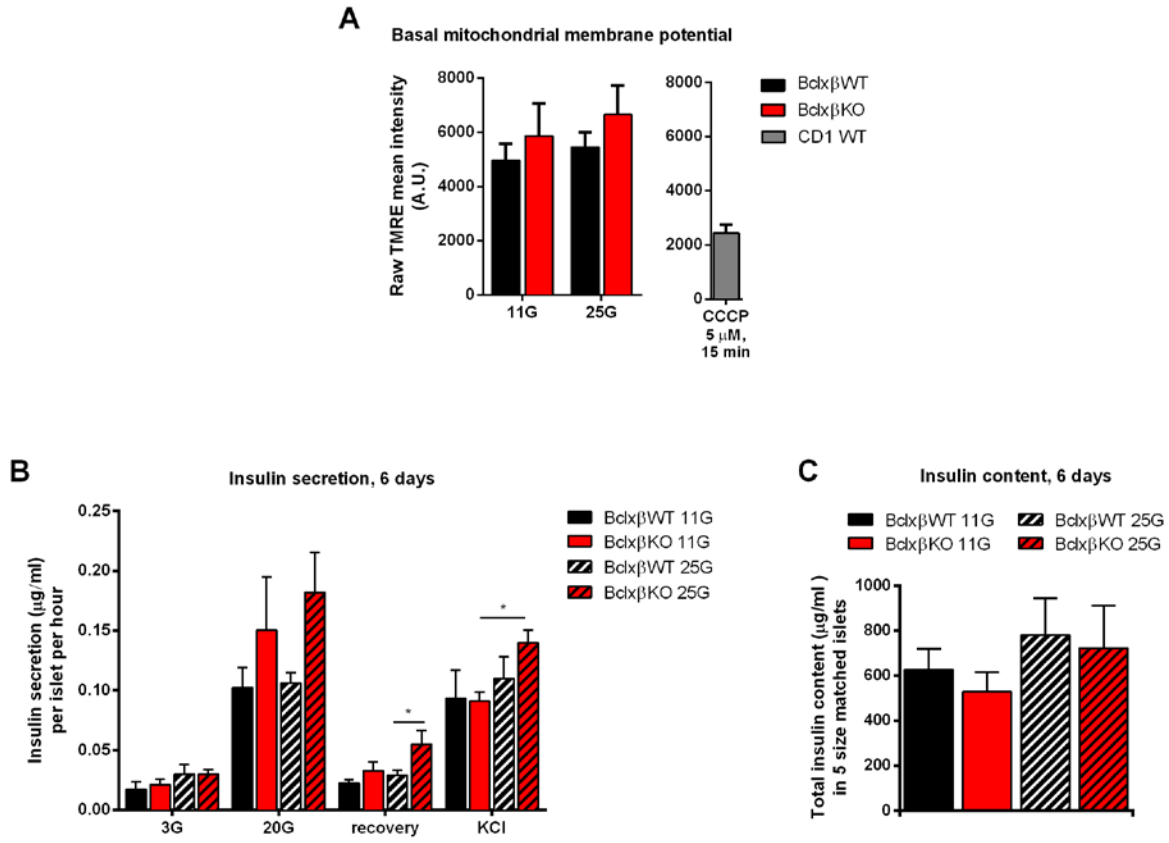

Figure 6. Endogenous Bcl-x_L helps maintains mitochondrial metabolism and insulin secretion in islets during prolonged exposure to high glucose. (A) Quantification of basal mitochondrial membrane potential ($\Delta\psi_m$) based on TMRE fluorescence intensity measured by flow cytometry. (n = 3) Prior to TMRE staining, islets were dispersed into single cells and cultured at 3 mM glucose media for 1 hour to recover from dispersion. (B) Glucose-stimulated insulin secretion in static incubation (n=4). (C) Total insulin content was measured from 5 size-matched islets at the end of each treatment (n=4). (All data are presented as mean ± SEM)

3.1.5 The antioxidant N-acetyl-L-cysteine does not prevent islet dysfunction following 6 day high glucose culture

We were interested to determine if the islet dysfunction induced by prolonged high glucose culture was due to oxidative stress. We therefore tested the effects of the antioxidant N-acetyl-L-cysteine (NAC) on islet $[Ca^{2+}]_i$ responses after 11 mM and 25 mM glucose culture for 6 days. NAC scavenges ROS such as hydrogen peroxides and superoxides directly or indirectly by enhancing the synthesis of the cellular antioxidant glutathione (208,209). NAC has been shown to restore β-cell dysfunction induced by glucotoxicity in models of T2D (118,210,211).

The results with NAC are somewhat unexpected. BclxβWT islets co-cultured with 5 mM NAC in 25 mM glucose, have significantly higher basal, peak and average steady state $[Ca^{2+}]_i$ responses to glucose compared to islets cultured in the absence of NAC (Figure 7A, B). In addition, NAC has no significant effects on islet $[Ca^{2+}]_i$ recovery in both genotypes, and does not prevent the high glucose- induced perturbations in the $[Ca^{2+}]_i$ recovery (Figure 7A, B). Lastly, the NAC-induced increase in baseline $[Ca^{2+}]_i$ of BclxβWT islets under 25G cultured is also associated with higher basal $\Delta\psi_m$ (Figure 7C).

These results show that NAC does not normalize islet $[Ca^{2+}]_i$ responses but, somewhat surprisingly, amplifies the effect of high glucose culture on islet cell metabolism and $[Ca^{2+}]_i$ dysregulation.

Figure 7.

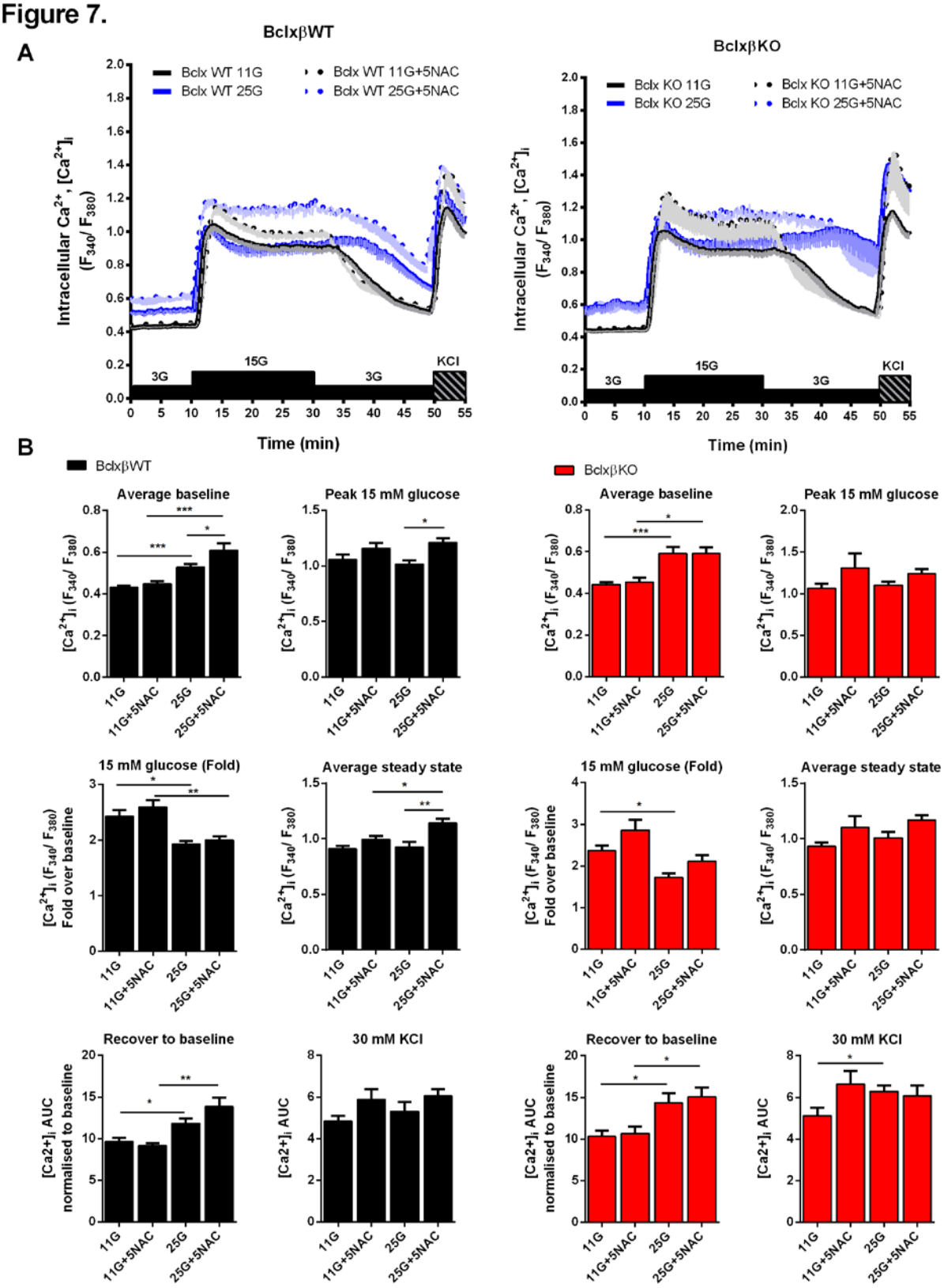
A
BclxβWT
Bclx WT 11G
Bclx WT 25G
Bclx WT 11G+5NAC
Bclx WT 25G+5NAC
Intracellular Ca2+, [Ca2+]i (F340/ F380)
3G
15G
3G
KCl
Time (min)
BclxβKO
Bclx KO 11G
Bclx KO 25G
Bclx KO 11G+5NAC
Bclx KO 25G+5NAC
Intracellular Ca2+, [Ca2+]i (F340/ F380)
3G
15G
3G
KCl
Time (min)
B
BclxβWT
Average baseline
Peak 15 mM glucose
15 mM glucose (Fold)
Average steady state
Recover to baseline
30 mM KCl
[Ca2+]i (F340/ F380)
[Ca2+]i (F340/ F380) Fold over baseline
[Ca2+]i AUC normalised to baseline
[Ca2+]i AUC
11G
11G+5NAC
25G
25G+5NAC
BclxβKO
Average baseline
Peak 15 mM glucose
15 mM glucose (Fold)
Average steady state
Recover to baseline
30 mM KCl
[Ca2+]i (F340/ F380)
[Ca2+]i (F340/ F380) Fold over baseline
[Ca2+]i AUC normalised to baseline
[Ca2+]i AUC
11G
11G+5NAC
25G
25G+5NAC

Figure 7. ctn

C

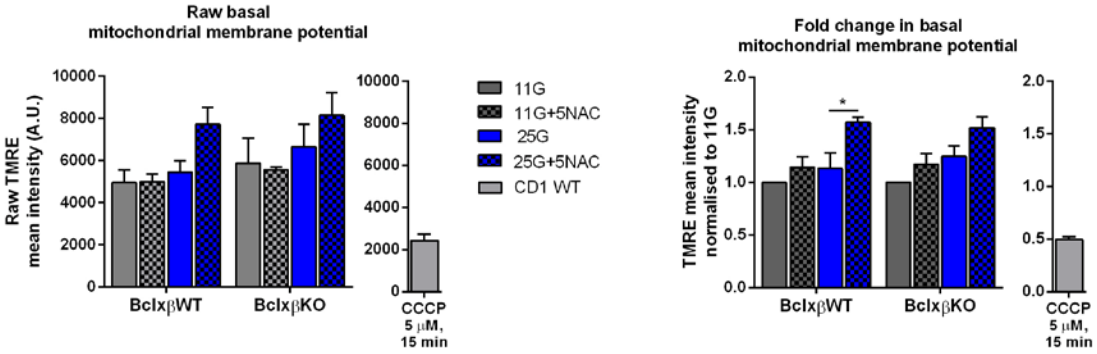

Figure 7. Effects of NAC in islet intracellular calcium and mitochondrial activity after 6 days. Intact islets of BclxβWT and BclxβKO mice were cultured in regular 11 mM glucose (11G) or 25 mM glucose (25G) in the presence or absence of 5 mM NAC (5NAC) for 48 hours. CD1 WT mouse islets were used for CCCP treatments due to the limited number of BclxβWT and KO islets available for the experiments. (A) Average $[Ca^{2+}]_i$ responses of Fura-2-loaded intact islets isolated. Shaded bars below data points represent SEM (11G n=5, 25G n=3) (B) Quantification and comparison of average F_{380}/F_{340} values during baseline, peak and average steady state of F_{380}/F_{340} values in response to glucose, and the AUC of the recovery period to baseline and the response to KCl. (11G n=5, 25G n=3). (C) Quantification of raw (left) and fold change (right) of basal mitochondrial membrane potential ($\Delta\psi_m$) based on TMRE fluorescence intensity measured by flow cytometry. *Left:* TMRE values were represented in arbitrary units (A.U.) *Right:* TMRE values were normalized to control culture (11G) of from BclxβWT (n = 3). (All data are presented as mean ± SEM)

3.1.6 Islet dysfunction following 6 days high glucose culture is not associated with oxidative stress, loss of β-cell enriched genes, or islet cell death

Intracellular Ca^{2+} homeostasis and mitochondrial membrane potential affect normal cell function and apoptosis (212). In addition, chronic hyperglycemia or glucotoxicity-induced oxidative stress is one of the main contributors to β-cell dysfunction. This involves transcriptional downregulation of the insulin genes, its key transcription factors such as Pdx-1 and MafA (67), glucose transporter 2 (Glut2) (213), glucose metabolism such as Gck (213,214), anti-apoptotic proteins including Bcl-x_L (213), and upregulation of mitochondrial bioenergetics proteins such as Ucp2 (215). We showed that NAC did not normalize islet $[Ca^{2+}]_i$ responses following 6 days high glucose culture, which suggests that the dysregulation may not be from oxidative stress. To clarify this, we further characterized overall islet pathophysiology in terms of superoxide production, cell death and gene expression after 6 days of 25 mM glucose culture compared to 11 mM glucose.

The results show that 6 days of 25G culture does not increase superoxide production and cell death (% efluor positive cells) in both BclxβWT and BclxβKO islets (Figure 8). Surprisingly, co-culture with 5 mM NAC strongly promotes superoxide production in islets (Figure 8A). This may be explained by previous studies, which indicated that NAC is protective against peroxides but not superoxide (209). Despite the increase in superoxide levels, no significant cell death is observed in islet cells of both genotypes co-cultured with NAC (Figure 8B). Perhaps islets are not sufficiently challenged to activate cell death by NAC-induced superoxide or NAC may have reduced hydrogen peroxide levels and so maintained overall ROS levels.

In addition, mRNA expression of several genes involved in regulation of insulin levels and secretion - Ins2, Pdx-1, MafA, Glut2, Gck, Ucp2 (Figure 8C) remain comparable across culture conditions and genotype. Lastly, Bcl-x_L transcript level remains significantly reduced in BclxβKO compared to WT controls after both 11G and 25G culture for 6 days (Figure 8C).

Figure 8.

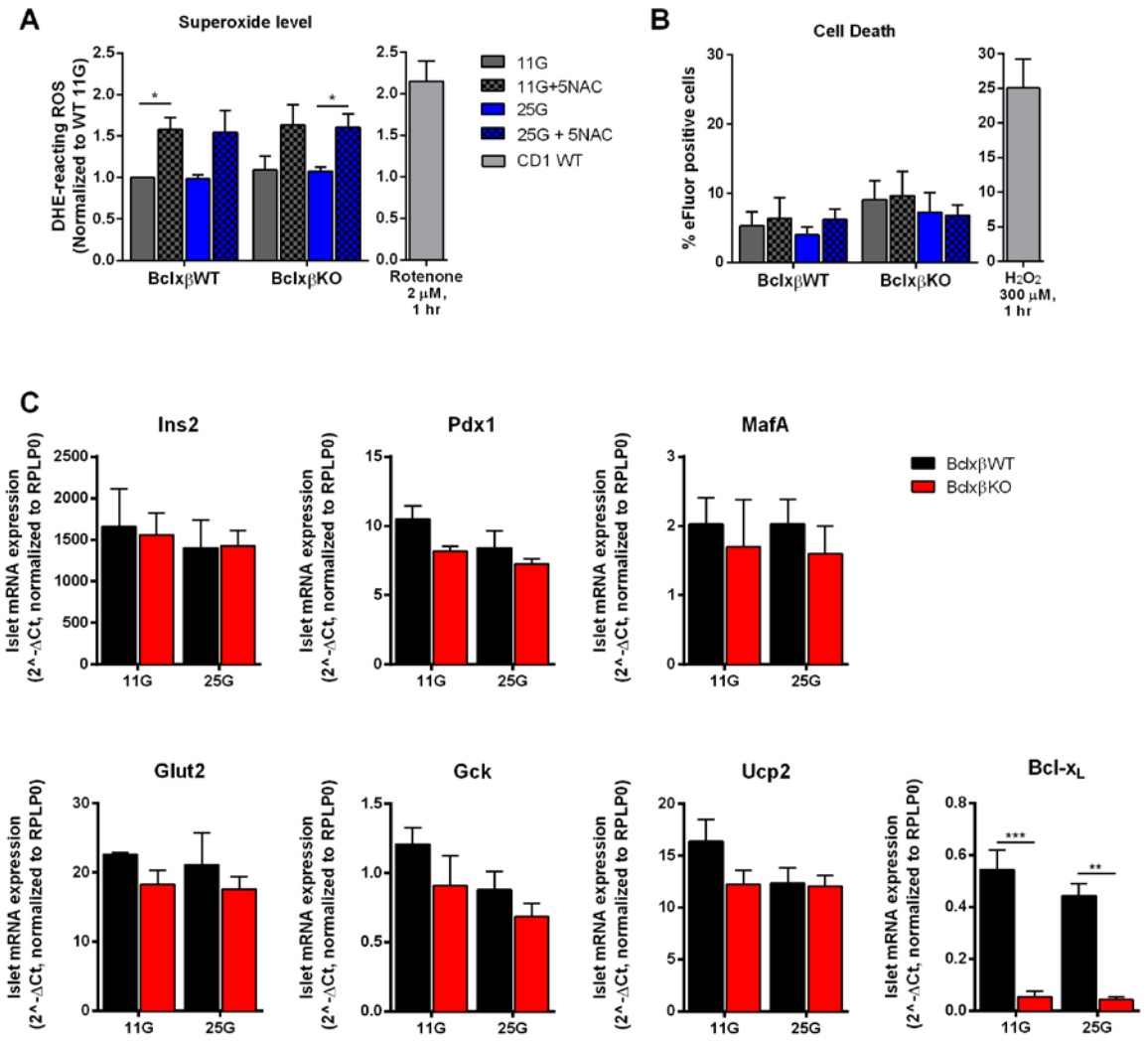

Figure 8. Loss of Bcl-x_L does not affect ROS production, cell death and gene expression under prolonged high glucose. Intact islets from BclxβWT and BclxβKO mice were culture for 6 days as indicated. (A, B) Prior to flow cytometry, islets were dispersed into single cells. (A) Cells were stained with the superoxide indicator DHE (20 μM) for 20 min. Rotenone (2 μM) was used to treat dispersed islet cells for 1 hour as a control for mitochondrial superoxide production. (B) Cells were co-stained with the viability dye eFluor780 for dead cells for 10 min after DHE staining. 300 μM H_2O_2 was used as a positive control for cell death. (C) At the end of 6 days culture, islet RNA was isolated, reverse transcribed into cDNA and expression of the selected genes were analyzed by Sybr RT-qPCR. (n = 3) (All data are presented as mean ± SEM)

3.1.7 Bcl-x_L protects islet cells against ribose- induced death but not against death under glucolipotoxic conditions

Bcl-x_L is a well-characterized anti-apoptotic member of the Bcl-2 family (216). It has been shown to protect β-cells against apoptosis resulting from chemical-induced ER stress, cytokines and gamma-irradiation (151,152). However its role in regulating β-cell survival under the oxidative stress associated with glucotoxicity or cell death induced by glucolipotoxic conditions remains unexplored.

Since culturing intact islets for 6 days in 25 mM glucose did not result in conditions of significant glucotoxicity, we used ribose, which is a highly reducing sugar, to induce oxidative stress in islets. This model is often used to study the effect of oxidative stress associated with glucotoxic conditions in β-cells (131,144,217). BclxβWT and BclxβKO islets were cultured for 4 days at 25 mM ribose (25R), 50 mM ribose (50R) or control 11 mM glucose (11G). At the end of each treatment, islets were dispersed into single cells for superoxide and cell death (% eFluor positive cells) measurements using flow cytometry. Our results demonstrate that only BclxβKO islets show an increase in superoxide production after 4 days culture with ribose at 25 mM and 50 mM (Figure 9A). In addition, 50 mM ribose treatment induces significantly more death of BclxβKO islet cells compared to BclxβWT cells (Figure9B), suggesting that Bcl-x_L prevents oxidative stress-induced cell death in this model.

We also investigated the effects of combined exposure to high glucose and fatty acids (glucolipotoxicity) on the survival of islet cells from BclxβWT and BclxβKO mice. Dispersed islet cells were cultured in regular 11 mM glucose, high 25 mM glucose, or in the presence of 25 mM glucose combined with 1.5 mM of the free fatty acid palmitate (in 6:1 molar ratio with BSA). In these experiments, the progression of islet cell death was imaged at 24, 48 and 72 hour time points based on propidium (PI) incorporation. In agreement with the results in Figure 8A, culture in high glucose for over 4 days does not induce significant death in islet cells from both BclxβWT and BclxβKO mice (Figure 9C). However, glucolipotoxic culture does induce significant islet cell death and, in contrast to ribose-induced death, BclxβKO islet cells are not more susceptible to this cell death than BclxβWT islet cells (Figure 9C).

Figure 9.

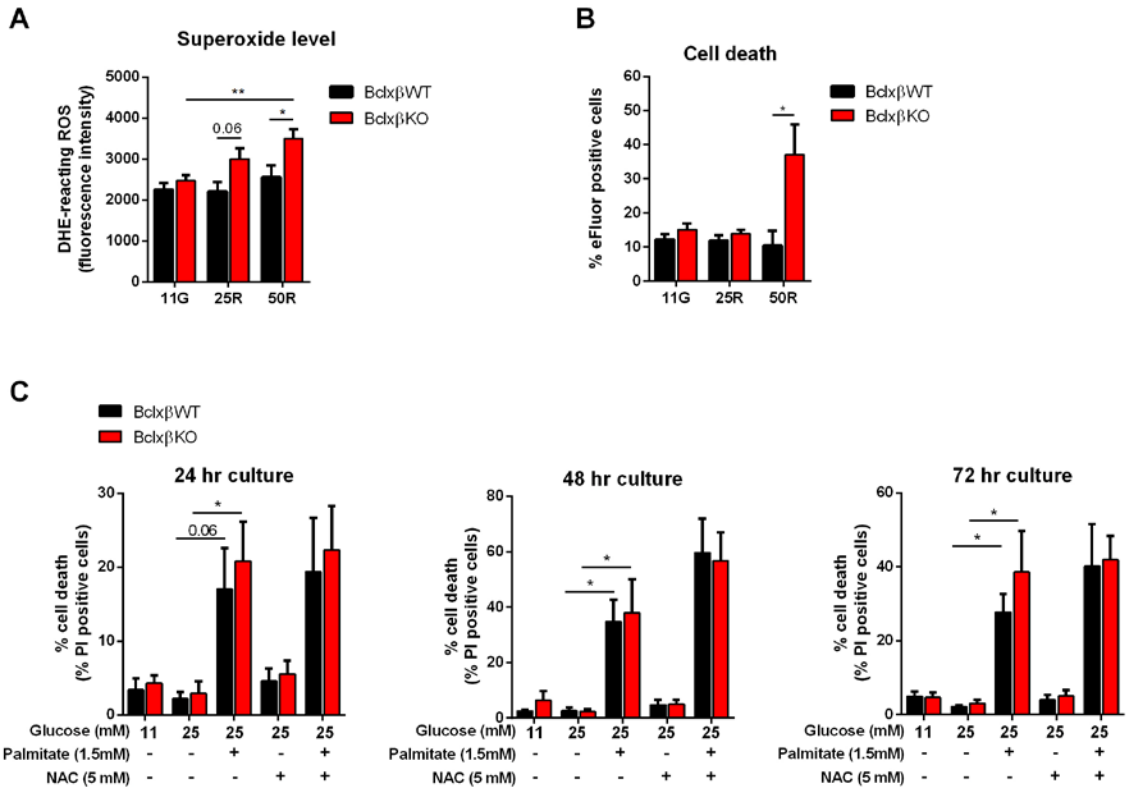

Figure 9. Bcl-x_L in gluco(lipo)toxic and oxidative stress-induced islet cell death. (A,B) Intact islets were cultured in regular 11 mM glucose (11G), 25 mM ribose (25R) or 50 mM ribose (50R) for 4 days. Prior to superoxide and cell death measurements by flow cytometry, islets were dispersed into single cells. (n = 4 - 11) (A) Islet single cells were stained with the superoxide indicator DHE (20 μM) for 20 min. Rotenone (2 μM) was used to treat dispersed islet cells for 1 hour as a control for mitochondrial superoxide production. (B) Islet single cells were co-stained with the viability dye eFluor780 for 10 min after DHE staining. 500 μM hydrogen peroxide was used as a positive control for cell death. (C) Dispersed islet single cells from BclxβWT and βKO islets were cultured as indicated in the presence of Hoecsht to stain for nuclei and propidium iodide (PI) to stain for dead cells. Total number of cells and dead cells were imaged by high content, high throughput microscope (IXM). Images were analyzed by CellProfiler, where cell death is presented as percentage of PI positive cells (n=3). (All data are presented as mean ± SEM)

3.2 Bcl-x_L Overexpression studies

3.2.1 Expression and localization of eYFP:Bcl-x_L

To further examine the effects of Bcl-x_L in primary islets cells, we have generated an adenovirus for overexpression of Bcl-x_L fused with a yellow fluorescence protein (Ad.eYFP:Bcl-x_L). To confirm that eYFP-tagged Bcl-x_L retain the mitochondrial localization reported of Bcl-x_L in β-cells (156,218), dispersed C57B6 WT mouse islets were transduced with Ad.eYFP:Bcl-x_L at MOI 5 for 24 hours. The islet cells were stained with using the mitochondria-specific fluorescence dye MitoTracker DeepRed and fluorescence was measured by confocal microscopy. eYFP fluorescence fom eYFP:Bcl-x_L mirrors the distribution of mitotracker staining (Figure 10A). eYFP florescence also strongly overlaps with the mitochondrial red fluorescence, suggesting that exogenous Bcl-x_L is expressed in the mitochondria (Figure 10B).

Figure 10.

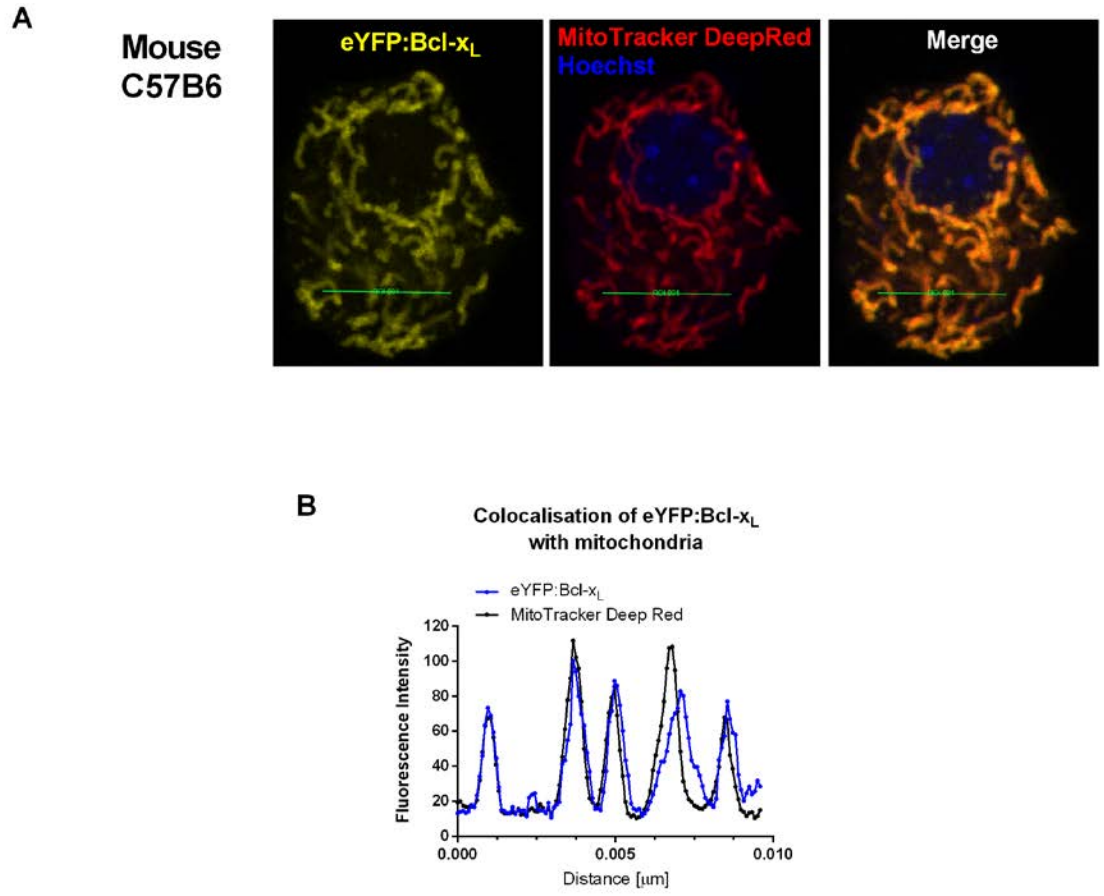

Figure 10. eYFP:Bcl-x_L localizes at the mitochondria of islet single cells. Dispersed islet cells from C57B6 mice were cultured on coverslips for 24 hours before transduction with Ad.eYFP:Bcl-x_L at MOI 5. After 24 hr of transduction, cells were stained with Hoechst (blue) and MitoTracker DeepRed (Red) for nuclei and mitochondria identification, respectively. (A) Representative confocal image of a single islet cell. (B) A histogram plot of fluorescence intensities across a line scan, as indicated in Figure 9A (green solid line), showing the degree of colocalisation between eYFP:Bcl-x_L (blue dotted line) and MitoTracker Deep Red (black dotted line).

3.2.2 Bcl-x_L overexpression impairs islet $[Ca^{2+}]_i$ responses and alters mitochondrial morphology

To further test the hypothesis that Bcl-x_L dampens metabolic activity, we overexpressed Bcl-x_L by transducing dispersed C67B6 mouse islets with Ad.eYFP:Bcl-x_L at MOI 5 or control virus Ad.eGFP at MOI 20. Ca^{2+} imaging was performed at 48 hour post transduction. Consistent with our Bcl-x_L knockout studies, eYFP:Bcl-x_L expression significantly reduces $[Ca^{2+}]_i$ response upon glucose stimulation and membrane depolarization by KCl (Figure 11A, B). Associated with eYFP:Bcl-x_L overexpression is the formation of mitochondrial clusters (Figure 11C). These clusters in eYFP:Bcl-x_L expressing cells appear to be aggregates of rounded and fragmented mitochondria (Figure 11D). Preliminary ultrastructural studies of MIN6 cells transfected with eYFP:Bcl-x_L show that mitochondria in some cells are aggregated into a large, highly dense and round structure with no visible defined cristae (Figure 11E, F). In contrast, mitochondria in other cells, which are likely to be non-transfected, are distributed across the cell (Figure 11G). Based on the distinct aggregates of mitochondria we observed by confocal microscopy we speculate that these abnormal mitochondria represent those of eYFP:Bcl-x_L overexpressing cell. In addition, superoxide measurements show a dose dependent increase with increasing transduction MOI of Ad.eYFP: Bcl-x_L (Figure 11H). Cells transduced with MOI 10 of Ad.eYFP:Bcl-x_L have almost double the level of superoxide compared to cells transduced with MOI 5 of Ad.eYFP:Bcl-x_L.

Figure 11.

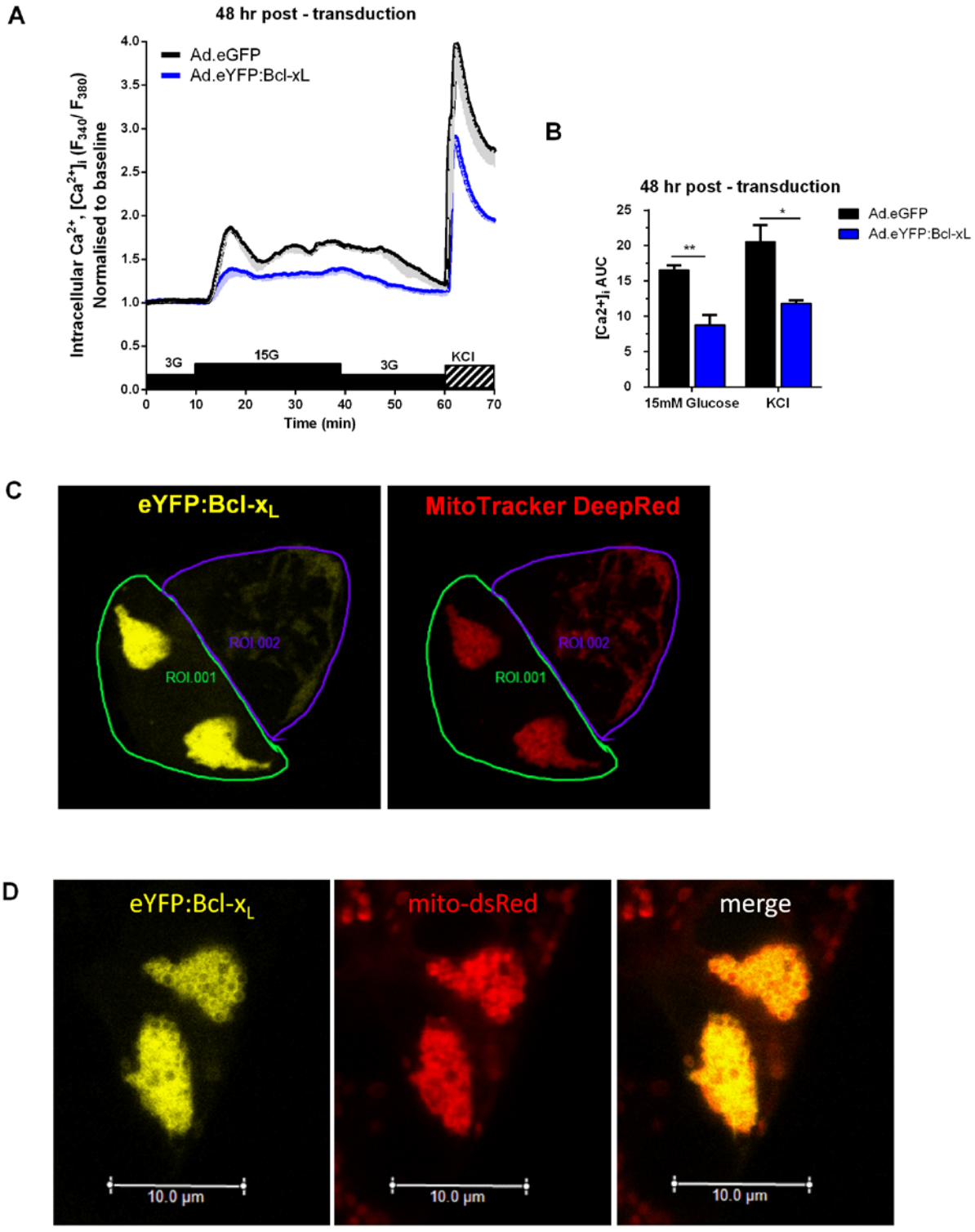
A
48 hr post - transduction
Ad.eGFP
Ad.eYFP:Bcl-xL
Intracellular Ca2+, [Ca2+]i (F340/ F380)
Normalised to baseline
3G
15G
3G
KCl
Time (min)
B
48 hr post - transduction
Ad.eGFP
Ad.eYFP:Bcl-xL
[Ca2+]i AUC
15mM Glucose
KCl
C
eYFP:Bcl-xL
MitoTracker DeepRed
ROI.002
ROI.001
D
eYFP:Bcl-xL
mito-dsRed
merge
10.0 µm

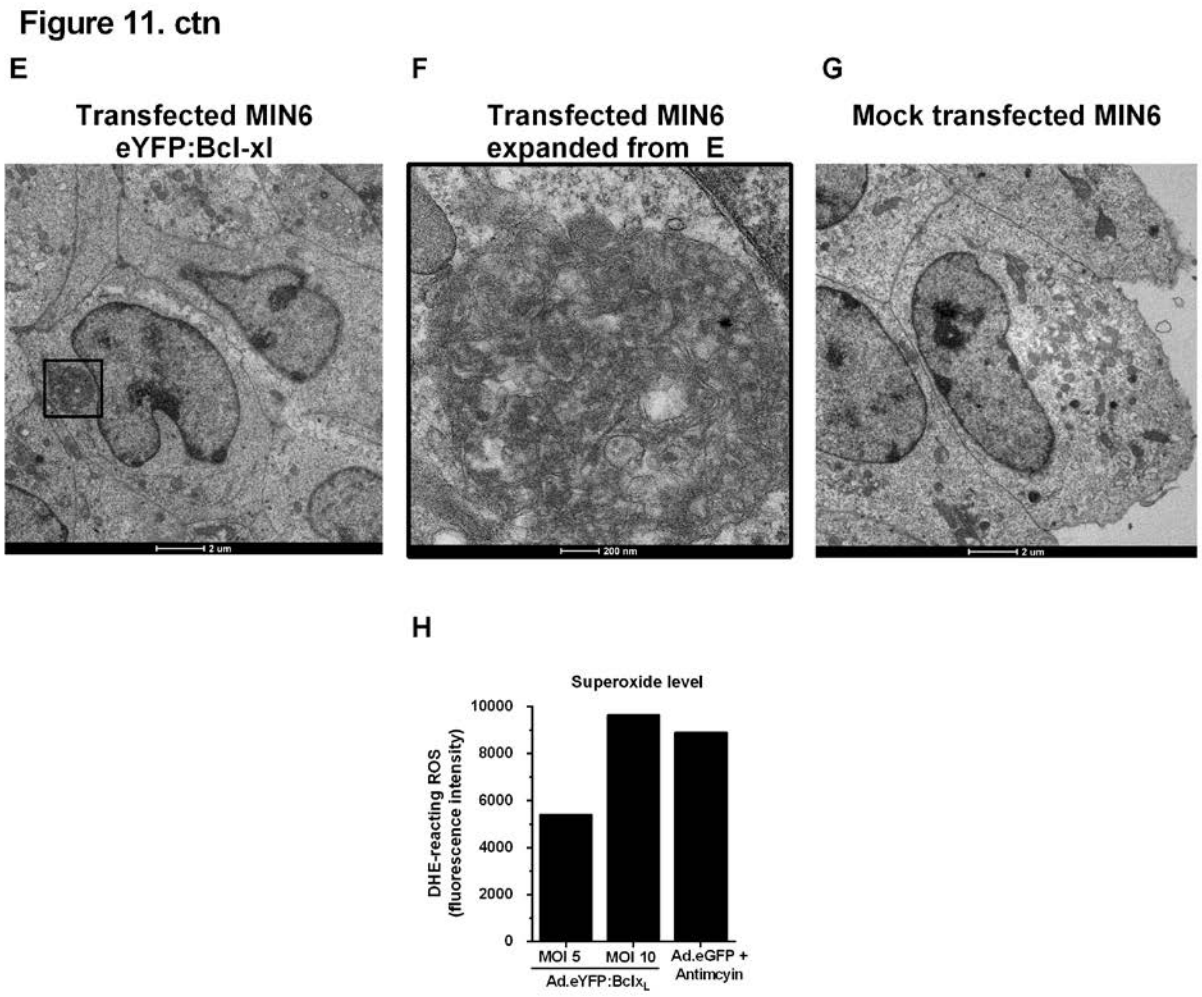

Figure 11. Overexpression of eYFP:Bcl-xL suppresses intracellular calcium signaling and alters mitochondrial morphology. Dispersed islets cells from WT C57B6 mice were transduced with Ad.eYFP:Bcl-x_L at MOI of 5. (A, B) At 48 hour post transduction, cells were stained with Fura-2 for Ca^{2+} imaging. (A) Traces of average cytosolic Ca^{2+} of eYFP:Bcl-x_L and eGFP control expressing cells. Shaded bars below data points represent SEM. (n=3) (B) Quantification of Ca^{2+} response to glucose and KCl as AUC (C) Representative confocal images and quantification of fluorescence intensities of dispersed islet cells expressing different levels of eYFP:Bcl-x_L (yellow) and morphology of mitochondria as identified by MitoTracker DeepRed (red). (D) MIN6 cells were co-transfected with eYFP:Bcl-x_L and a mitochondrial targeted red fluorescence protein Mito ds-Red. (E-G) Electron micrographs of MIN6 cells transfected with eYFP:Bcl-x_L. (n=1) (E) Preliminary image of cell displaying mitochondrial aggregation. (F) Enlarged image of insert in E of aggregated mitochondria. (G) Preliminary image of cell with normal distributed mitochondria. (H) Superoxide measurements of MIN6 cells transduced with Ad.eYFP:Bcl-x_L or control virus Ad.eGFP (n=1). (All data are presented as mean ± SEM)

Chapter 4: Conclusions

4.1 Overall summary and findings

This study used β-cell specific Bcl-x knockout mice and overexpression of exogenous Bcl-x_L to provide evidence for novel non-apoptotic roles of Bcl-x_L in islet β-cells, as well as for the apoptotic functions of Bcl-x_L in β-cells under oxidative stress. Our results further reinforce the hypothesis that endogenous Bcl-x_L dampens β-cell mitochondrial metabolism as reported previously and maintain intracellular calcium homeostasis (156). We demonstrated that endogenous Bcl-x_L reduces superoxide levels and protects β-cells against death during the oxidative stress induced by supraphysiological levels of the highly reducing sugar, ribose. Moreover, overexpression of Bcl-x_L suppresses intracellular calcium signaling in response to glucose stimulation and membrane depolarization, which is associated with significant changes in mitochondrial structure and preliminary indications of increased superoxide production. This suggests that both too low and too high levels of Bcl-x_L can result in dysregulation of β-cell mitochondrial function and ROS levels. Finally, we identified that Bcl-x_L deletion does not sensitize β-cells to death under glucolipotoxic conditions of up to 72 hours, in contrast to a significant sensitization during ribose treatment.

4.2 Discussion

In order to determine the physiological role of Bcl-x_L in β-cell under both healthy and metabolically stressful conditions, we examined the effects of both 2 and 6 days culture in normal condition (11 mM glucose) and high glucose (25 mM) on intracellular Ca^{2+} homeostasis, mitochondrial membrane potential ($\Delta\psi_m$), superoxide production and cell death. In addition, we also overexpressed exogenous Bcl-x_L (eYFP:Bcl-x_L) in islet cells to examine its effects on Ca^{2+} responses, mitochondria morphology and superoxide production. Lastly, we identified the roles of Bcl-x_L in islet cell death under ribose-induced oxidative stress and glucolipotoxicity.

4.2.1 Function of Bcl-x_L in islets under normal culture

After 2 days of normal culture in 11 mM glucose, we observed an oscillatory $[Ca^{2+}]_i$ response to glucose in BclxβWT islets but a non-oscillatory and non-biphasic plateau $[Ca^{2+}]_i$ response in BclxβKO islets (Figure 2A). Electrophysiological and imaging studies of glucose-stimulated islets have shown that when healthy islets are stimulated with a moderate level of glucose such as 11 mM, they commonly respond with cycles of oscillating cytosolic Ca^{2+} due to periodic bursts of membrane depolarization (219). Islets stimulated with higher concentration of glucose (20 mM or higher), on the other hand respond with a rapid spike in $[Ca^{2+}]_i$, which quickly plateaus and sustains throughout the duration of glucose stimulation, and this reflects a continuous electrical spiking activity (219). The change from oscillatory to plateau Ca^{2+} response reflects the thresholds for glycolytic and electrical oscillations during glucose metabolism (220). Based on this model, the different $[Ca^{2+}]_i$ patterns seen in response to 15 mM glucose between BclxβWT and BclxβKO islets are likely to reflect islet sensitivity to glucose, where islets deficient in Bcl-x_L are metabolically more sensitive. This is also consistent with previously published data which shows that dispersed islet single cells deficient in Bcl-x_L have increased $[Ca^{2+}]_i$ response to 10 mM glucose compared WT controls (156). Moreover, it fits with the trend towards higher $\Delta\psi_m$ we observed under both basal and glucose-stimulated conditions, although this did not reach statistical significance (Figure 3). Lastly, we also overexpressed Bcl-x_L in dispersed C57B6 islet cells, which showed suppressed $[Ca^{2+}]_i$ response to glucose compared to control (Figure 11A,B), suggesting metabolic inhibition by Bcl-x_L.

4.2.2 Function of Bcl-x_L in islets during prolonged culture under high glucose

When glucose concentration in culture media was raised from 11 mM to 25 mM for 2 days, both BclxβWT and BclxβKO islets displayed a small but significant increase in basal $[Ca^{2+}]_i$. (Figure 4A, B). In addition, the ability of islets to restore basal $[Ca^{2+}]_i$ levels after glucose-stimulation was significantly hampered in BclxβKO islets, and similar trend occured in BclxβWT islets (Figure 4A, B). Such effects of high glucose and Bcl-x_L ablation on islet $[Ca^{2+}]_i$ homeostasis were further potentiated after 6 days. Basal $[Ca^{2+}]_i$ of BclxβWT islets cultured at 25 mM glucose for 6 days was significantly higher and the islet $[Ca^{2+}]_i$ recovery after a glucose washout was

impaired compared to those cultured in normal 11 mM glucose media (Figure 5A, B), and the observed $[Ca^{2+}]_i$ perturbations were furthered exacerbated in BclxβKO islets (Figure 5A,B). These high glucose-induced $[Ca^{2+}]_i$ changes were also associated with a trend towards increased $\Delta\psi_m$ (Figure 5C) and insulin secretion (Figure 5D) under basal glucose conditions in islets of both genotype, although the basal effect did not reach statistical significance. BclxβKO islets in particularly had a significantly higher insulin secretion during glucose washout i.e. the recovery period, and trended towards higher $\Delta\psi_m$ compared to BclxβWT islets (Figure 5C). Lastly, these changes in islet β-cell physiology after 6 days of high glucose did not appear to be due to increased glucose-induced oxidative stress since they were not prevented by the antioxidant NAC (Figure 7) and we did not observe any increase in superoxide production, cell death, or reduced expression of genes that are important for β-cell function (Figure 8). Instead of glucotoxicity, which irreversibly impairs insulin secretion, our model of prolonged high glucose culture is likely to reflect changes that are observed during an early stage of prediabetes.

Prediabetes is a period at which insulin production is increased to compensate for insulin resistance (12), in which increase β-cell mass is a major adaption to achieve this. In addition to β-cell hyperplasia, functional physiology of β-cells also undergoes significant adaptations to promote insulin secretion. Ob/ob mice are often used as a model of prediabetes since these mice are glucose intolerant, insulin resistant, have high circulating insulin and normal fasting blood glucose level but elevated post-meal blood glucose level (221). A recent study has demonstrated that the metabolic activity of β-cells from female ob/ob mice is increased in order to enhance overall insulin secretion (222). These metabolic adaptions include increases in glucose-stimulated NAD(P)H level, Ca^{2+} response and $\Delta\psi_m$ compared to lean controls (222). In addition, ob/ob islets also lack oscillatory Ca^{2+} response compared to control islets (222). These observations are in some ways similar to our results with high glucose culture, especially in islets deficient of Bcl-x_L. However, we did not observe significant increases in insulin gene expression, content and secretion with 6 days high glucose culture or genotypic differences, which were found in ob/ob mice. It is possible that the time point and glucose concentration we used in this study are inducing an earlier stage of the prediabetic phenotype. Therefore, our results suggest that Bcl-x_L suppresses islet metabolic activities, which are part of β-cell adaptation to compensate for insulin resistance during prediabetes.

The mechanisms by which Bcl-x_L regulates mitochondrial activities in islet β-cells may be similar to that in neurons, as they are both highly dependent on glucose for their normal functions. In neurons, Bcl-x_L is found to stabilize $\Delta\psi_m$, physically interact with ATP synthase and increase ATP production efficiency (164,165). More specifically Bcl-x_L interacts with the β-subunit of F_0F_1 ATP synthase, promotes proton flux across mitochondrial inner membrane, inhibits superfluous ion flux and therefore prevents potentially harmful fluctuations in $\Delta\psi_m$ and improves ATP synthesis as an adaptive mechanism to cellular stress (164,165). Our conclusion that Bcl-x_L dampens mitochondrial metabolic activity in islets therefore appears contradictory to these studies. However, studies on tumor cells show that Bcl-x_L reduces glucose-derived citrate, α-ketoglutarate and overall cytosolic acetyl-CoA levels (223). Both acetyl-CoA and citrate are important intermediates of the TCA cycle to produce reducing equivalents for ATP production during oxidative phosphorylation (204). If the observation that Bcl-x_L suppresses the production of acetyl-CoA and other TCA cycle intermediates also applies to islet β-cells, then this is a possible mechanism by which Bcl-x_L suppresses islet mitochondrial metabolism, including under prolonged high glucose stress.

The mechanisms of Bcl-x_L on mitochondrial metabolic pathways could very likely also contribute to the effects of high glucose culture on the basal and glucose-stimulated $[Ca^{2+}]_i$ that were amplified in BclxβKO islets compared to BclxβWT islets. However, Bcl-x_L may also directly regulate Ca^{2+} flux through channels in the mitochondria or the ER such as the voltage dependent anionic channel (VDAC) (171,172) or inositol 1,4,5-triphosphate receptor ($InsP_3R$) (159,161,170), respectively. VDAC is abundantly expressed in the outer mitochondrial membrane to facilitate metabolite transport between the mitochondrial intermembrane space and the cytosol (224). In its opened state, VDAC facilitates metabolites such as ATP transport into the cytosol, while a closed VDAC prevents ATP transport but promotes Ca^{2+} uptake into the mitochondria (224). Bcl-x_L has been shown to physically interact with VDAC (225) to regulate mitochondrial Ca^{2+} uptake under both basal and apoptotic conditions (159–161,170). For instance, it has been reported that the BH-4 domain of Bcl-x_L interacts with the N-terminal of VDAC and promote a closed state and mitochondrial Ca^{2+} uptake (160,161,170), while another group, in contrast, has shown that Bcl-x_L promotes an opened VDAC to prevent mitochondrial Ca^{2+} overload and therefore apoptosis (159). Despite a lack of consensus on the effect of Bcl-x_L

on VDAC conformations and activities, it will be worthwhile to test whether the impaired $[Ca^{2+}]_i$ recovery in BclxβKO islets is due to suppression on mitochondrial Ca^{2+} uptake using a mitochondria-specific Ca^{2+} probe such as Rhod-2 (226). If this is the case, it would seem likely that Bcl-x_L promotes a closed form of VDAC to promote Ca^{2+} uptake into the mitochondria. Apart from the mitochondria, the ER is another major calcium buffering organelle (227). Bcl-x_L has been shown to bind $InsP_3R$ and enhance Ca^{2+} release from the ER (171,172). It is unlikely that the inability of BclxβKO islets to restore Ca^{2+} homeostasis during glucose washout is due to such Bcl-x_L- facilitated Ca^{2+} release from the ER, as loss of such release mechanisms would be expected to reduce, not increase, intracellular Ca^{2+} levels.

The results from NAC treatment (Figure 7) and, superoxide measurements after 6 days of high glucose culture (Figure 8A), suggest that ROS or oxidative stress did not contribute to the high glucose-induced dysregulation of islet $[Ca^{2+}]_i$ at the time-points examined. However, a lack of observable increase in superoxide level could possibly be attributed to superoxide conversion into hydrogen peroxide via MnSOD. Therefore additional ROS measurements using 2',7'-dichlorofluorescein (H2DCF) to detect hydrogen peroxides (228) may provide information on the overall contribution of different ROS to islet dysfunction after prolonged high glucose culture. Having said that, it is unlikely that the observed $[Ca^{2+}]_i$ dysregulation is due to increased hydrogen peroxide since NAC, which predominately reduces hydrogen peroxide by increasing cellular glutathione level, did not prevent the islet $[Ca^{2+}]_i$ dysregulation (Figure 7).

4.2.3 Function of Bcl-x_L in islets during oxidative stress associated with glucotoxicity

To test the role of Bcl-x_L in oxidative stress, we treated intact BclxβWT and BclxβKO islets with the highly reducing sugar ribose at 25 mM or 50 mM for 4 days. Loss of Bcl-x_L in islet β-cells significantly increased ribose-mediated superoxide production and cell death (Figure 9).

The mechanisms in which Bcl-x_L prevents ribose induced ROS production and islet β-cell death may involve mitochondrial metabolism since ribose can be converted into glucose via the pentose phosphate pathway (229). Our data from prolonged high glucose culture support the dampening effect of Bcl-x_L on mitochondrial metabolic activities, which will theoretically reduce the semi-reduction of oxygen into superoxide ions. However, while both glucose and ribose are inducers of ROS, the mechanisms involved could also be different. Glucose largely promotes mitochondrial ROS during oxidative phosphorylation while ribose has mostly been reported to promote non-mitochondrial ROS through formation of advanced glycation end products (AGEs) in the cytosol of β-cell lines (217,230,231). Various methods are available to identify whether Bcl-x_L protection against ribose-induced superoxide production is specifically mitochondrial. For example, the use of MitoSox, which is a mitochondrial specific superoxide fluorescent indicator (232) and the use of mitochondrial specific ROS scavengers such as MnTBAP, MitoQ (233) and others.

Alternatively, Bcl-x_L may exert antioxidant activities through modulation of mitochondrial morphology and membrane integrity via interactions with other redox-regulated proteins such as reactive oxygen species modulator 1 (ROMO1) and mitochondrial fusion proteins such as mitofusins (Mfn), which have been identified as binding partners of Bcl-x_L (176,182). ROMO1 has shown to respond to oxidative stress and recruits Bcl-x_L in order to maintain $\Delta\psi_m$, and therefore prevent apoptosis (176,177). More recently, ROMO1 was demonstrated to couple oxidative stress to mitochondrial morphology by promoting fusion activities of OPA1 at the mitochondrial inner membrane (234). Given the intricate relationships between mitochondria morphology, metabolic activities, apoptosis and the implications of Bcl-x_L in these pathways, additional analysis of these mechanisms of BclxβWT and BclxβKO islets after ribose treatment will be valuable to understand how Bcl-x_L protects islet cell death against ribose-induced oxidative stress.

4.2.4 Function of Bcl-x_L in islets survival during glucolipotoxic stress

It was previously reported that in human islets, after 5 days of high glucose culture (16.7 mM) Bcl-x_L expression was downregulated while Bcl-2 levels remained unchanged (66), indicating that Bcl-x_L but not Bcl-2 is a target of glucotoxicity at the transcriptional level. Our finding, that deletion of Bcl-x_L sensitizes β-cells to ribose-induced oxidative stress and death, suggests that such downregulation of endogenous Bcl-x_L under glucotoxicity may be a contributing event in the resulting β-cell apoptosis. Our result that BclxβKO islet cells did not die more under combined glucolipotoxic conditions indicate that it is possible that other antiapoptotic proteins such as Bcl-2 and Mcl-1 play a more important role than Bcl-x_L in preventing glucolipotoxic β-cell apoptosis. Future experiments on the expression level of Bcl-x_L and other Bcl-2 family members remained in BclxβWT relative to BclxβKO islets after glucolipotoxicity will provide insight on the dynamic regulation of apoptosis under these stress conditions.

Our results also raise the question of what the relative contributions of apoptosis and other cell death pathways are under the various conditions of β-cell stress. Although apoptosis is by far the most characterized form of β-cell death under glucolipotoxic and other stress conditions, necrosis or other pathways of programmed cell death, such as autophagic cell death and programmed necrosis, may potentially be involved (91,235). Since our cell death experiments were based on PI or eFluor incorporations, which label any dead cells with damaged plasma membrane, late-stage apoptotic cell death cannot be distinguished from necrosis or other forms of cell death. However, unpublished data from our lab suggest that glucolipotoxicity can also kill Bax-Bak double knockout β-cells, which strongly indicates involvement of non-apoptotic death (191). Additional apoptosis specific detection methods such as cleaved caspase 3/7, annexin V or TUNEL assays, and pathway-specific inhibitors, will be required to conclusively establish the relative contribution of apoptotic and non-apoptotic islet cell death under glucolipotoxicity.

4.2.5 Function of Bcl-x_L in mitochondrial morphology

The generation of an adenovirus expressing a fluorescently tagged Bcl-x_L (Ad.eYFP:Bcl-xL) is a useful tool to study its role in primary islet cells as well as allowing me to visually identify islet cells overexpressing exogenous Bcl-x_L and compare these to cells expressing only endogenous Bcl-x_L. One of the interesting findings in our overexpression study is that high levels of Bcl-x_L promoted the formation of mitochondrial aggregates, which may be associated with higher superoxide production.

Consistent with studies on Bcl-x_L localization, our data showed that the fluorescent-tagged Bcl-x_L was found in islet mitochondria (156). It is widely acknowledged that endogenous Bcl-x_L localizes in the mitochondrial outer membrane in order to control mitochondrial membrane permeability (236). However, Bcl-x_L has also been found in the inner mitochondrial membranes, where it is reported to stabilize membrane potential in neurons (164,165). Since our result was based on mitochondria-specific fluorescence staining using MitoTracker DeepRed and was limited to the magnification power of confocal imaging, it was difficult to distinguish the precise localization of Bcl-x_L within the islet mitochondria. We observed that cells with high levels of fluorescence eYFP:Bcl-x_L displayed aggregation of what appeared to be fragmented mitochondria. Our results were consistent with previous studies, which provide evidence for a role of Bcl-x_L in regulating mitochondrial morphology through its C-terminal transmembrane domain (183,237). The effects of eYFP:Bcl-x_L overexpression on mitochondria aggregation is likely to be mediated through interaction between Bcl-x_L and mitochondrial fusion-fission proteins, as Bcl-x_L has been shown to mediate extensive mitochondrial fusion through interaction with mitofusions 1 & 2 (182,238).

It is worth noting that one study has reported that co-expression of Bcl-2 family proteins including Bcl-x_L with GFP causes mitochondrial aggregation and promotes apoptosis, while they found that other variants of GFP, such as eGFP and eYFP do not alter mitochondrial morphology (239). Moreover, the mitochondrial aggregation in the presence of GFP requires the C-terminal of Bcl-x_L, suggesting that physical interaction between Bcl proteins and fluorescence proteins can have notable consequences in mitochondrial dynamics and functional activities. In addition to primary islet cells transduced with Ad.eYFP:Bcl-x_L, we found that mitochondrial aggregation

also occurs in MIN6 cells where eYFP:Bcl-x_L was overexpressed by lipofectamine-based transfection. In preliminary experiments we have not seen such mitochondrial aggregation in MIN6 cells after similar overexpression of a mitochondria-targeted YFP, indicating the effect is Bcl-x_L-dependent. To conclusively confirm that mitochondrial aggregation is indeed mediated through Bcl-x_L but not eYFP, an ideal control will be a mitochondrial targeted eYFP. An alternative approach is to overexpress native form of Bcl-x_L i.e. untagged Bcl-x_L and analyze its localization and associated mitochondrial morphology by immunohistochemistry.

4.2.6 Effects of NAC on islets mitochondrial physiology

The studies of hyperglycemia with NAC treatment have yielded some interesting results and questions on the relative contribution of superoxide and peroxide ROS species in islet mitochondrial dysfunction and the potential relevance of using NAC as an antioxidant in islet physiology. After culturing islets for 6 days in high glucose at 25 mM, co-culture with 5 mM NAC significantly elevated basal, peak and average steady state $[Ca^{2+}]_i$ response to glucose as well as $\Delta\psi_m$ in BclxβWT islets only (Figure 7A,B,C). In addition, NAC treatment alone significantly increased superoxide production in both BclxβWT and BclxβKO islets under normal 11G culture, and a trend was seen towards higher superoxide production in high glucose culture (Figure 7D). Despite increase in superoxide production, there was no observable islet cell death with NAC treatment (Figure 7E).

Although NAC is a well-known antioxidant, the precise mechanisms by which NAC inhibits cytosolic versus mitochondrial ROS, and also superoxide versus hydrogen peroxide remain ambiguous. NAC is thought mostly to scavenge hydrogen peroxides, as it is a precursor of glutathione, which together with glutathione peroxidase, reduce hydrogen peroxides into water (208). It is possible that the effects of NAC on islet mitochondrial metabolism are related to the fact that NAC promotes biosynthesis of glutathione, as this can affect the mitochondrial uncoupling protein Ucp2 (240). In islets, Ucp2 activity is induced by ROS as a feedback mechanism to suppress the mitochondrial superoxide production that occurs during coupled respiration. A recent study has shown that Ucp2 activity is post-translationally regulated by

glutathionylation, which is the formation of a disulphide bond between the thiol group of the protein to glutathione. Reversible glutathionylation of Ucp2 serves as a redox sensor of local ROS production and Ucp2 glutathionylation inhibits proton leak, which acutely promotes local superoxide production acutely and amplifies glucose-stimulated insulin secretion in β-cells (240). Conveivably, NAC may therefore increase glucose-induced $\Delta\psi_m$ and superoxide production via glutathione-dependent inhibition of Ucp2.

In summary, in addition to the canonical role of Bcl-x_L in regulating apoptosis, Bcl-x_L affects β-cell function. Previously, Luciani et al (156) provided evidence for a metabolic dampening effects of endogenous Bcl-x_L in β-cells cultured under physiological conditions. This thesis has provided additional evidence to support the dampening effect of Bcl-x_L in β-cells in terms of mitochondrial membrane potential, intracellular Ca^{2+} and insulin homeostasis, particularly under conditions of prolonged exposure to high glucose. Since Bcl-x_L may preserve β-cell survival at the cost of β-cell function, caution may be warranted caution when considering the effectiveness of exploiting Bcl-x_L as a therapeutic target for diabetes treatments. Further studies will be required to determine the mechanisms by which Bcl-x_L dampens metabolism and affects overall β-cell physiology, as well as the potential contribution of Bcl-x_L-dependent effects in the pathogenesis of type 2 diabetes.

References

1. International Diabetes Federation. IDF Diabetes Atlas update poster, 6th edn. Brussels, Belgium: International Diabetes Federation, 2014.

2. Mathers CD, Loncar D. Projections of global mortality and burden of disease from 2002 to 2030. PLoS Med. 2006;3(11):2011–30.

3. Goldenberg R, Punthakee Z. Definition, Classification and Diagnosis of Diabetes, Prediabetes and Metabolic Syndrome. Can J Diabetes. 2013;37:8–11.

4. Wållberg M, Cooke A. Immune mechanisms in type 1 diabetes. Trends Immunol. 2013;34(12):583–91.

5. Noble JA, Erlich HA. Genetics of type 1 diabetes. Cold Spring Harbor perspectives in medicine. 2012. p. 485–94.

6. Rosenfeld L. Insulin: discovery and controversy. Clin Chem. 2002;48:2270–88.

7. Liew A, O'Brien T. The potential of cell-based therapy for diabetes and diabetes-related vascular complications. Curr Diab Rep. 2014;14(3).

8. Services C for DC and PUSD of H and H. National diabetes fact sheet: national estimates and general information on diabetes and prediabetes in the United States, 2011. 2011;CS217080A:1–12.

9. Prentki M, Nolan CJ. Islet β cell failure in type 2 diabetes. J Clin Invest. 2006;116(7):1802–12.

10. Boden G. Obesity, insulin resistance and free fatty acids. Curr Opin Endocrinol Diabetes Obes. 2011;18:139–43.

11. Boden G, Chen X, Ruiz J, White J V, Rossetti L. Mechanism of fatty acid-induced inhibition of glucose uptake. J Clin Invest. 1994;93:2438–46.

12. Tabák AG, Herder C, Rathmann W, Brunner EJ, Kivimäki M. Prediabetes: A high-risk state for diabetes development. Lancet. 2012;379:2279–90.

13. Pierce M, Keen H, Bradley C. Risk of Diabetes in Offspring of Parents with Non-insulin-dependent Diabetes. 1995;6–13.

14. Stumvoll M, Goldstein BJ, van Haeften TW. Type 2 diabetes: principles of pathogenesis and therapy. Lancet. 2010;365:1333–46.

15. Froguel BA. Perspective Rare and Common Genetic Events in Type 2 Diabetes : What Should Biologists Know? Cell Metab. 2015;1–12.

16. Aronoff SL, Berkowitz K, Shreiner B, Want L. Glucose Metabolism and Regulation: Beyond Insulin and Glucagon. Diabetes Spectr. 2004;17:183–90.

17. Canadian Diabetes Association Clinical Practice Expert Committee. Canadian Diabetes Association 2013 Clinical Practice Guidelines for the Prevention and Management of Diabetes in Canada. Can J Diabetes. 2013;37:212.

18. Robertson RP, Harmon J, Tran PT, Poitout V. β-cell glucose toxicity,lipotoxicity,and chronic Oxidative Stress in Type 2 Diabetes. Diabetes. 2004;53(9):S119–24.

19. Steiner DJ, Kim A, Miller K, Hara M. Pancreatic islet plasticity: Interspecies comparison of islet architecture and composition. Islets. 2010;2(3):135–45.

20. Hauge-Evans AC, King AJ, Carmignac D, Richardson CC, Robinson ICAF, Low MJ, et al. Somatostatin secreted by islet δ-cells fulfills multiple roles as a paracrine regulator of islet function. Diabetes. 2009;58:403–11.

21. Molina J, Rodriguez-Diaz R, Fachado A, Silva CJ-, Berggren P-O, Caicedo A. Control of Insulin Secretion by Cholinergic Signaling in the Human Pancreatic Islet. Diabetes. 2014;63(August):2714–26.

22. Kaiser D, Oetjen E. Something old, something new, and something very old - drugs for treating type 2 diabetes. Br J Pharmacol. 2014;49(171):2940–50.

23. Stein SA, Lamos EM, Davis SN. A review of the efficacy and safety of oral antidiabetic drugs. Expert Opin Drug Saf. 2013;12(2):153–75.

24. Seino Y, Fukushima M, Yabe D. GIP and GLP-1, the two incretin hormones: Similarities and differences. J Diabetes Investig. 2010;1(1):8–23.

25. Lund PK. The discovery of glucagon-like peptide 1. Regul Pept. 2005;128:93–6.

26. Pederson RA, Brown JC. Interaction of gastric inhibitory polypeptide, glucose, and arginine on insulin and glucagon secretion from the perfused rat pancreas. Endocrinology. 1978;103:610–5.

27. Butler AE, Janson J, Bonner-weir S, Ritzel R, Rizza RA, Butler PC. Beta-Cell Deficit and Increased beta-Cell Apoptosis in Humans With Type 2 Diabetes. 2003;52(January).

28. O'Hagan C, De Vito G, Boreham C a G. Exercise prescription in the treatment of type 2 diabetes mellitus: Current practices, existing guidelines and future directions. Sport Med. 2013;43:39–49.

29. Fu Z, Gilbert ER, Liu D. Regulation of insulin synthesis and secretion and pancreatic beta-cell dysfunction in diabetes. Curr Diabetes Rev. 2013;9(1):25–53.

30. Vaulont S, Vasseur-Cognet M, Kahn a. Glucose regulation of gene transcription. J Biol Chem. 2000;275:31555–8.

31. Steiner DF. Pancreatic Beta Cell in Health and Disease - The Biosynthesis of Insulin [Internet]. 2008. 31-49 p. Available from: http://www.springerlink.com/index/10.1007/978-4-431-75452-7

32. Rhodes CJ, White MF. Molecular insights into insulin action and secretion. Eur J Clin Invest. 2002;32 Suppl 3:3–13.

33. Macfarlane WM, McKinnon CM, Felton-Edkins Z a., Cragg H, James RFL, Docherty K. Glucose stimulates translocation of the homeodomain transcription factor PDX1 from the cytoplasm to the nucleus in pancreatic beta-cells. J Biol Chem. 1999;274(2):1011–6.

34. Kishi A, Nakamura T, Nishio Y, Maegawa H, Kashiwagi A. Sumoylation of Pdx1 is associated with its nuclear localization and insulin gene activation. Am J Physiol Endocrinol Metab. 2003;284:E830–40.

35. Iype T, Francis J, Garmey JC, Schisler JC, Nesher R, Weir GC, et al. Mechanism of insulin gene regulation by the pancreatic transcription factor Pdx-1: Application of pre-mRNA analysis and chromatin immunoprecipitation to assess formation of functional transcriptional complexes. J Biol Chem. 2005;280(17):16798–807.

36. Stoffers D, Ferrer J, Clarke WL, Habener JF. Early-onset type-II diabetes mellitus (MODY4) linked to IPF1. Nature genetics. 1997. p. 138–9.

37. Vanderford NL. Regulation of beta-cell-specific and glucose-dependent MafA expression. Islets. 2011;3(January 2015):35–7.

38. Matsuoka T, Artner I, Henderson E, Means A, Sander M, Stein R. The MafA transcription factor appears to be responsible for tissue-specific expression of insulin. Proc Natl Acad Sci U S A. 2004;101:2930–3.

39. Zhao L, Guo M, Matsuoka TA, Hagman DK, Parazzoli SD, Poitout V, et al. The islet beta cell-enriched MafA activator is a key regulator of insulin gene transcription. J Biol Chem. 2005;280(12):11887–94.

40. Zhang C, Moriguchi T, Kajihara M, Esaki R, Harada A, Shimohata H, et al. MafA is a key regulator of glucose-stimulated insulin secretion. Mol Cell Biol. 2005;25(12):4969–76.

41. Guo S, Dai C, Guo M, Taylor B, Harmon JS, Sander M, et al. Inactivation of specific β cell transcription factors in type 2 diabetes. J Clin Invest. 2013;123(8):3305–16.

42. Matsuoka T, Kaneto H, Kawashima S, Miyatsuka T, Tochino Y, Yoshikawa A, et al. Preserving Mafa expression in diabetic islet β-cells improves glycemic control in vivo. J Biol Chem. 2015;jbc.M114.595579.

43. Ohneda K, Mirmira RG, Wang J, Johnson JD, German MS. The homeodomain of PDX-1 mediates multiple protein-protein interactions in the formation of a transcriptional activation complex on the insulin promoter. Mol Cell Biol. 2000;20(3):900–11.

44. Andrali SS, Qian Q, Özcan S. Glucose mediates the translocation of neuroD1 by O-linked glycosylation. J Biol Chem. 2007;282:15589–96.

45. Fajans SS, Bell GI, Polonsky KS. Molecular mechanisms and clinical pathophysiology of maturity-onset diabetes of the young. N Engl J Med. 2001;345(13):971–80.

46. Le Lay J, Stein R. Involvement of PDX-1 in activation of human insulin gene transcription. J Endocrinol. 2006;188:287–94.

47. Aramata S, Han SI, Yasuda K, Kataoka K. Synergistic activation of the insulin gene promoter by the beta-cell enriched transcription factors MafA, Beta2, and Pdx1. Biochim Biophys Acta - Gene Struct Expr. 2005;1730:41–6.

48. Poitout V, Olson LK, Robertson RP. Chronic exposure of betaTC-6 cells to supraphysiologic concentrations of glucose decreases binding of the RIPE3b1 insulin gene transcription activator. J Clin Invest. 1996;97(4):1041–6.

49. Jonas JC, Sharma A, Hasenkamp W, Ilkova H, Patanè G, Laybutt R, et al. Chronic hyperglycemia triggers loss of pancreatic β cell differentiation in an animal model of diabetes. J Biol Chem. 1999;274:14112–21.

50. Harmon JS, Stein R, Robertson RP. Oxidative stress-mediated, post-translational loss of MafA protein as a contributing mechanism to loss of insulin gene expression in glucotoxic beta cells. J Biol Chem. 2005;280(12):11107–13.

51. Itoh N, Okamoto H. Translational control of proinsulin synthesis by glucose. Nature. 1980;283:100–2.

52. Welsh M, Scherberg N, Gilmoret R. Translational control of insulin biosynthesis. Biochem J. 1986;235:459–67.

53. Kimball SR. Eukaryotic initiation factor eIF2. Int J Biochem Cell Biol. 1999;31:25–9.

54. Vander Mierde D, Scheuner D, Quintens R, Patel R, Song B, Tsukamoto K, et al. Glucose activates a protein phosphatase-1-mediated signaling pathway to enhance overall translation in pancreatic β-cells. Endocrinology. 2007;148(January):609–17.

55. Scheuner D, Mierde D Vander, Song B, Flamez D, Creemers JWM, Tsukamoto K, et al. Control of mRNA translation preserves endoplasmic reticulum function in beta cells and maintains glucose homeostasis. 2005;11(7):757–64.

56. Harding HP, Ron D. Endoplasmic reticulum stress and the development of diabetes: a review. Diabetes. 2002;51(3):455–61.

57. Nolan CJ, Prentki M. The islet β-cell: fuel responsive and vulnerable. Trends Endocrinol Metab. 2008;19(September):285–91.

58. Maechler P. Mitochondrial function and insulin secretion. Mol Cell Endocrinol. Elsevier Ireland Ltd; 2013;379(June):12–8.

59. Prentki M, Matschinsky FM, Madiraju SRM. Metabolic signaling in fuel-induced insulin secretion. Cell Metab. 2013;18:162–85.

60. Keane K, Newsholme P. Metabolic regulation of insulin secretion. 1st ed. Vitamins and Hormones. Elsevier Inc.; 2014. 1-33 p.

61. Abumrad N, Harmon C, Ibrahimi A. Membrane transport of long-chain fatty acids: evidence for a facilitated process. J Lipid Res. 1998;39(12):2309–18.

62. Itoh Y, Kawamata Y, Harada M, Kobayashi M, Fujii R, Fukusumi S, et al. Free fatty acids regulate insulin secretion from pancreatic beta cells through GPR40. Nature. 2003;422(2000):173–6.

63. Kwan EP, Xie L, Sheu L, Nolan CJ, Prentki M, Betz A, et al. Munc13-1 deficiency reduces insulin secretion and causes abnormal glucose tolerance. Diabetes. 2006;55(May):1421–9.

64. Pratley RE, Weyer C. Progression from IGT to Type 2 Diabetes Mellitus : The Central Role of Impaired Early Insulin Secretion. 2002;

65. Hou ZQ, Li HL, Gao L, Pan L, Zhao JJ, Li GW. Involvement of chronic stresses in rat islet and INS-1 cell glucotoxicity induced by intermittent high glucose. Mol Cell Endocrinol. 2008;291:71–8.

66. Federici M, Hribal M, Perego L, Ranalli M, Caradonna Z, Perego C, et al. High Glucose Causes Apoptosis in Cultured Human Pancreatic Islet of Langerhans. Diabetes. 2001;50(June):1290–301.

67. Robertson a. P. Chronic oxidative stress as a central mechanism for glucose toxicity in pancreatic islet beta cells in diabetes. J Biol Chem. 2004;279:42351–4.

68. Poitout V, Robertson RP. Glucolipotoxicity: Fuel excess and β-cell dysfunction. Endocr Rev. 2008;29(3):351–66.

69. Bensellam M, Laybutt DR, Jonas J-C. The molecular mechanisms of pancreatic β-cell glucotoxicity: Recent findings and future research directions. Mol Cell Endocrinol. Elsevier Ireland Ltd; 2012;364(1-2):1–27.

70. Robertson RP, Harmon J, Tran PO, Tanaka Y, Takahashi H. Glucose toxicity in β-cells: Type 2 diabetes, good radicals gone bad, and the glutathione connection. Diabetes. 2003. p. 581–7.

71. Lu H, Koshkin V, Allister EM, Gyulkhandanyan A V., Wheeler MB. Molecular and metabolic evidence for mitochondrial defects associated with beta-cell dysfunction in a mouse model of type 2 diabetes. Diabetes. 2010;59(February):448–59.

72. Szegezdi E, Logue SE, Gorman AM, Samali A. Mediators of endoplasmic reticulum stress-induced apoptosis. EMBO Rep. 2006;7(9):880–5.

73. Tang C, Koulajian K, Schuiki I, Zhang L, Desai T, Ivovic a., et al. Glucose-induced beta cell dysfunction in vivo in rats: Link between oxidative stress and endoplasmic reticulum stress. Diabetologia. 2012;55:1366–79.

74. Seo HY, Yong DK, Lee KM, Min AK, Kim MK, Kim HS, et al. Endoplasmic reticulum stress-induced activation of activating transcription factor 6 decreases insulin gene expression via up-regulation of orphan nuclear receptor small heterodimer partner. Endocrinology. 2008;149:3832–41.

75. Zhang K, Kaufman RJ. From endoplasmic-reticulum stress to the inflammatory response. Nature. 2008;454:455–62.

76. Pascal SMA, Veiga-da-Cunha M, Gilon P, Van Schaftingen E, Jonas JC. Effects of fructosamine-3-kinase deficiency on function and survival of mouse pancreatic islets after prolonged culture in high glucose or ribose concentrations. Am J Physiol Endocrinol Metab. 2010;298:E586–96.

77. Tajiri Y, Möller C, Grill V. Long term effects of aminoguanidine on insulin release and biosynthesis: Evidence that the formation of advanced glycosylation end products inhibits B cell function. Endocrinology. 1997;138:273–80.

78. Tajiri Y, Grill V. Aminoguanidine exerts a beta-cell function-preserving effect in high glucose-cultured beta-cells (INS-1). Int J Exp Diabetes Res. 2000;1:111–9.

79. Coughlan MT, Yap FYT, Tong DCK, Andrikopoulos S, Gasser A, Thallas-Bonke V, et al. Advanced glycation end products are direct modulators of β-cell function. Diabetes. 2011;60:2523–32.

80. Lin N, Zhang H, Su Q. Advanced glycation end-products induce injury to pancreatic beta cells through oxidative stress. Diabetes & Metabolism. 2012. p. 250–7.

81. Ehses JA, Perren A, Eppler E, Ribaux P, Pospisilik J, Maor-Cahn R, et al. Increased number of islet-associated macrophages in type 2 diabetes. Diabetes. 2007;56(September):2356–70.

82. Donath MY, Ehses JA, Maedler K, Schumann DM, Ellingsgaard H, Eppler E, et al. Mechanisms of beta-cell death in type 2 diabetes. Diabetes. 2005;54 Suppl 2(December):S108–13.

83. Maedler K, Sergeev P, Ris F, Oberholzer J, Joller-jemelka HI, Spinas GA, et al. Glucose-induced beta cell production of IL-1 beta contributes to glucotoxicity in human pancreatic islets. J Clin Invest. 2002;110(6):851–60.

84. Gurlo T, Ryazantsev S, Huang C, Yeh MW, Reber HA, Hines OJ, et al. Evidence for proteotoxicity in beta cells in type 2 diabetes: toxic islet amyloid polypeptide oligomers form intracellularly in the secretory pathway. Am J Pathol. 2010;176(2):861–9.

85. Westwell-Roper CY, Ehses JA, Verchere CB. Resident macrophages mediate islet amyloid polypeptide-induced islet IL-1β production and β-cell dysfunction. Diabetes. 2014. 1698-1711 p.

86. Weir GC, Laybutt DR, Kaneto H, Bonner-Weir S, Sharma A. Beta-cell adaptation and decompensation during the progression of diabetes. Diabetes. 2001. p. S154–9.

87. Boden G. Obesity and Free Fatty Acids. Endocrinology and Metabolism Clinics of North America. 2008. p. 635–46.

88. Cnop M, Igoillo-Esteve M, Cunha D a, Ladrière L, Eizirik DL. An update on lipotoxic endoplasmic reticulum stress in pancreatic beta-cells. Biochem Soc Trans. 2008;36:909–15.

89. Maedler K, Oberholzer J, Bucher P, Spinas GA, Donath MY. Monounsaturated fatty acids prevent the deleterious effects of palmitate and high glucose on human pancreatic β-cell turnover and function. Diabetes. 2003;52(March):726–33.

90. Shimabukuro M, Ohneda M, Lee Y, Unger RH. Role of nitric oxide in obesity-induced beta cell disease. J Clin Invest. 1997;100(2):290–5.

91. El-Assaad W, Buteau J, Peyot ML, Nolan C, Roduit R, Hardy S, et al. Saturated fatty acids synergize with elevated glucose to cause pancreatic β-cell death. Endocrinology. 2003;144(January):4154–63.

92. Poitout V, Amyot J, Semache M, Zarrouki B, Hagman D, Fontés G. Glucolipotoxicity of the pancreatic beta cell. Biochim Biophys Acta. 2010;1801(3):289–98.

93. Zhou YP, Grill VE. Long-term exposure of rat pancreatic islets to fatty acids inhibits glucose-induced insulin secretion and biosynthesis through a glucose fatty acid cycle. J Clin Invest. 1994;93:870–6.

94. Ritz-Laser B, Meda P, Constant I, Klages N, Charollais A, Morales A, et al. Glucose-induced preproinsulin gene expression is inhibited by the free fatty acid palmitate. Endocrinology. 1999;140(9):4005–14.

95. Kelpe CL, Moore PC, Parazzoli SD, Wicksteed B, Rhodes CJ, Poitout V. Palmitate inhibition of insulin gene expression is mediated at the transcriptional level via ceramide synthesis. J Biol Chem. 2003;278:30015–21.

96. Hagman DK, Hays LB, Parazzoli SD, Poitout V. Palmitate inhibits insulin gene expression by altering PDX-1 nuclear localization and reducing MafA expression in isolated rat islets of Langerhans. J Biol Chem. 2005;280(37):32413–8.

97. Piro S, Anello M, Di Pietro C, Lizzio MN, Patanè G, Rabuazzo AM, et al. Chronic exposure to free fatty acids or high glucose induces apoptosis in rat pancreatic islets: Possible role of oxidative stress. Metabolism. 2002;51(10):1340–7.

98. Lupi R, Dotta F, Marselli L, Guerra S Del, Masini M, Santangelo C, et al. Prolonged exposure to free fatty acids has cytostatic and pro-apoptotic effects on human pancreatic islets. Diabetes. 2002;51:1437–42.

99. El-Assaad W, Joly E, Barbeau A, Sladek R, Buteau J, Maestre I, et al. Glucolipotoxicity alters lipid partitioning and causes mitochondrial dysfunction, cholesterol, and ceramide deposition and reactive oxygen species production in INS832/13 β-cells. Endocrinology. 2010;151(July 2010):3061–73.

100. Alejandro EU, Gregg B, Blandino-rosano M, Cras-méneur C, Bernal-mizrachi E. Natural history of β-cell adaptation and failure in type 2 diabetes. Mol Aspects Med. 2014;1–24.

101. Ow Y-LP, Green DR, Hao Z, Mak TW. Cytochrome c: functions beyond respiration. Nat Rev Mol Cell Biol. 2008;9(July):532–42.

102. Holmström KM, Finkel T. Cellular mechanisms and physiological consequences of redox-dependent signalling. Nat Rev Mol Cell Biol. Nature Publishing Group; 2014;15(6):411–21.

103. Henquin JC. The dual control of insulin secretion by glucose involves triggering and amplifying pathways in beta-cells. Diabetes Res Clin Pract. Elsevier Ireland Ltd; 2011;93:S27–31.

104. Henquin JC. Regulation of insulin secretion: A matter of phase control and amplitude modulation. Diabetologia. 2009;52:739–51.

105. Hamanaka RB, Chandel NS. Mitochondrial reactive oxygen species regulate cellular signaling and dictate biological outcomes. Trends in Biochemical Sciences. 2010. p. 505–13.

106. Sena LA, Chandel NS. Physiological roles of mitochondrial reactive oxygen species. Mol Cell. Elsevier Inc.; 2012;48(2):158–66.

107. Leloup C, Tourrel-Cuzin C, Magnan C, Karaca M, Castel J, Carneiro L, et al. Mitochondrial reactive oxygen species are obligatory signals for glucose-induced insulin secretion. Diabetes. 2009;58(March):673–81.

108. Pi J, Bai Y, Zhang Q, Wong V, Floering LM, Daniel K, et al. Reactive Oxygen Species as a Signal in Glucose- Stimulated Insulin Secretion. Diabetes. 2007;56(July):1783–91.

109. Jensen M V, Joseph JW, Ronnebaum SM, Burgess SC, Sherry AD, Newgard CB. Metabolic cycling in control of glucose-stimulated insulin secretion. Am J Physiol Endocrinol Metab. 2008;295:E1287–97.

110. Ivarsson R, Quintens R, Dejonghe S, Tsukamoto K, In't Veld P, Renström E, et al. Redox control of exocytosis: Regulatory role of NADPH, thioredoxin, and glutaredoxin. Diabetes. 2005;54(July):2132–42.

111. Panten U, Rustenbeck I. Fuel-induced amplification of insulin secretion in mouse pancreatic islets exposed to a high sulfonylurea concentration: Role of the NADPH/NADP+ ratio. Diabetologia. 2008;51:101–9.

112. Supale S, Li N, Brun T, Maechler P. Mitochondrial dysfunction in pancreatic β cells. Trends Endocrinol Metab. 2012;23(9):477–87.

113. Prentki M, Matschinsky FM, Madiraju SRM. Metabolic signaling in fuel-induced insulin secretion. Cell Metab. Elsevier Inc.; 2013;18(2):162–85.

114. Murphy MP. How mitochondria produce reactive oxygen species. Biochem J. 2009;417:1–13.

115. Karunakaran U, Park KG. A systematic review of oxidative stress and safety of antioxidants in diabetes: Focus on islets and their defense. Diabetes Metab J. 2013;37:106–12.

116. Drews G, Krippeit-Drews P, Duïfer M. Oxidative stress and beta-cell dysfunction. Pflugers Arch Eur J Physiol. 2010;460:703–18.

117. Lei XG, Vatamaniuk MZ. Two tales of antioxidant enzymes on β cells and diabetes. Antioxid Redox Signal. 2011;14(3):489–503.

118. Harmon JS, Bogdani M, Parazzoli SD, Mak SSM, Oseid EA, Berghmans M, et al. β-cell-specific overexpression of glutathione peroxidase preserves intranuclear MafA and reverses diabetes in db/db Mice. Endocrinology. 2009;150(November 2009):4855–62.

119. Lenzen S, Drinkgern J. Low antioxidant enzyme gene expression in pancreatic islets compared with various other mouse tissues. Free Radic Biol Med. 1996;20(3):463–6.

120. Lenzen S. Oxidative stress: the vulnerable beta-cell. Biochem Soc Trans. 2008;36:343–7.

121. Li N, Stojanovski S, Maechler P. Mitochondrial Hormesis in Pancreatic β Cells: Does Uncoupling Protein 2 Play a Role? Oxid Med Cell Longev. 2012;2012.

122. Chan CB, De Leo D, Joseph JW, McQuaid TS, Ha XF, Xu F, et al. Increased uncoupling protein-2 levels in beta-cells are associated with impaired glucose-stimulated insulin secretion: mechanism of action. Diabetes. 2001;50:1302–10.

123. Patanè G, Anello M, Piro S, Vigneri R, Purrello F, Rabuazzo AM. Role of ATP production and uncoupling protein-2 in the insulin secretory defect induced by chronic exposure to high glucose or free fatty acids and effects of peroxisome proliferator-activated receptor-gamma inhibition. Diabetes. 2002;51:2749–56.

124. Krauss S, Zhang CY, Scorrano L, Dalgaard LT, St-Pierre J, Grey ST, et al. Superoxide-mediated activation of uncoupling protein 2 causes pancreatic beta cell dysfunction. J Clin Invest. 2003;112(12):1831–42.

125. Robson-Doucette CA, Sultan S, Allister EM, Wikstrom JD, Koshkin V, Bhattacharjee A, et al. Beta-Cell Uncoupling Protein 2 Regulates Reactive Oxygen Species Production, Which Influences Both Insulin and Glucagon Secretion. Diabetes. 2011;60(November):2710–9.

126. Moore PC, Ugas MA, Hagman DK, Parazzoli SD, Poitout V. Evidence Against the Involvement of Oxidative Stress in Fatty Acid Inhibition of Insulin Secretion. Diabetes. 2004;53:2610–6.

127. Tanaka Y, Tran POT, Harmon J, Robertson RP. A role for glutathione peroxidase in protecting pancreatic beta cells against oxidative stress in a model of glucose toxicity. Proc Natl Acad Sci U S A. 2002;99:12363–8.

128. Nishikawa T, Edelstein D, Du XL, Yamagishi S, Matsumura T, Kaneda Y, et al. Normalizing mitochondrial superoxide production blocks three pathways of hyperglycaemic damage. Nature. 2000;404:787–90.

129. Anello M, Lupi R, Spampinato D, Piro S, Masini M, Boggi U, et al. Functional and morphological alterations of mitochondria in pancreatic beta cells from type 2 diabetic patients. Diabetologia. 2005;48:282–9.

130. Olson LK, Redmon JB, Towle HC, Robertson RP. Chronic exposure of HIT cells to high glucose concentrations paradoxically decreases insulin gene transcription and alters binding of insulin gene regulatory protein. J Clin Invest. 1993;92(July):514–9.

131. Wali JA, Rondas D, Zhao Y, Elkerbout L, Fynch S, Gurzov EN, et al. The proapoptotic BH3-only proteins Bim and Puma are downstream of endoplasmic reticulum and mitochondrial oxidative stress in pancreatic islets in response to glucotoxicity. Cell Death Dis. Nature Publishing Group; 2014;5(3):e1124–9.

132. Liesa M, Shirihai OS. Mitochondrial dynamics in the regulation of nutrient utilization and energy expenditure. Cell Metab. 2013;17(2):491–506.

133. Molina AJA, Wikstrom JD, Stiles L, Las G, Mohamed H, Elorza A, et al. Mitochondrial networking protects beta-cells from nutrient-induced apoptosis. Diabetes. 2009;58(October):2303–15.

134. Picard M, Shirihai OS, Gentil BJ, Burelle Y. Mitochondrial morphology transitions and functions: implications for retrograde signaling? Am J Physiol Regul Integr Comp Physiol. 2013;304(January):R393–406.

135. Dlasková A, Špaček T, Šantorová J, Plecitá-Hlavatá L, Berková Z, Saudek F, et al. 4Pi microscopy reveals an impaired three-dimensional mitochondrial network of pancreatic islet β-cells, an experimental model of type-2 diabetes. Biochim Biophys Acta - Bioenerg. 2010;1797:1327–41.

136. Bindokas VP, Kuznetsov A, Sreenan S, Polonsky KS, Roe MW, Philipson LH. Visualizing superoxide production in normal and diabetic rat islets of Langerhans. J Biol Chem. 2003;278(11):9796–801.

137. Jhun BS, Lee H, Jin ZG, Yoon Y. Glucose Stimulation Induces Dynamic Change of Mitochondrial Morphology to Promote Insulin Secretion in the Insulinoma Cell Line INS-1E. PLoS One. 2013;8(4):1–11.

138. Zhang Z, Wakabayashi N, Wakabayashi J, Tamura Y, Song W-J, Sereda S, et al. The dynamin-related GTPase Opa1 is required for glucose-stimulated ATP production in pancreatic beta cells. Mol Biol Cell. 2011;22:2235–45.

139. Cnop M, Welsh N, Jonas J, Jörns A, Lenzen S, Eizirik DL. Mechanisms of pancreatic beta-cell death in type 1 and type 2 diabetes: many differences, few similarities. Diabetes. 2005;54 Suppl 2(6):S97–107.

140. Kroemer G, Galluzzi L, Vandenabeele P, Abrams J, Alnemri E, Baehrecke E, et al. Classification of Cell Death 2009. Cell Death Differ. 2009;16(1):3–11.

141. Danial NN, Danial NN, Korsmeyer SJ, Korsmeyer SJ. Cell death: critical control points. Cell. 2004;116:205–19.

142. Tait SWG, Green DR. Mitochondria and cell death: outer membrane permeabilization and beyond. Nat Rev Mol Cell Biol. Nature Publishing Group; 2010;11(9):621–32.

143. McKenzie MD, Carrington EM, Kaufmann T, Strasser A, Huang DCS, Kay TWH, et al. Proapoptotic BH3-only protein bid is essential for death receptor-induced apoptosis of pancreatic β-cells. Diabetes. 2008;57(May):1284–92.

144. McKenzie MD, Jamieson E, Jansen ES, Scott CL, Huang DCS, Bouillet P, et al. Glucose induces pancreatic islet cell apoptosis that requires the BH3-only proteins bim and puma and multi-BH domain protein bax. Diabetes. 2010;59(March):644–52.

145. Cunha DA, Igoillo-Esteve M, Gurzov EN, Germano CM, Naamane N, Marhfour I, et al. Death protein 5 and p53-upregulated modulator of apoptosis mediate the endoplasmic reticulum stress-mitochondrial dialog triggering lipotoxic rodent and human β-cell apoptosis. Diabetes. 2012;61(November):2763–75.

146. Maedler K, Spinas G a., Lehmann R, Sergeev P, Weber M, Fontana A, et al. Glucose Induces β-Cell Apoptosis Via Upregulation of the Fas Receptor in Human Islets. Diabetes. 2001;50:1683–90.

147. Leber B, Lin J, Andrews DW. Still embedded together binding to membranes regulates Bcl-2 protein interactions. Oncogene. Nature Publishing Group; 2010;29(38):5221–30.

148. Cheng EH, Levine B, Boise LH, Thompson CB, Hardwick JM. Bax-independent inhibition of apoptosis by Bcl-XL. Nature. 1996;379:554–6.

149. Gross A, Mcdonnell JM, Korsmeyer SJ. BCL-2 family members and the mitochondria in apoptosis BCL-2 family members and the mitochondria in apoptosis. 1999;1899–911.

150. Harris MH, Thompson CB. The role of the Bcl-2 family in the regulation of outer mitochondrial membrane permeability. Cell Death Differ. 2000;7:1182–91.

151. Zhou YP, Pena JC, Roe MW, Mittal A, Levisetti M, Baldwin AC, et al. Overexpression of Bcl-x(L) in beta-cells prevents cell death but impairs mitochondrial signal for insulin secretion. Am J Physiol Endocrinol Metab. 2000;278:E340–51.

152. Carrington EM, McKenzie MD, Jansen E, Myers M, Fynch S, Kos C, et al. Islet beta-cells deficient in Bcl-xL develop but are abnormally sensitive to apoptotic stimuli. Diabetes. 2009;58(October):2316–23.

153. Cunha DA, Hekerman P, Ladrière L, Bazarra-Castro A, Ortis F, Wakeham MC, et al. Initiation and execution of lipotoxic ER stress in pancreatic beta-cells. J Cell Sci. 2008;121(0 14):2308–18.

154. Shimabukuro M, Wang MY, Zhou YT, Newgard CB, Unger RH. Protection against lipoapoptosis of beta cells through leptin-dependent maintenance of Bcl-2 expression. Proc Natl Acad Sci U S A. 1998;95(August):9558–61.

155. Michels J, Kepp O, Senovilla L, Lissa D, Castedo M, Kroemer G, et al. Functions of BCL-XL at the Interface between Cell Death and Metabolism. Int J Cell Biol. 2013;2013:705294.

156. Luciani DS, White SA, Widenmaier SB, Saran V V., Taghizadeh F, Hu X, et al. Bcl-2 and Bcl-xL suppress glucose signaling in pancreatic β-cells. Diabetes. 2013;62:170–82.

157. Gottlieb E, Armour SM, Harris MH, Thompson CB. Mitochondrial membrane potential regulates matrix configuration and cytochrome c release during apoptosis. Cell Death Differ. 2003;10:709–17.

158. Shoshan-Barmatz V, Keinan N, Zaid H. Uncovering the role of VDAC in the regulation of cell life and death. J Bioenerg Biomembr. 2008;40:183–91.

159. Vander Heiden MG, Li XX, Gottleib E, Hill RB, Thompson CB, Colombini M. Bcl-xL Promotes the Open Configuration of the Voltage-dependent Anion Channel and Metabolite Passage through the Outer Mitochondrial Membrane. J Biol Chem. 2001;276:19414–9.

160. Shimizu S, Konishi a, Kodama T, Tsujimoto Y. BH4 domain of antiapoptotic Bcl-2 family members closes voltage-dependent anion channel and inhibits apoptotic mitochondrial changes and cell death. Proc Natl Acad Sci U S A. 2000;97:3100–5.

161. Arbel N, Ben-Hail D, Shoshan-Barmatz V. Mediation of the antiapoptotic activity of Bcl-xL protein upon interaction with VDAC1 protein. J Biol Chem. 2012;287(27):23152–61.

162. Shimizu S, Narita M, Tsujimoto Y. Bcl-2 family proteins regulate the release of apoptogenic cytochrome c by the mitochondrial channel VDAC. Nature. 1999;399(1992):483–7.

163. Vander Heiden MG, Chandel NS, Williamson EK, Schumacker PT, Thompson CB. Bcl-xL regulates the membrane potential and volume homeostasis of mitochondria. Cell. 1997;91:627–37.

164. Alavian KN, Li H, Collis L, Bonanni L, Zeng L, Sacchetti S, et al. Bcl-xl regulates metabolic efficiency of neurons through interaction with the mitochondrial F1FoATP synthase. Nat Cell Biol. Nature Publishing Group; 2011;13(10):1224–33.

165. Chen Y-B, Aon MA, Hsu Y-T, Soane L, Teng X, McCaffery JM, et al. Bcl-xL regulates mitochondrial energetics by stabilizing the inner membrane potential. J Exp Med. 2011;208(2):i29–i29.

166. Gottlieb E, Vander Heiden MG, Thompson CB. Bcl-x(L) prevents the initial decrease in mitochondrial membrane potential and subsequent reactive oxygen species production during tumor necrosis factor alpha-induced apoptosis. Mol Cell Biol. 2000;20(15):5680–9.

167. Orrenius S, Zhivotovsky B, Nicotera P. Regulation of cell death: the calcium-apoptosis link. Nat Rev Mol Cell Biol. 2003;4(July):552–65.

168. Bonneau B, Prudent J, Popgeorgiev N, Gillet G. Non-apoptotic roles of Bcl-2 family: The calcium connection. Biochim Biophys Acta - Mol Cell Res. Elsevier B.V.; 2013;1833(7):1755–65.

169. Pinton P, Rizzuto R. Bcl-2 and Ca2+ homeostasis in the endoplasmic reticulum. Cell Death Differ. 2006;13:1409–18.

170. Huang H, Hu X, Eno CO, Zhao G, Li C, White C. An interaction between Bcl-xL and the Voltage-dependent Anion Channel (VDAC) promotes mitochondrial Ca2+ uptake. J Biol Chem. 2013;288:19870–81.

171. White C, Li C, Yang J, Petrenko NB, Madesh M, Thompson CB, et al. The endoplasmic reticulum gateway to apoptosis by Bcl-X(L) modulation of the InsP3R. Nat Cell Biol. 2005;7(10):1021–8.

172. Li C, Wang X, Vais H, Thompson CB, Foskett JK, White C. Apoptosis regulation by Bcl-x(L) modulation of mammalian inositol 1,4,5-trisphosphate receptor channel isoform gating. Proc Natl Acad Sci U S A. 2007;104:12565–70.

173. Susnow N, Zeng L, Margineantu D, Hockenbery DM. Bcl-2 family proteins as regulators of oxidative stress. Semin Cancer Biol. 2009;19:42–9.

174. Zimmermann AK, Loucks FA, Schroeder EK, Bouchard RJ, Tyler KL, Linseman DA. Glutathione binding to the Bcl-2 homology-3 domain groove: A molecular basis for BCL-2 antioxidant function at mitochondria. J Biol Chem. 2007;282(40):29296–304.

175. Chen ZX, Pervaiz S. Bcl-2 induces pro-oxidant state by engaging mitochondrial respiration in tumor cells. Cell Death Differ. 2007;14:1617–27.

176. Kim JJ, Lee SB, Park JK, Yoo YD. TNF-alpha-induced ROS production triggering apoptosis is directly linked to Romo1 and Bcl-X(L). Cell Death Differ. Nature Publishing Group; 2010;17(9):1420–34.

177. Lee SB, Kim HJ, Shin J, Kang ST, Kang S, Yoo YDO. Bcl-XL prevents serum deprivation-induced oxidative stress mediated by Romo1. Oncol Rep. 2011;25:1337–42.

178. Hildeman DA, Mitchell T, Aronow B, Wojciechowski S, Kappler J, Marrack P. Control of Bcl-2 expression by reactive oxygen species. Proc Natl Acad Sci U S A. 2003;100(25):15035–40.

179. Li D, Ueta E, Kimura T, Yamamoto T, Osaki T. Reactive oxygen species (ROS) control the expression of Bcl-2 family proteins by regulating their phosphorylation and ubiquitination. Cancer Sci. 2004;95(8):644–50.

180. Mehmeti I, Lenzen S, Lortz S. Modulation of Bcl-2-related protein expression in pancreatic beta cells by pro-inflammatory cytokines and its dependence on the antioxidative defense status. Mol Cell Endocrinol. Elsevier Ireland Ltd; 2011;332(1-2):88–96.

181. Autret A, Martin SJ. Emerging Role for Members of the Bcl-2 Family in Mitochondrial Morphogenesis. Mol Cell. 2009;36:355–63.

182. Delivani P, Adrain C, Taylor RC, Duriez PJ, Martin SJ. Role for CED-9 and Egl-1 as regulators of mitochondrial fission and fusion dynamics. Mol Cell. 2006;21:761–73.

183. Zheng J-Y, Tsai Y-C, Kadimcherla P, Zhang R, Shi J, Oyler GA, et al. The C-terminal transmembrane domain of Bcl-xL mediates changes in mitochondrial morphology. Biophys J. 2008;94(January):286–97.

184. Li H, Chen Y, Jones AF, Sanger RH, Collis LP, Flannery R, et al. Bcl-xL induces Drp1-dependent synapse formation in cultured hippocampal neurons. Proc Natl Acad Sci U S A. 2008;105(6):2169–74.

185. Li H, Alavian KN, Lazrove E, Mehta N, Jones A, Zhang P, et al. A Bcl-xL-Drp1 complex regulates synaptic vesicle membrane dynamics during endocytosis. Nat Cell Biol. 2013;15(May):773–85.

186. Berman SB, Chen YB, Qi B, McCaffery JM, Rucker EB, Goebbels S, et al. Bcl-x L increases mitochondrial fission, fusion, and biomass in neurons. J Cell Biol. 2009;184(5):707–19.

187. Picard M, Turnbull DM. Linking the metabolic state and mitochondrial dna in chronic disease, health, and aging. Diabetes. 2013;62:672–8.

188. Feil S, Valtcheva N, Feil R. Inducible cre mice. Methods Mol Biol. 2009;530:343–63.

189. Friedel RH, Wurst W, Wefers B, Kühn R. Generating conditional knockout mice. Methods Mol Biol. 2011;693:205–31.

190. Orban PC, Chui D, Marth JD. Tissue- and site-specific DNA recombination in transgenic mice. Proc Natl Acad Sci U S A. 1992;89:6861–5.

191. White S. Pro-apoptotic Bax and Bak control beta-cell deatg and early endoplasmic reticulum stress signalling. [Thesis] Univ Bristish Columbia, Circ. 2013;(June).

192. Schwerk C, Schulze-Osthoff K. Regulation of apoptosis by alternative pre-mRNA splicing. Mol Cell. 2005;19:1–13.

193. Motoyama N, Wang F, Roth KA, Sawa H, Nakayama K, Nakayama K, et al. Massive cell death of immature hematopoietic cells and neurons in Bcl-x-deficient mice. Science. 1995;267:1506–10.

194. Gittes GK. Developmental biology of the pancreas: A comprehensive review. Dev Biol. Elsevier B.V.; 2009;326(1):4–35.

195. Campbell SC, Macfarlane WM. Regulation of the pdx1 gene promoter in pancreatic beta-cells. Biochem Biophys Res Commun. 2002;299:277–84.

196. Serup P, Petersen H V, Pedersen EE, Edlund H, Leonard J, Petersen JS, et al. The homeodomain protein IPF-1/STF-1 is expressed in a subset of islet cells and promotes rat insulin 1 gene expression dependent on an intact E1 helix-loop-helix factor binding site. Biochem J. 1995;310 (Pt 3:997–1003.

197. Miller CP, McGehee RE, Habener JF. IDX-1: a new homeodomain transcription factor expressed in rat pancreatic islets and duodenum that transactivates the somatostatin gene. EMBO J. 1994;13(5):1145–56.

198. Zhang N, He Y-W. The antiapoptotic protein Bcl-xL is dispensable for the development of effector and memory T lymphocytes. J Immunol. 2005;174:6967–73.

199. Wicksteed B, Brissova M, Yan W, Opland DM, Plank JL, Reinert RB, et al. Conditional gene targeting in mouse pancreatic β-cells: Analysis of ectopic cre transgene expression in the brain. Diabetes. 2010;59(18):3090–8.

200. Gu G, Dubauskaite J, Melton D a. Direct evidence for the pancreatic lineage: NGN3+ cells are islet progenitors and are distinct from duct progenitors. Development. 2002;129:2447–57.

201. Johnson JD, Ford EL, Bernal-Mizrachi E, Kusser KL, Luciani DS, Han Z, et al. Suppressed insulin signaling and increased apoptosis in Cd38-null islets. Diabetes. 2006;55(October):2737–46.

202. Jeffrey KD, Alejandro EU, Luciani DS, Kalynyak TB, Hu X, Li H, et al. Carboxypeptidase E mediates palmitate-induced beta-cell ER stress and apoptosis. Proc Natl Acad Sci U S A. 2008;105:8452–7.

203. Wojtala A, Bonora M, Malinska D, Pinton P, Duszynski J, Wieckowski MR. Methods to monitor ROS production by fluorescence microscopy and fluorometry. Methods Enzymol. 2014;542:243–62.

204. Jitrapakdee S, Wutthisathapornchai A, Wallace JC, MacDonald MJ. Regulation of insulin secretion: Role of mitochondrial signalling. Diabetologia. 2010. p. 1019–32.

205. Thibault C, Guettet C, Laury MC, N'Guyen JM, Tormo MA, Bailbé D, et al. In vivo and in vitro increased pancreatic beta-cell sensitivity to glucose in normal rats submitted to a 48-h hyperglycaemic period. Diabetologia. 1993;36:589–95.

206. Yoshikawa H, Tajiri Y, Sako Y, Hashimoto T, Umeda F, Nawata H. Effects of biotin on glucotoxicity or lipotoxicity in rat pancreatic islets. Metabolism. 2002;51:163–8.

207. Ling Z, Kiekens R, Mahler T, Schuit FC, Pipeleers-Marichal M, Sener a, et al. Effects of chronically elevated glucose levels on the functional properties of rat pancreatic beta-cells. Diabetes. 1996;45(July 1995):1774–82.

208. Kerksick C, Willoughby D. The antioxidant role of glutathione and N-acetyl-cysteine supplements and exercise-induced oxidative stress. J Int Soc Sports Nutr. 2005;2(2):38–44.

209. Cotgreave IA. N-acetylcysteine: pharmacological considerations and experimental and clinical applications. Adv Pharmacol. 1997;38(September):205–27.

210. Tanaka Y, Gleason CE, Oseid E a., Hunter-Berger KK, Tran POT, Harmon JS, et al. Prevention of glucose toxicity in HIT-T15 cells and ZDF rats by an antioxidant, N-acetyl-L-cysteine. Investig Ophthalmol Vis Sci. 1996;37(September):10857–62.

211. Kaneto H, Kajimoto Y, Miyagawa J ichiro, Matsuoka T aki, Fujitani Y, Umayahara Y, et al. Beneficial effects of antioxidants in diabetes: Possible protection of pancreatic β-cells against glucose toxicity. Diabetes. 1999;48(December):2398–406.

212. Pinton P, Giorgi C, Siviero R, Zecchini E, Rizzuto R. Calcium and apoptosis: ER-mitochondria Ca2+ transfer in the control of apoptosis. Oncogene. 2008;27(50):6407–18.

213. Wang H, Kouri G, Wollheim CB. ER stress and SREBP-1 activation are implicated in beta-cell glucolipotoxicity. J Cell Sci. 2005;118:3905–15.

214. Kim WH, Lee JW, Suh YH, Hong SH, Choi JS, Lim JH, et al. Exposure to chronic high glucose induces β-cell apoptosis through decreased interaction of glucokinase with mitochondria: Downregulation of glucokinase in pancreatic β-cells. Diabetes. 2005;54(September):2602–11.

215. Kassis N, Bernard C, Pusterla A, Casteilla L, Pénicaud L, Richard D, et al. Correlation between pancreatic islet uncoupling protein-2 (UCP2) mRNA concentration and insulin status in rats. Int J Exp Diabetes Res. 2000;1:185–93.

216. Czabotar PE, Lessene G, Strasser A, Adams JM. Control of apoptosis by the BCL-2 protein family: implications for physiology and therapy. Nat Rev Mol Cell Biol. Nature Publishing Group; 2014;15(1):49–63.

217. Kaneto H, Fujii J, Myint T, Miyazawa N, Islam KN, Kawasaki Y, et al. Reducing sugars trigger oxidative modification and apoptosis in pancreatic beta-cells by provoking oxidative stress through the glycation reaction. Biochem J. 1996;320 (Pt 3:855–63.

218. Gurzov EN, Germano CM, Cunha D a., Ortis F, Vanderwinden JM, Marchetti P, et al. p53 up-regulated modulator of apoptosis (PUMA) activation contributes to pancreatic β-cell apoptosis induced by proinflammatory cytokines and endoplasmic reticulum stress. J Biol Chem. 2010;285(26):19910–20.

219. Nunemaker CS, Bertram R, Sherman A, Tsaneva-Atanasova K, Daniel CR, Satin LS. Glucose modulates [Ca2+]i oscillations in pancreatic islets via ionic and glycolytic mechanisms. Biophys J. 2006;91(September):2082–96.

220. Bertram R, Sherman A, Satin LS. Metabolic and electrical oscillations: partners in controlling pulsatile insulin secretion. Am J Physiol Endocrinol Metab. 2007;293:E890–900.

221. Lindström P. β-cell function in obese-hyperglycemic mice [ob/ob mice]. Advances in Experimental Medicine and Biology. 2010. p. 463–77.

222. Irles E, Ñeco P, Lluesma M, Villar-Pazos S, Santos-Silva JC, Vettorazzi JF, et al. Enhanced glucose-induced intracellular signaling promotes insulin hypersecretion: Pancreatic beta-cell functional adaptations in a model of genetic obesity and prediabetes. Mol Cell Endocrinol. Elsevier Ireland Ltd; 2015;404:46–55.

223. Yi CH, Pan H, Seebacher J, Jang I, Hyberts SG, Heffron GJ, et al. Metabolic Regulation of Protein N-Alpha-Acetylation by Bcl-xL Promotes Cell Survival. Cell. 2011;146(4):607–20.

224. Colombini M. VDAC structure, selectivity, and dynamics. Biochimica et Biophysica Acta - Biomembranes. 2012. p. 1457–65.

225. Malia TJ, Wagner G. NMR structural investigation of the mitochondrial outer membrane protein VDAC and its interaction with antiapoptotic Bcl-XL. Biochemistry. 2007;46:514–25.

226. Fonteriz RI, de la Fuente S, Moreno A, Lobatón CD, Montero M, Alvarez J. Monitoring mitochondrial [Ca2+] dynamics with rhod-2, ratiometric pericam and aequorin. Cell Calcium. Elsevier Ltd; 2010;48(1):61–9.

227. Prins D, Michalak M. Organellar calcium buffers. Cold Spring Harb Perspect Biol. 2011;3:1–16.

228. Carter WO, Narayanan PK, Robinson JP. Intracellular hydrogen peroxide and superoxide anion detection in endothelial cells. J Leukoc Biol. 1994;55(March):253–8.

229. Segal S, Foley J. The metabolism of D-ribose in man. J Clin Invest. 1958;37(15):719–35.

230. Matsuoka TA, Kajimoto Y, Watada H, Kaneto H, Kishimoto M, Umayahara Y, et al. Glycation-dependent, reactive oxygen species-mediated suppression of the insulin gene promoter activity in HIT cells. J Clin Invest. 1997;99:144–50.

231. Newsholme P, Haber EP, Hirabara SM, Rebelato ELO, Procopio J, Morgan D, et al. Diabetes associated cell stress and dysfunction: role of mitochondrial and non-mitochondrial ROS production and activity. J Physiol. 2007;583(2007):9–24.

232. Kalyanaraman B. Oxidative chemistry of fluorescent dyes: implications in the detection of reactive oxygen and nitrogen species. Biochemical Society Transactions. 2011. p. 1221–5.

233. Smith RAJ, Murphy MP. Animal and human studies with the mitochondria-targeted antioxidant MitoQ. Ann N Y Acad Sci. 2010;1201:96–103.

234. Norton M, Ng AC-H, Baird S, Dumoulin A, Shutt T, Mah N, et al. ROMO1 is an essential redox-dependent regulator of mitochondrial dynamics. Sci Signal. 2014;7(January):ra10.

235. Las G, Serada SB, Wikstrom JD, Twig G, Shirihai OS. Fatty acids suppress autophagic turnover in beta-cells. J Biol Chem. 2011;286:42534–44.

236. Kaufmann T, Schlipf S, Sanz J, Neubert K, Stein R, Borner C. Characterization of the signal that directs Bcl-xL, but not Bcl-2, to the mitochondrial outer membrane. J Cell Biol. 2003;160:53–64.

237. Boustany NN, Tsai Y-C, Pfister B, Joiner WM, Oyler GA, Thakor N V. BCL-xL-dependent light scattering by apoptotic cells. Biophys J. 2004;87(December):4163–71.

238. Cleland MM, Norris KL, Karbowski M, Wang C, Suen D-F, Jiao S, et al. Bcl-2 family interaction with the mitochondrial morphogenesis machinery. Cell Death Differ. 2011;18:235–47.

239. Aokage T, Ohsawa I, Ohta S. Green fluorescent protein causes mitochondria to aggregate in the presence of the Bcl-2 family proteins. Biochem Biophys Res Commun. 2004;314:711–6.

240. Mailloux RJ, Fu A, Robson-Doucette C, Allister EM, Wheeler MB, Screaton R, et al. Glutathionylation state of uncoupling protein-2 and the control of glucose-stimulated insulin secretion. J Biol Chem. 2012;287(47):39673–85.